# Doctoral Thesis

# The analysis of roles of a single-stranded DNA binding protein complex, RPA, in yeast meiosis by Auxin-inducible degron system

**Arivarasan Sampathkumar**

**Laboratory of Genome and Chromosome Functions, Institute for Protein Research, Graduate School of Science, Osaka University**

**PI: Prof. Akira Shinohara**

## Table of Contents

## List of Abbreviations

| | |
|---|---|
| °C | degree Celsius |
| 911 clamp | Rad9, Hus1, and Rad1 |
| AE | Axial elements |
| AID | Auxin inducible degron |
| ATM | Ataxia- Telangiectasia-Mutated |
| ATP | Adenosine triphosphate |
| ATR | ATM- and Rad3-related |
| BSA | Bovine serum albumin |
| Cdks | Cyclin dependent Kinases |
| CHEF | Clamped homogenous electric field. |
| COs | Crossovers |
| D-loop | Displacement Loop |
| DAPI | 4′,6-diamidino-2-phenylindole |
| DDR | DNA Damage Response |
| dHJ | Double Holliday junction |
| DNA | Deoxyribonucleic acid |
| DNA-PK | DNA dependent Protein Kinase |
| DSB | Double Stranded Breaks |
| dsDNA | double stranded DNA |
| DTT | Dithiothreitol |
| EDTA | Ethylene diamine tetra acetic acid |
| EtBr | Ethidium Bromide |
| FACS | Fluorescence activated cell sorting. |
| H3-pT11 | Histone H3 threonine 11 phosphorylation |
| JMs | Joint molecules |
| LiAc | Lithium Acetate |
| LMP | Low melting point |
| MI | Meiosis I |
| MII | Meiosis II |
| MRX | Mre11, Rad50, Xrs2 |
| nm | nanometer |
| OD | Optical Density |
| PAGE | Polyacrylamide gel electrophoresis |
| PEG | Polyethylene Glycol |
| PFA | Paraformaldehyde |
| PI | Propidium Iodide |
| RPA | Replication Protein A |
| Rpm | Rotations per minute |
| RT | Room Temperature |
| S. cerevisiae | Saccharomyces cerevisiae |
| SC | Synaptonemal Complex |
| SDS | Sodium dodecyl sulfate |
| SEI | Single End Invasion |
| SIC | Synapsis initiation complexes. |
| SPM | Sporulation medium |
| SPS | Pre Sporulation medium |
| ssDNA | single stranded DNA |

| | |
|---|---|
| TCA | Trichloro acetic acid |
| TE | Tris-EDTA |
| TIR1 | Transport Inhibitor Response 1 |
| ZMM | Zip-Msh-Mer |
| µl | microliters |

# Abstract:

Replication Protein A (RPA) stands as a pivotal player in various facets of eukaryotic DNA metabolism, particularly in safeguarding single-stranded DNA (ssDNA) structures. This study delves into the diverse functions of RPA, revealing its significant involvement in double-strand break (DSB) formation and repair. Notably, RPA's role extends to axis formation post-S-phase replication and the elongation of the synaptonemal complex, evidenced by the absence of linear immunostaining with Rec8 and Zip1.

Furthermore, findings from this study indicate a crucial interplay between RPA and Rad51 assembly during meiosis. Depletion of Rfa1, a subunit of RPA, resulted in observable impacts on Rad51 assembly, shedding light on the intricate connections between these essential components during meiotic processes.

In addition to its structural contributions, RPA emerges as a key sensor for ssDNA, activating a checkpoint mechanism pivotal for recombination. This activation involves the orchestrated interplay of Mek1, Hop1, and Ndt80, underscoring RPA's role as a molecular sentinel in the cellular response to DNA recombination events.

Collectively, this comprehensive exploration highlights the multifunctional nature of RPA, emphasizing its indispensable role in maintaining genomic integrity through its participation in various DNA processes, ranging from replication and recombination to checkpoint activation.

# Introduction:

## 1.1 Meiosis:

Meiosis is a fundamental biological process that plays a crucial role in the reproduction and genetic diversity of sexually reproducing organisms. It is a specialized form of cell division that occurs in eukaryotic cells, leading to the formation of gametes, which are essential for sexual reproduction. Meiosis involves a complex series of events that ensure the proper distribution of genetic material, resulting in the production of genetically distinct haploid cells. The process of meiosis consists of two consecutive divisions, referred to as meiosis I and meiosis II, each comprising distinct phases. Meiosis I is particularly remarkable as it involves homologous chromosomes pairing and exchange of genetic material through a process known as recombination or crossing-over. This genetic recombination promotes genetic diversity by shuffling genetic information between homologous chromosomes, leading to the formation of unique combinations of alleles.

## 1.2 Budding yeast as a model organism:

Budding yeast (Saccharomyces cerevisiae) is a widely used model organism in the study of meiosis. It has been extensively researched and provides several advantages for investigating the molecular mechanisms and genetic regulation of meiosis. Budding yeast is a unicellular organism with a relatively simple life cycle, making it easier to study and manipulate in the laboratory compared to more complex multicellular organisms. Its compact genome and well-annotated genetic map facilitate the identification and characterization of genes involved in meiosis. Despite being a unicellular organism, budding yeast shares many

essential meiotic processes with higher eukaryotes, including plants and animals. The basic events of meiosis, such as recombination, chromosome pairing, and segregation, are conserved across species. Studying these processes in yeast can provide insights into meiotic mechanisms that are relevant to other organisms, including humans. Budding yeast can be induced to undergo synchronized meiosis under controlled laboratory conditions. This characteristic is particularly advantageous for studying the sequential events of meiosis in a uniform and highly reproducible manner. By inducing meiosis at specific time points, it will be convenient to investigate the temporal regulation of meiotic events and the interactions between different molecular components.

### 1.3 Meiotic Cell Cycle:

Meiosis consists of two phases, meiosis I (MI) and meiosis II (MII). Prior to entering meiosis, a dividing cell goes through interphase, which is divided into three stages: G1, S, and G2. In the G1 phase, the cell determines whether it will undergo meiosis. Following G1 is the Pre-meiotic S phase, also known as the S phase. In budding yeast, when nutrient supply is limited, two genes, IME1 and IME2, are expressed. These genes regulate the initiation of meiosis by promoting entry into the pre-meiotic S phase and expressing the necessary genes for meiosis. During the pre-meiotic S phase, DNA replication is triggered by S-phase cyclin-dependent kinases consisting of Cdc28 catalytic subunits and S-phase-specific cyclins, Clb5 or Clb6.

## 1.4 DNA damage response and repair:

The eukaryotic cell possesses a set of biological processes known as the DNA damage response (DDR), which is activated in the presence of DNA lesions (Ciccia and Elledge, 2010). The DDR is crucial for efficient and timely DNA damage repair and cell cycle regulation, ultimately ensuring cell survival. One of the key components of the DDR is a kinase-dependent signaling cascade. In mammals, this pathway involves kinases such as ATM, ATR, and DNA-PK (Blackford and Jackson, 2017), while in Saccharomyces cerevisiae (S. cerevisiae), the homologs of ATM (Mec1) and ATR (Tel1) are involved (Weinert et al., 1994; Greenwell et al., 1995). These kinases act as transducers, detecting DNA damage and initiating a signaling cascade by phosphorylating numerous proteins (Falck et al., 2005; Marechal and Zou, 2013).

At the sites of DNA damage, a ring-shaped heterotrimeric protein complex called the 9-1-1 clamp (composed of Rad9, Hus1, and Rad1 in mammals, and Ddc1, Mec2, and Rad17 in S. cerevisiae) is loaded near the damaged DNA (Roeder and Bailis, 2000; Hong and Roeder, 2002). In meiotic cells, the 9-1-1 clamp also loads near the meiotic double-strand break (DSB) sites, which are intentionally induced by the protein Spo11 to initiate meiotic recombination (Keeney et al., 1997; Prieler et al., 2005). Once loaded, the 9-1-1 clamp triggers downstream signaling events in the DDR cascade, including the activation of Mec1.

## 1.5 Pre meiotic S-phase:

Meiotic S phase refers to the DNA synthesis phase that occurs during meiosis in budding yeast (Saccharomyces cerevisiae). It is a crucial step in the meiotic cell cycle where DNA replication takes place, resulting in the duplication of the genetic material before subsequent stages of meiosis. During meiotic S phase, the DNA replication machinery is

activated to ensure that each chromosome is faithfully duplicated. The process of DNA replication in budding yeast follows a highly conserved mechanism similar to that observed in other eukaryotic organisms. During the pre-meiotic S phase, Replication Protein A (RPA) plays a crucial role in DNA replication. RPA binds to single-stranded DNA regions and stabilizes them, preventing their degradation and facilitating the assembly of the replication machinery, ensuring efficient and accurate DNA replication.

## 1.6 Prophase I:

Meiotic prophase I in budding yeast (Saccharomyces cerevisiae) is a complex and critical phase of meiosis. It is characterized by chromosome condensation, homologous chromosome pairing, recombination, and synapsis. Numerous significant events occur during the prophase, including reciprocal recombination between homologues known as crossover recombination, the formation of the synaptonemal complex (SC) that maintains the connection between homologous chromosomes, and the activation of the recombination (pachytene) checkpoint. Based on the morphology of chromosomes, the prophase of meiosis I (MI) is divided into several stages: leptotene, zygotene, pachytene, diplotene, and diakinesis

### 1.6.1 Leptotene:

Leptotene marks the initial phase of prophase I. During this stage, sister chromatids undergo condensation in synchronization with pre-S phase, leading to the formation of a chromosome axis consisting of multiple chromatin loops. This condensed structure, known as the axial element, is a component of the Synaptonemal Complex (SC). The axial element is composed of specific meiosis-related proteins, including Hop1, Red1, Mek1, and Rec8. While DNA double-strand breaks (DSBs) are formed in the loop regions, the actual formation

of DSBs occurs on the axial element through the tethering of loops around DSB sites to the axis region via histone modification. Spo11, in meiotic programmed DSB formation, cleaves the DNA and binds to the 5' end of each strand at the DSB site. The DSB ends are processed to generate 3'-overhangs, and Rad51 and Dmc1 proteins are recruited to these overhangs. At this stage, the formation of DSBs facilitates the alignment of homologous chromosomes, positioning their homologous axes at approximately 400 nm along their length.

### 1.6.2 Zygotene

Zygotene is characterized by the initiation of Synaptonemal Complex (SC) formation. During this stage, the SC central element connects homologous chromosomes by linking the axial/lateral elements of the homologs. The main component of the central element is the ZMM (Zip-Msh-Mer) complex, consisting of Zip1, Zip2, Zip3, Mer3, Msh4, Msh5, Spo16, and Spo22/Zip4. All the components of the ZMM complex form a ZMM nodule, while only Zip1 polymerizes as the SC transverse element along the entire length of the homologous chromosomes. Zip1 and Zip3 are recruited to the centromere independently of ZMM nodule formation during leptotene. The stages of SC formation can be observed by staining Zip1 on chromosome spreads, where Zip1 localization on centromeres and ZMM nodules appears as dots, while polymerized Zip1 from ZMM nodules appears as a partial line. Other components of the ZMM complex can also be detected as dots. The polymerization of Zip1 relies on the Gmc2-Ecm11 complex, a novel SC component in Saccharomyces cerevisiae. The Gmc2-Ecm11 complex, although meiosis-specific, lacks orthologs in other organisms. However, functional analogs such as Corona in Drosophila melanogaster and SYCE1-3 and TEX12 in mice exist. The recruitment of the Gmc2-Ecm11 complex occurs on ZMM nodules before SC elongation in a Zip3 and Spo22-dependent manner. During this stage, the processed ends of double-strand breaks (DSBs), along with the recombinases Rad51 and Dmc1, invade the

homologous sequences of the homologous chromosome, forming a D-loop structure. Once the homologous region is stabilized, the D-loop becomes a stable asymmetric structure known as a single-end invasion (SEI). ZMM proteins contribute to the stabilization of SEI. ZMM proteins are recruited to the DSB site through physical interactions between the 9-1-1 complex (Rad9-Rad1-Hus1) and the Ddc1-Rad17-Mec3 complex in budding yeast. Subsequently, SC elongation initiates from the DSB sites through ZMM nodules.

### 1.6.3 Pachytene

During the pachytene stage, the single-end invasion (SEI) structure is converted into a double Holliday junction (dHJ) structure through DNA synthesis and ligation of each end. These dHJs are stabilized by the ZMM complex, which can be observed cytologically on chromosome spreads during both the zygotene and pachytene stages. At the beginning of pachytene, the synapsed regions are extended through SC elongation along the entire length of the chromosomes, resulting in the formation of a full-length synaptonemal complex (SC). The two axes of the homologous chromosomes are joined together by the full-length SC, a process referred to as "synapsis." By the mid- to late-pachytene, the SC is fully matured and consists of paired axes known as the "lateral element." At this stage, the full length of Zip1 and Gmc2-Ecm11 can be detected. In the mid-pachytene, the dHJs are resolved, leading to the generation of reciprocal crossovers (COs), accompanied by the disassembly of SC components from the chromosomes. The exit from the pachytene stage is regulated by Ndt80, a transcription factor for middle sporulation genes.

### 1.6.4 Diplotene

After the pachytene stage, the diplotene stage follows, where meiotic chromosomes begin to decondense. During this stage, the synaptonemal complex (SC) completely

disassembles, and the chromosomes lose most of their components. Additionally, while the sister arms of the chromosomes remain closely connected, the homologous chromosomes become widely separated, except in regions where chiasmata are present. These chiasmata hold the chromosomes together during diakinesis until the beginning of metaphase I.

### 1.6.5 Diakinesis

During diakinesis, the chiasmata, which are physical connections between homologous chromosomes, become more visible. This visibility is due to the tension exerted by the spindle apparatus, which pulls the homologous chromosomes in opposite directions. The late stage of diakinesis is followed by metaphase I, where the chromosomes are aligned and positioned by microtubule-directed motion at the kinetochore. As the tension between all homologs becomes equal, Securin, an inhibitory protein, is degraded. This degradation releases Separase from its inactive state. Separase is a protease that cleaves the kleisin subunit of the cohesin complex. Consequently, the meiosis-specific cohesin complex dissociates from the chromosomes, except for the kinetochore region, which is protected by Shugosin.

## 1.7 Meiotic Recombination:

Following pre-meiotic DNA replication, sister chromatids are connected by cohesin, but there is no physical link between homologous chromosomes, which can lead to inaccurate chromosome segregation. To address this, cells undergo homologous recombination, a vital

process for maintaining genome integrity by repairing DNA damage, including double-strand breaks (DSBs). Homologous recombination involves the exchange of DNA molecules with identical sequences between chromosomes (Handel and Schimenti, 2010). It is essential in both mitotic and meiotic cell cycles, playing a role in the recovery of collapsed DNA replication forks, establishing connections between homologous chromosomes for proper separation during the meiotic division, and generating genetic diversity by reshuffling gene alleles (Handel and Schimenti, 2010). During meiosis, homologous recombination is initiated by the formation of DSBs at recombination hotspots. The topoisomerase-related protein Spo11, aided by other accessory proteins, catalyzes the breakage of phosphodiester bonds in DNA strands, leading to the covalent attachment of Spo11 to the 5'-end of the DNA at the DSB site (Keeney et al., 1997; Page and Hawley, 2004; Handel and Schimenti, 2010). The MRX complex (Mre11, Rad50, Xrs2) recognizes the protein-DNA adduct, and with the assistance of Sae2 protein, removes Spo11 from the 5'-end, resulting in the formation of a single-stranded 3'-overhang tail. Nucleases and helicases then extend this tail by several hundred to a few thousand nucleotides (Krogh and Symington, 2004; Shim et al., 2010). RPA is a ssDNA binding protein which binds to this 3’ ssDNA overhang tail. This ensures that the ssDNA overhang does not form any secondary structures which will hinder progression of recombination. The single-stranded DNA with a 3'-end is coated by the recombinase proteins Rad51 and Dmc1, forming nucleoprotein filaments. With the aid of accessory proteins Rad54 and Tid1, these filaments initiate a search for homologous DNA sequences. Upon finding a complementary strand in the homologous duplex DNA, the single-stranded DNA invades the duplex, forming a displacement loop (D-loop). The transient D-loop is then converted into a stable single-end invasion (SEI) accompanied by DNA synthesis. Capture of the extended SEI with the single-stranded DNA at the other DSB end, followed by further extension of the 3'-overhang tail and gap ligation, leads to the formation of double Holliday junctions (dHJs).

These dHJs are subsequently resolved to generate reciprocal crossovers (COs) (Matos et al., 2011). The formation of COs is tightly regulated to ensure non-random distribution along chromosomes, with at least one crossover per pair of homologs. This phenomenon, known as crossover interference, reduces the likelihood of having multiple COs in proximity (Borner et al., 2004).

## 1.8 Rad51 and Dmc1 ssDNA filament formation:

The S. cerevisiae Rad51 protein shares 30% sequence identity with the catalytic domain of the bacterial RecA protein, which is present in both mitotic and meiotic cells (Shinohara et al., 1992). In contrast, Dmc1 exhibits 45% sequence identity with Rad51 and shows significant similarity to RecA, but it is specifically expressed during meiosis (Krogh and Symington, 2004). Rad51 and Dmc1 play crucial roles in the conversion of double-strand breaks (DSBs) into joint molecules (JMs), such as single-end invasions (SEIs) and double Holliday junctions (dHJs), during meiosis (Shinohara et al., 2000).

Rad51 forms helical filaments on single-stranded DNA and catalyzes strand exchange between circular single-stranded DNA and homologous linear double-stranded DNA to generate JMs (Shinohara and Ogawa, 1998). In vitro studies have shown that Rad52 protein facilitates the formation of Rad51 filaments for strand exchange (Shinohara and Ogawa, 1998). Consistent with this, in vivo localization of Rad51 to DSB sites requires Rad52 as an essential factor for loading Rad51 onto single-stranded DNA coated by RPA (Krogh and Symington, 2004; Seeber et al., 2013).

On the other hand, Dmc1 plays a vital role in repairing homologous non-sister chromatids during meiosis (Schwacha and Kleckner, 1997). The assembly of Dmc1 is promoted by Rad51, as well as a meiosis-specific protein complex called Mei5-Sae3 (Hayase et al., 2004). Rad51 and Dmc1 co-localize to form foci that correspond to DSB sites during meiosis,

suggesting their involvement in the same recombination events, such as inter-homolog recombination (Bishop, 1994; Shinohara et al., 2000). Mutations in rad51 lead to partial defects in meiotic recombination and result in inviable meiotic products (Shinohara et al., 1992). Conversely, dmc1 null mutants show the accumulation of resected but unrepaired DSBs during meiosis, as observed through various physical assays (Bishop et al., 1992). Overall, Rad51 and Dmc1 play critical roles in meiotic recombination.

## 1.9 Synaptonemal Complex:

The process of homologous recombination and accurate chromosome segregation in meiotic prophase is intricately connected to the dynamics of chromosome pairing and synapsis. In yeast, it has been observed that the formation of double-strand breaks (DSBs) is essential for synapsis, and the processing of DSB ends is crucial for efficient synapsis (Roeder, 1995). Synapsis occurs within a ladder-like protein structure called the synaptonemal complex (SC), which is prominently visible during the pachytene stage. The assembly, rearrangement, and disassembly of the SC take place during the prophase of meiosis I (Page and Hawley, 2004).

The formation of the SC begins at the leptotene stage. Sister chromatids, connected by cohesion, start to condense and become highly organized within the axial elements. As leptotene progresses, bridges called axial associations form at sites corresponding to DSBs between homologs. Rad51 and Dmc1 are crucial for the formation of axial associations. These associations serve as sites for the assembly of synapsis initiation complexes (SICs), which consist of a group of ZMM (Zip1-Zip2-Zip3) proteins, including Zip1, Zip2, Zip3, Msh4, Msh5, Spo22, Spo16, and Mer3 (Nakagawa and Ogawa, 1999; Shinohara et al., 2008). Axial associations play a vital role in meiotic synapsis by facilitating the assembly of the SC and are important for the maturation of DSBs into meiotic crossovers (Chua and Roeder,

1998). The axial associations initiate the formation of the SC between the axial elements, which then become part of the lateral elements within the SC structure (Miyazaki and Orr-Weaver, 1994).

At the zygotene stage, the two axial elements are joined together by the formation of a short local SC. During pachytene, chromosomes undergo synapsis, wherein the lateral elements pair homologous chromosomes together through connections provided by the central elements. As mentioned earlier, the formation of the SC is facilitated by the action of ZMM proteins. Among the ZMMs, the binding of Zip3 to the axial associations recruits Zip2, and both Zip2 and Zip3 promote the binding of Zip1. Subsequently, Zip1 binding to the axial associations promotes the polymerization of the full-length SC along the entire length of the chromosomes by depositing Zip1 as a component of the transverse filament (Agarwal and Roeder, 2000). Following pachytene, the SC disassembles, and homologs separate. Despite the SC being discovered over 50 years ago, the complete understanding of its assembly and disassembly mechanisms is still a subject of ongoing research.

## 1.10 Recombination checkpoint

The orderly progression of events during the meiotic cell cycle is crucial for the accurate transmission of genetic information to offspring. Cell cycle checkpoints play a vital role in ensuring that late events are not initiated until earlier events have been successfully completed, thus maintaining the integrity of the process (Marston and Amon, 2004; Handel and Schimenti, 2010; Kerr et al., 2012). One such checkpoint, known as the recombination checkpoint or pachytene checkpoint, detects errors during meiotic prophase-I and eliminates

unresolved defects, leading to a delay or arrest in cell cycle progression (Perez-Hidalgo et al., 2003; Handel and Schimenti, 2010; Kerr et al., 2012).

The recombination checkpoint specifically monitors events related to meiotic chromosome metabolism, such as DNA double-strand break (DSB) repair and chromosome synapsis (Perez-Hidalgo et al., 2003). Errors in meiotic DSB repair can activate this checkpoint, causing an arrest at mid-pachytene of prophase-I in yeast and inducing apoptosis in mice (Perez-Hidalgo et al., 2003). The signal transduction pathway of the recombination checkpoint is initiated by sensor proteins that detect DNA damage, such as DSB ends or single-stranded DNAs. These sensor proteins generate a signal that is recognized and transmitted by sensor protein kinases, leading to the activation of checkpoint effector proteins that trigger various cellular responses to address the damage (Roeder and Bailis, 2000; Perez-Hidalgo et al., 2003; Marston and Amon, 2004).

The recombination checkpoint involves highly conserved protein kinases, including Tel1/ATM (ataxia-telangiectasia-mutated) and Mec1/ATR (ATM- and Rad3-related), serving as sensor kinases. Meiosis-specific chromosome axis proteins, such as Red1, Mek1, and Hop1, are also required for checkpoint activation. Additionally, the checkpoint clamp Rad17/Mec3/Ddc1 (known as the 9-1-1 complex in humans) and its loader Rad24-RFC play a role in checkpoint activation. Other factors responsible for checkpoint activation include Pch2 (a meiosis-specific AAA+ ATPase) and the histone methyltransferase enzyme Dot1 (Roeder and Bailis, 2000; Perez-Hidalgo et al., 2003; Longhese et al., 2009; Kerr et al., 2012).

The recombination checkpoint is triggered upon or shortly after DSB formation. In response to un-resected DSBs, Tel1 is recruited to the DNA damage site through its interaction with the MRX component Xrs2, leading to checkpoint activation (Usui et al., 2001; Clerici et al., 2001; Hochwagen and Amon, 2006; Longhese et al., 2009). Once the DSB termini undergo

resection, the signaling activity of Tel1 is attenuated, although the mechanism of Tel1 attenuation is not yet known. In the dmc1 mutant, where DSBs are hyper resected, resulting in the accumulation of single-stranded DNAs due to the failure to perform interhomolog repair, Mec1-dependent checkpoint activation occurs in response to these unresolved meiotic defects. This activation depends on the regulators Rad24, Rad17, Mec3, and Ddc1 (Lydall et al., 1996; Hong and Roeder, 2002; Longhese et al., 2009).

In response to these unresolved meiotic defects, the recombination checkpoint induces cell cycle arrest at mid-pachytene by preventing the activation of cyclin-dependent kinases (Cdks), which consist of a catalytic Cdc28 core protein and its regulator cyclins. Cdks are inhibited by Swe1 kinase, which phosphorylates Cdc28 on Tyr19, thereby inhibiting its catalytic activity (Leu and Roeder, 1999; Hochwagen and Amon, 2006). Swe1 activity is controlled by the checkpoint, and upon checkpoint activation, Swe1 becomes hyperphosphorylated, enhancing its function (Leu and Roeder, 1999).

Furthermore, upon checkpoint activation, the level of Sum1, a transcriptional repressor that down-regulates pachytene exit factors, remains high, while the transcription factor Ndt80, required for exiting mid-pachytene, is inhibited. This leads to the suppression of cyclin transcription, such as Clb1, and other key cell cycle regulators for pachytene, including Polo-like kinase Cdc5. Notably, the activation of Cdc5 leads to the resolution of double Holliday junctions (dHJs) and the disassembly of the synaptonemal complex (SC) (Page and Hawley, 2004; Sourirajan and Lichten, 2008; Kerr et al., 2012). Thus, the relative balance of Sum1 and Ndt80 levels determines whether cells exit mid-pachytene or remain arrested (Page and Hawley, 2004; Kerr et al., 2012).

### 1.11 Ndt80 function in meiosis I exit.

In the yeast Saccharomyces cerevisiae, the initiation of meiosis is triggered by nitrogen starvation, which leads to the activation of a transcriptional program involving approximately 1,600 yeast genes (Chu et al., 1998; Primig et al., 2000). Two key transcription factors, Ime1 and Ndt80, play crucial roles in this process. Ime1 is responsible for the expression of early genes, while Ndt80 controls the transcription of middle genes. Proper transcriptional regulation mediated by Ndt80 is essential for exiting the pachytene stage and ensuring successful meiotic recombination. The transcriptional regulation of Ndt80 occurs in a stepwise manner.

In vegetative cells, the transcriptional repressor Sum1 binds to the promoter region of the NDT80 gene, inhibiting its expression. Upon meiosis entry, Ime1 binds upstream of the Sum1 binding site, effectively removing the repressor through phosphorylation. This allows Ime1 to switch on the expression of Ndt80. However, for the exit from pachytene, Ndt80 must be expressed above a threshold level through a positive feedback mechanism. Ndt80 itself becomes phosphorylated and binds to the promoter of the NDT80 gene, triggering a positive feedback loop (Lo et al., 2012). The recombination checkpoint, however, inhibits this positive feedback (Tung et al., 2000).

Ndt80 is a critical regulator that promotes the transcription of approximately 200 genes involved in various processes associated with meiotic commitment and sporulation completion (Chu et al., 1998; Chu and Herskowitz, 1998; Xu et al., 1995). One of the targets of Ndt80 is the Polo-like kinase Cdc5, which is required for the resolution of double Holliday junctions (dHJs) to form crossovers (COs). Cdc5 also plays a role in promoting the co-orientation of sister chromatids by facilitating the association of the monopolin complex with kinetochores (Clyne et al., 2003; Lee and Amon, 2003; Shinohara et al., 2008).

Furthermore, Ndt80 is involved in the negative feedback regulation of double-strand break (DSB) formation (Carballo et al., 2013; Gray et al., 2013; Rockmill et al., 2013). This

negative regulation of DSBs by Ndt80 is inhibited by the Mec1/Tel1 pathway. Additionally, Ndt80 directly or indirectly contributes to the degradation of Rtt107, an essential protein for DSB initiation on the synaptonemal complex (SC) axial/lateral elements.

## 1.12 Auxin inducible degron

Auxin inducible degron system is a conditional depletion system. The Auxin Inducible Degron (AID) is a powerful tool used in molecular biology to control the targeted degradation of specific proteins in a rapid and reversible manner. AID technology is based on the plant hormone auxin, which triggers the degradation of a protein fused to the AID tag when exogenously applied to the cell or organism. (Nishimura 2009)

The AID tag consists of a small peptide sequence that is recognized by an E3 ubiquitin ligase called TIR1 (Transport Inhibitor Response 1) or its homologs. TIR1 binds to the AID tag in the presence of auxin, leading to the transfer of ubiquitin molecules to the tagged protein. This ubiquitination marks the protein for proteasomal degradation, resulting in its rapid elimination from the cell. AID system can be utilized to investigate the immediate consequences of protein depletion on meiotic recombination without permanently altering the genome. By expressing a protein of interest fused to the AID tag, the protein can be depleted in a time-controlled manner by adding auxin to the system

# Introduction Figures

## Intro Fig 1: Schematic representation for Meiosis

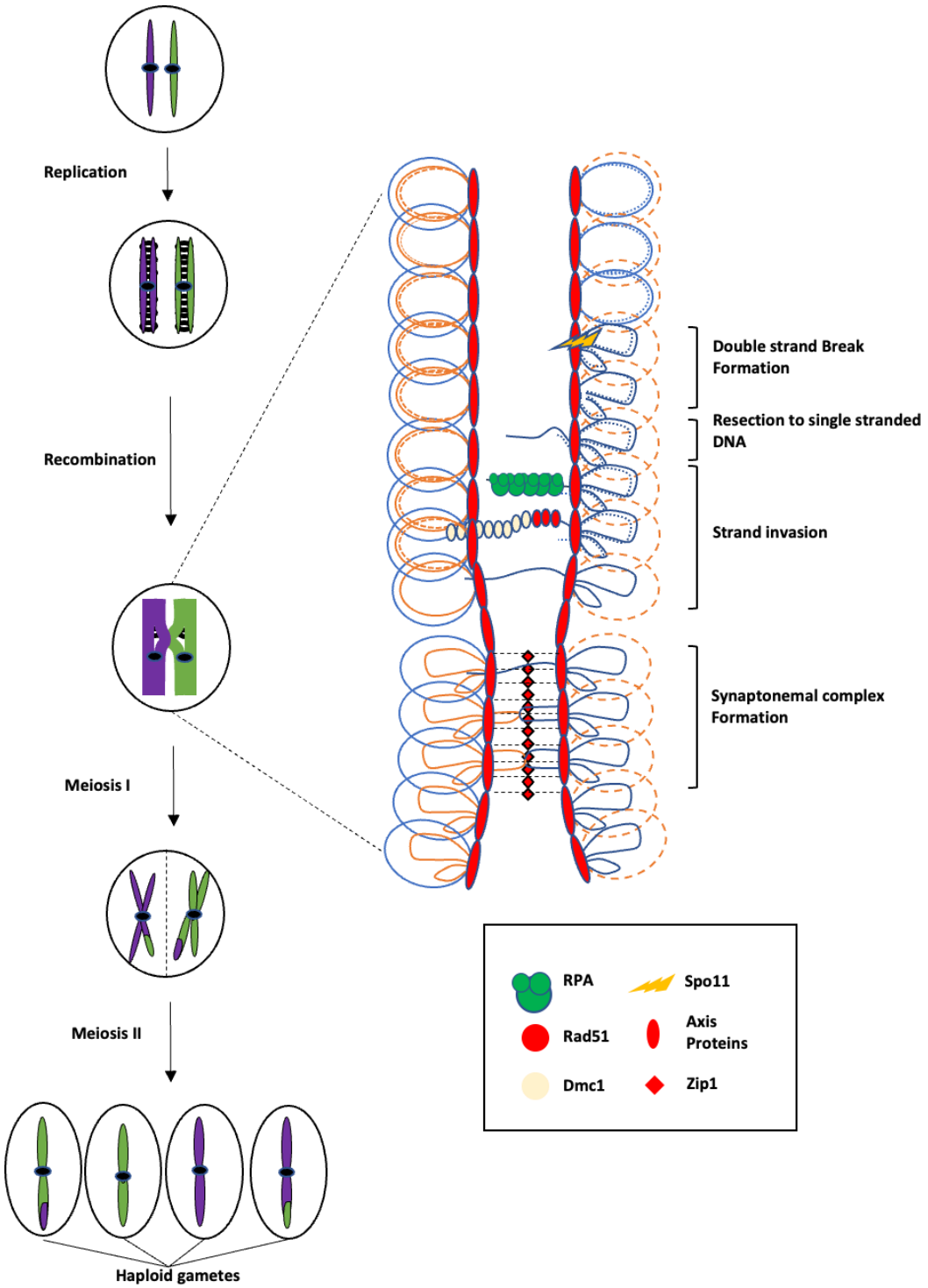

**Intro Fig 2: Role of RPA in replication and recombination**

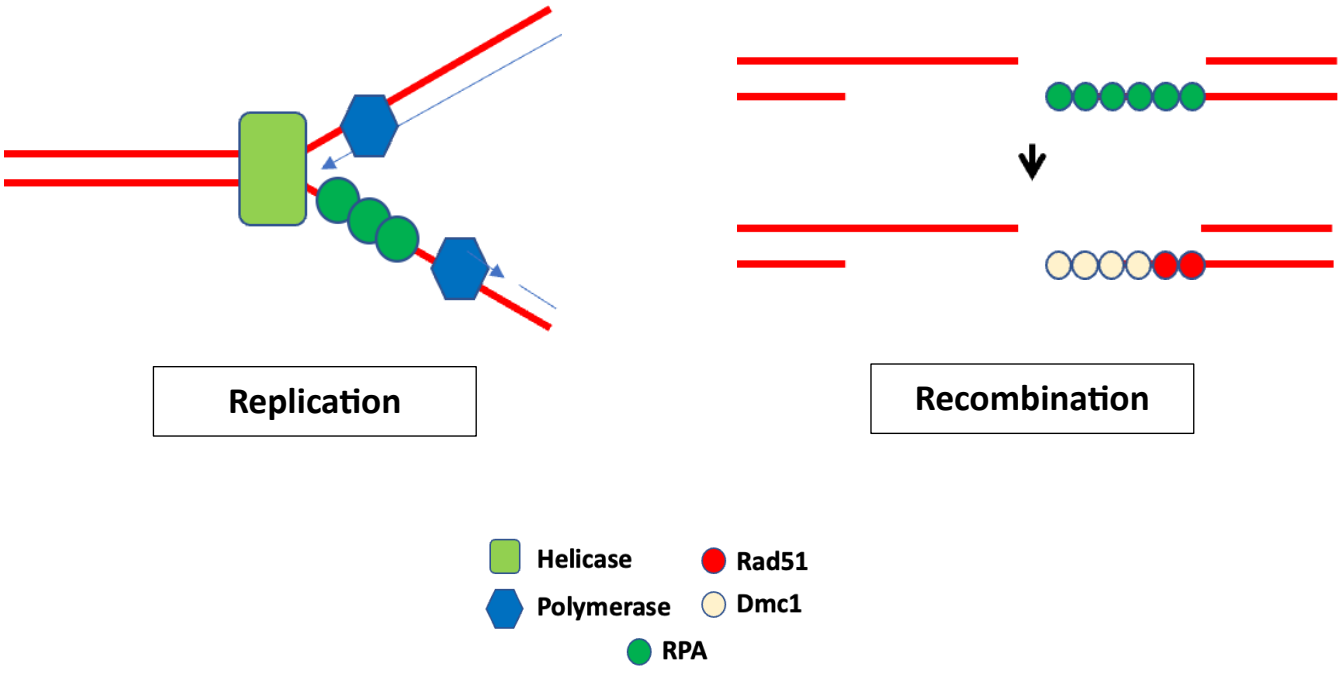

**Intro Fig 3: Meiotic Recombination in dmc1⊿**

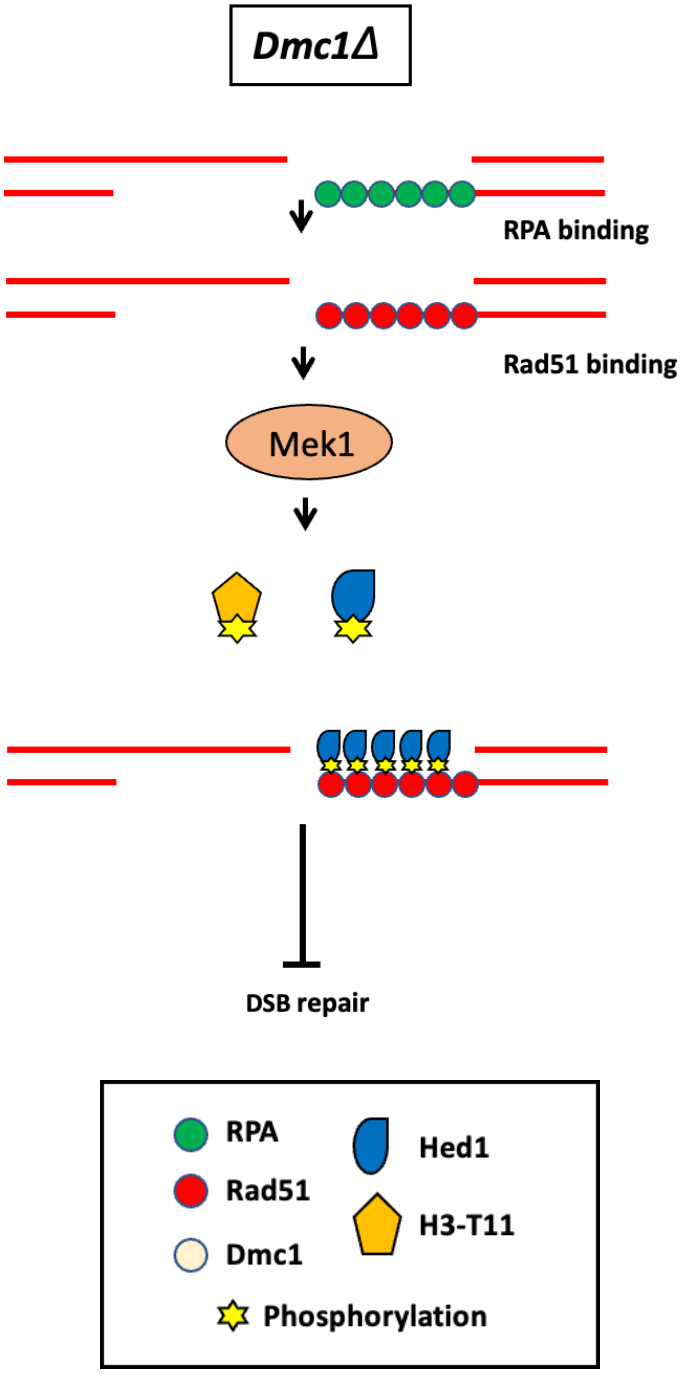

# Materials and Methods:

## 2.1 Strains and Plasmids:

All strains used in this study were originated from the S. cerevisiae SK1 diploid strain MSY832/833 (MATα/MATa, ho::LYS2/", ura3/", leu2::hisG/", trp1::hisG/", lys2 /") and NKY 1303/1543(MATα/MAT a, ho::LYS2, ura3, leu2::hisG, lys2, his4B-LEU2, arg4- Bgl). The genotypes of strains used in this study are mentioned in Table-1.

## 2.2 Yeast Transformation

Yeast cells were cultured overnight in 3 ml of YPAD liquid medium (containing 1% Bacto Yeast Extract, 2% Bacto Peptone, 2% Glucose, and 1% Adenine). The overnight culture was then diluted 1/200 in 50-100 ml of YPAD in a 500 ml flask and grown at 230 rpm at 30°C using a shaker for approximately 2.5 to 4 hours until the optical density (OD) reached 0.4 to 0.6. The cells were subsequently centrifuged for 2 minutes at 3000 rpm, suspended in 1 ml of LiAc/TE solution (containing 0.1 M LiAc and 1x TE buffer), and transferred to a new Eppendorf tube. After another centrifugation at 5000 rpm for 1 minute, the cells were resuspended in 200 µl of LiAc/TE solution. Carrier DNA (15 µl of 10 mg/ml deoxyribonucleic acid from salmon sperm) was added and mixed with the cells. Then, 50 µl of the cell suspension was transferred to new Eppendorf tubes. Plasmid or DNA fragments (1-10 µl) were added to each tube and thoroughly mixed. Subsequently, 350 µl of PEG/LiAc/TE solution (containing 40% PEG4000, 0.1 M LiAc, and 1x TE buffer) was added, and the cells were mixed by inverting the tubes. The tubes were incubated at 30°C

with rotation for 30 minutes, followed by a 15-minute incubation at 42°C on a heat block. After centrifugation at 5000 rpm for 1 minute, the supernatants were aspirated, and the cells were resuspended in 1 ml of YPAD. The cells were incubated for 3-6 hours or overnight and then centrifuged at 1500 rpm for 2 minutes. The resulting pellets were suspended in 100 µl of TE and spread onto selective medium plates.

### 2.3 Preparation of E. coli plasmid DNA (Miniprep)

The preparation of E. coli plasmid was conducted following the standard procedure in Shinohara Lab. A single colony of E. coli was inoculated into 1.5 – 2.0 ml of LB liquid media containing ampicillin (50µg/ml) and incubated overnight at 37°C. The following day, the overnight culture was transferred to Eppendorf tubes and centrifuged at 10,000 rpm for 1 minute. The supernatants were completely removed using a Pasteur pipette. The cells were then suspended in 100 µl of GTE buffer (50 mM Glucose, 25 mM Tris-HCL, pH 8.0, 10 mM EDTA) and vortexed until no pellet was observed. Next, 200 µl of Alkaline-SDS solution (0.2 N NaOH, 1% SDS) was added, and the samples were inverted five times and kept on ice for 5 minutes. To the samples, 150 µl of 7.5 M Ammonium acetate was added, and the samples were inverted again and kept on ice for at least 10 minutes. After centrifugation at 15,000 rpm for 10 minutes at 4°C, the supernatants were transferred to new Eppendorf tubes containing 400 µl of 2-propanol. The samples were inverted and centrifuged again at 15,000 rpm for 10 minutes at room temperature. They were then washed with 70% ethanol and subsequently with 100% ethanol. The samples were dried for 10 minutes using a centrifugal concentrator. Finally, 50-100 µl of a 10:1 TE solution (10 mM Tris-HCL, 1 mM EDTA) was added to dissolve the DNA.

## 2.4 Genomic DNA isolation

Overnight, yeast cells were cultured in 1-2 ml of YPAD liquid medium. The cells were then harvested in Eppendorf tubes. The resulting pellets were suspended in 500 µl of Zymolyase 100T and vortexed to ensure proper mixing. The tubes were incubated at 37°C for 30 minutes to facilitate cell lysis. To lyse the cells, 5 µl of Proteinase-K (10 mg/ml) and 100 µl of Lysing buffer (containing 0.25 M EDTA, 0.5 M Tris base, and 2.5% SDS) were added to the cell suspension. The mixture was thoroughly mixed and incubated at 65°C for 1 hour with intermittent mixing at least twice. Next, 100 µl of 5 M potassium acetate solution was added to the cell suspension, which was then shaken well and incubated on ice for 15 minutes. The cells were centrifuged at 15,000 rpm for 10 minutes, and the resulting supernatants were transferred to new Eppendorf tubes containing 500 µl of ice-cold 100% ethanol. The samples were gently inverted five times and centrifuged at 12,000 rpm for 30 seconds. The supernatant was discarded, and the pellets were washed with 1 ml of 70% ethanol. After removing the supernatant, the pellets were washed again with 1 ml of 100% ethanol. The samples were dried for 10 minutes using a centrifugal concentrator. The extracted DNA was suspended in 500 µl of 1x TE buffer, followed by treatment with RnaseA at a concentration of 10 µg/ml at room temperature for 30 minutes. Then, 500 µl of 2-propanol was added to the samples, which were gently inverted five times and centrifuged at 15,000 rpm. The supernatant was removed, and the pellets were washed with 70% ethanol, followed by washing with 100% ethanol. After drying the samples for 10 minutes, the DNA was suspended in 100-200 µl of 1x TE buffer.

## 2.5 Meiotic Time course

Yeast cells were streaked onto YPG plates (containing 1% Bacto Yeast Extract, 2% Bacto Peptone, and 2% Glycerol) from the freezing stock (-80°C). The plates were then incubated at 30°C for 12 hours. Afterward, the cells were streaked onto YPAD plates and incubated for an additional 2 days at 30°C to obtain individual colonies. A single diploid colony was selected and inoculated into 3 ml of liquid YPAD medium, which was then incubated overnight in a rotator at 30°C. Subsequently, 1 ml of the culture was added to 100 ml of SPS culture medium (containing 0.5% Bacto Yeast Extract, 1% Bacto Peptone, 0.5% Ammonium sulfate, 1% potassium acetate, 1.02% potassium hydrogen phthalate, and 0.17% Yeast Nitrogen Base). The SPS culture was incubated at 30°C with 230 rpm using a shaker (Innova 44) for 16-17 hours. On the following day, the SPS culture was centrifuged, and the resulting pellets were washed twice with sterilized distilled water. The yeast cells were then suspended in 100 ml of SPM medium (containing 1% Potassium acetate and 0.02% Raffinose). The cells were incubated at 30°C with 230 rpm to initiate meiosis, and samples were collected at specific time points for further analysis.

## 2.6 Western Blotting

A total of 5 ml of SPM culture was collected, and the cell precipitates were initially washed twice with 5 ml of cold water. Subsequently, the precipitates were suspended in 20% trichloroacetic acid (TCA) at a concentration of 10% (w/v). To disrupt the cells, a beads shocker (Yasui Kikai Co. Ltd., Osaka, Japan) was utilized with a 60-second on-60-second off cycle, repeated five times. The precipitated proteins were recovered by centrifugation and

then suspended in 200 µl of sodium dodecyl sulfate polyacrylamide gel electrophoresis (SDS-PAGE) sample buffer. The pH of the samples was adjusted to 8.8 using 1M Tris-HCl (pH 9.5), followed by boiling at 95°C for 5 minutes. After SDS-PAGE, the proteins were transferred from the gel to a Nylon membrane (Immobilon, MILLIPORE) using a semi-dry transfer unit (ATTO TRANSWESTERN). Antibodies against myc, Hop1, Cdc5, Rec8, H3pT11, Hed1 and Tubulin were used at dilutions of 1:1000.

### 2.7 Whole Cell immunostaining:

For immunostaining of whole cells, pre-coated poly L-lysine slides were used. To prepare the slide, 200 µl of a 1 mg/ml poly L-lysine solution was added to a glass slide (S2441 micro slide glass, super frost Matsunami glass, IND., LTD) and covered with a cover glass. The slide was then incubated at room temperature for 15 minutes. The cover glass was removed by immersing it in MilliQ water and washed with MilliQ water for 2 minutes twice. Subsequently, the slides were air-dried at room temperature for 15 minutes. 900 µl of meiotic SPM culture was collected, and 100 µl of 37% formaldehyde was added for cell fixation. The sample tube was centrifuged, and the pellet was suspended in 1 ml of ZK buffer. Then, 20 µl of 1 M DTT was added, and the mixture was left at room temperature for 2 minutes before centrifugation. The pellet was resuspended in 1 ml of ZK buffer, and 5 µl of 5 mg/ml Zymolyase 100T was added. The cells were mixed and incubated at 30°C for 1.5 hours. After collection, the cells were suspended in 1X PBS. Next, 200 µl of the cell suspension was added to the poly L-lysine-coated slides, covered with a coverslip, and incubated at room temperature for 15 minutes. The cells were fixed with cold 100% methanol for 6 minutes and 30 seconds, followed by cold 100% acetone for 2 minutes. After fixation, the slides were blocked with 5% BSA in 1X PBS for 15 minutes. The blocking buffer was drained, and 90 µl of PBS/BSA solution containing the primary antibody (diluted 1:1000) was added to the

slides, covered with a coverslip, and incubated at 4°C overnight. To remove the cover glass, the slides were immersed at a 45° angle in PBST washing buffer (1X PBS, 0.1% Tween 20) and washed twice for 10 minutes using a Coplin jar. Then, 90 µl of PBS/BSA solution with the secondary antibody (diluted 1:2000 of fluorochrome-conjugated IgG) was added to the slides, covered with a coverslip, and incubated at room temperature for 2 hours in a dark moist chamber. The coverslip was removed, and the slides were washed as described above, followed by a 2-minute wash with sterilized distilled water. The slides were air-dried for 10 minutes, and 10-15 µl of mounting medium VectaShield containing 0.2 µg/ml DAPI was added to the slides. The slides were covered with a cover glass, sealed with nail polish, and stored in the dark at 4°C until use. The sample slides were observed using an epi-fluorescence microscope.

## 2.8 DAPI analysis:

A total of 1 ml of meiotic cell culture was collected and centrifuged. The resulting pellets were fixed with 70% ethanol (v/v). After another round of centrifugation, 100 µl of 1 M sorbitol containing DAPI (1 mg/ml, diluted 1:1000) was added. Subsequently, 5 µl of the sample was spotted onto a slide (S2226 micro slide glass, Matsunami glass, IND., LTD), covered with a cover glass, and sealed with nail polish. The slide was observed using an epifluorescent microscope (ZIESS Axioplan2), and a total of 200 nuclei were counted for each sample.

## 2.9 Preparation of chromosomal spreads (Lipsol method)

To prepare chromosome spread slides, a volume of 5 ml of diploid yeast cells (SPM culture) was collected and centrifuged in a 15 ml screw cap tube. The pellet was then suspended in 1 ml of ZK buffer (25 mM Tris-Cl, pH 7.5, 0.8 M Potassium chloride), and 20 µl of 1 M DTT was added. After a 2-minute incubation at room temperature, the tube was centrifuged again. The resulting pellet was resuspended in 1 ml of ZK buffer, and 5 µl of 5 mg/ml Zymolyase 100T was added. The mixture was mixed and incubated at 30°C for 30 minutes. The samples were then centrifuged, washed with 1 ml of cold MES/Sorbitol solution (0.1 M MES, pH 6.5, 1 M Sorbitol, 0.5 mM MgCl2, 1 mM EDTA), centrifuged again to remove the supernatant, and suspended in 1 ml of cold MES/Sorbitol solution. The suspension was stored on ice until the Lipsol treatment.

For chromosome spreads, 20 µl of the cell suspension was spotted onto a clean glass slide (S2441 micro slide glass, Matsunami glass, IND., LTD) using a micropipette. Then, 40 µl of PFA/sucrose solution (3.5% PFA, 3.4% sucrose, freshly prepared) was added and gently swirled. At the same time, 80 µl of 1% Lipsol and 80 µl of PFA/sucrose solution were added and gently swirled to ensure even distribution throughout the slide without leaving any gaps. The slide was observed under a light microscope to confirm that about 80-90% of the cells had been lysed. Finally, the slide was dried overnight and stored at -20°C.

## 2.10 Immunostaining of chromosomal spreads:

The prepared chromosome spread slides were immersed in a Coplin jar containing 0.2% Photoflo (Photo-Flo 200 solution Kodak) for 2 minutes. Afterward, the slides were air

dried for 10 minutes and then blocked with TBS/BSA solution (1X TBS, 1% BSA) for 15 minutes. The blocking buffer was removed, and 90 µl of TBS/BSA solution containing the primary antibody (diluted 1:1000) was added to the slides. The slides were covered with a coverslip and incubated overnight at 4°C. The coverslip was removed by immersing the slides at a 45° angle in 1X TBS washing buffer. The slides were washed twice in 1X TBS using a Coplin jar for 10 minutes each. Next, 90 µl of TBS/BSA solution with the secondary antibody (diluted 1:2000) conjugated to a fluorochrome was added to the slides, covered with a coverslip, and incubated at room temperature for 2 hours in a dark moist chamber. After removing the coverslip, the slides were washed as described earlier, followed by a final wash with sterilized distilled water for 2 minutes. The slides were air dried for 10 minutes, and then 10-15 µl of Vecta shield mounting medium (Vector laboratories Inc., H-1000) containing 0.2 µg/ml DAPI was added to each slide. A coverslip was placed on top, sealed with nail polish, and the slides were stored in the dark at 4°C until use. The sample slides were observed using an epi-fluorescence microscope.

## 2.11 CHEF analysis:

DNA plugs were created using a mixture of 1.8% LMP (Low melting point) agarose (SeaPlaque○R Agarose, LONZA) in 125 mM EDTA (pH 7.5). The agarose gel was melted and incubated at 45-50°C until ready for use. A 15 ml SPM culture containing meiotic cells was collected, washed twice with 5 ml of 50 mM EDTA, and centrifuged. The cell pellets were resuspended in 500 µl of 50 mM EDTA and transferred to 1.5 ml Eppendorf tubes, followed by centrifugation. After removing the supernatant, the cell pellets were resuspended in 100 µl of 50 mM EDTA (pH 7.5). The cell suspension was incubated at 45°C for 30 seconds. Then, 200 µl of pre-warmed LMP/solution 1 mixture (0.83 ml of 1.8% LMP agarose

mix and 0.17 ml of Plug DNA solution 1) was added to the cell suspension, and the mixture was immediately vortexed. Next, 90 µl of the LMP/solution 1/cells mixture was transferred into a plug mold and allowed to solidify. The sample blocks were removed from the plug mold and transferred to a 15 ml tube containing 3 ml of Plug DNA solution 2. The samples were incubated at 37°C for one hour, and then Plug DNA solution 2 was replaced with 3 ml of Plug DNA solution 3. After overnight incubation at 50°C, Plug DNA solution 3 was removed and replaced with 3 ml of 50 mM EDTA (pH 7.5). The plugs were incubated on a rotator for 15 minutes (twice), and then 50 mM EDTA was removed and replaced with 4 ml of Plug DNA storage solution. The DNA plugs were stored at -20°C in Eppendorf tubes containing the DNA storage solution. A 150 ml gel containing 1.3% agarose (Pulse Field Certified Agarose, BIORAD) was prepared in a gel mold (20 cm x 14 cm) and equilibrated at 55°C for a few hours. One-third of the DNA plug was immersed in 1.5 ml of filter-sterilized 0.5 x TBE in an Eppendorf tube and rotated for 15 minutes. The DNA plugs were then placed in the wells of the agarose gel and sealed with a drop of 1.3% agarose gel. The gel was left to set for 30 minutes at room temperature. The CHEF apparatus (CHEF-DR III system, BIORAD) was assembled, and the gel was equilibrated in the buffer at 14°C for 15 minutes. Pulse-field gel electrophoresis was conducted with specific parameters (e.g., switch times, switch angles, voltage, run time) depending on the gel size. After electrophoresis, the gel was stained with ethidium bromide (EtBr), rinsed with water, and photographed.

## 2.12 FACS analysis:

1ml of SPM was collected and centrifuged at 3000 RPM for 3 mins. The pellet was then suspended in 70% ethanol. Fixed cells were centrifuged at 10000 RPM for 1 min at 4ºC and resuspended in 1ml of 50mM sodium citrate buffer then centrifuged at 10000 RPM for 1 min at 4ºC. The cells were resuspended in 0.5ml of sodium citrate buffer and sonicated for

20s at RT. Sonicated cells were incubated with 12.5ul of 10mg/mL RNAseA for 1h at 50ºC and in 25ul of 15mg/ml proteinase K for 1h at 50ºC. 0.5ml of 16ug/mL PI solution was added and incubated for 30min at RT in dark. The samples were then analyzed using Sony SA-3800 Spectral analyzer. Floreada.io was used for gating and plotting graphs.

### 2.13 Auxin induced degron.

To induce the degradation of Rfa1 during Auxin-Induced Degradation at 2h and 4 h after meiotic induction, 50 μM of CuSO4 (Wako, 033-04415) was introduced to induce the expression of pCUP1-OsTIR1, 30 minutes prior to the addition of auxin. The cell cultures were divided, and either 2 mM of auxin (3-indoleacetic acid, Wako 096-00182, dissolved in DMSO) or an equivalent amount of Dimethyl sulfoxide (DMSO; Dojindo, 349-01025) alone was added to the control at the specified times. A subsequent addition of 1 mM auxin was made after 2h from the initial addition and another 1mM dose of auxin was added after 2h from the addition of previous dose. A total of 4mM auxin was added.

# Results:

### 3.1 Rfa1 Depletion using AID:

RPA is a single-stranded DNA-binding protein highly conserved among eukaryotes. It was composed of three different subunits in budding yeast such as Rfa1, Rfa2 and Rfa3 (Wold MS 1997). It plays a significant role in both mitosis and meiosis in DNA replication, recombination, and DNA repair etc. Although RPA is known to protect ssDNA tails during meiosis, it remains unknown about the precise role of RPA in meiosis (Zou and Elledge, 2003). Since RPA is important during mitotic replication and repair (Ruff 2016), a deletion mutant of any subunit of RPA will be lethal to cells. So, to study the functions of RPA in meiosis a conditional mutant of RPA is required so that RPA can be depleted only at specific phases of meiosis.

In this study I have used the Auxin inducible degron that conditionally depleted RPA (Nishimura 2009). An AID tag is added to the target protein such as RFA1, which encodes the largest subunit of RPA. When Auxin is added, auxin bridges the binding between Tir1 and the AID-tagged protein. Tir1 is an adaptor protein for E3 ubiquitin ligase and leads to the degradation of the target protein through protein ubiquitylation. To promote meiosis-specific degradation, the Tir1 gene is placed under the control of the Cupper-inducible CUP1 promoter (Fig 2A).

I checked the expression level of Rfa1 protein in *RFA1-AID* cells by western blotting using anti-myc antibody and calculated the level of protein by quantifying the band intensity as tubulin as a control. After induction of meiosis, I added auxin to the Sporulation medium (SPM) at either 2 h or 4 h (Fig 1E, 6E). Without auxin addition, the level of Rfa1 was constant during meiosis. When auxin was added at 2 h, the Rfa1 level reduced to ~15% at 4 h relative to that at 2 h and maintained at a low level till later time points up to 10 h (Fig:1A, 1B). Under the condition, I concluded that auxin addition efficiently depletes Rfa1 in a

meiotic cell with *Rfa1-AID*. To check chromosome-bound RPA in *RFA1-AID* cells, immunostaining for Rfa2, the second subunit of RPA, was performed on chromosomal spreads. In wild-type, Rfa2 forms punctuate staining which was referred to as foci (Gasior SL 1997). In the wildtype cells, Rfa2 foci appeared at 2 h (~10%), peaked at 5 h (~76%) 6 h (~71%) and gradually decreased till later time points at 8 h (~27%) and 10 h (~9%) (Fig 1D). Rfa2 foci in the *RFA1-AID* mutant appear at 2 h, reach a plateau at about 5 h (~74%) or 6 h (~75%), and gradually decrease in the later time points (Fig 1D). When Auxin is added at 2 h, very few chromosomes bound Rfa2 foci were observed at 4 h (~0.5%), 6 h (~0.5%), and 8 h (~9%) (Fig: 1C, 1D).

When the auxin was added at 4 h, I found ~80% reduction of Rfa1 at 6 h compared to that at 4 h on western blots (Fig: 7A, 7B). And Rfa2 foci rapidly disappeared even at 5 h and 6 h (Fig 7C, 7D). This suggests that Auxin addition rapidly indued the depletion of the RPA complex from the meiotic chromosome. In the following section, I used these conditions to examine the effect of the depletion of Rfa1, thus RPA, in various meiotic events.

### 3.18 RPA is necessary for meiotic cell cycle progression:

To study the roles of RPA in the meiotic division, Rfa1 was depleted from 2 h after induction of synchronous meiosis by nitrogen starvation and samples were collected at the indicated times (Fig: 1E). The cells were fixed with 70% ethanol and stained with DAPI (4′,6-diamidino-2-phenylindole). Cells containing 1, 2, 3, or 4 DAPI bodies in a cell were examined under a microscope and the number of cells with each class was counted at each time point to analyze the meiotic division, thus meiosis I and II. In the absence of auxin, Rfa1-AID cells entered MI at 5 h and MII at 8 h (Fig). When auxin was added at 2 h, cells did not enter meiosis I or II. Only ~1% of cells had 2 or more DAPI bodies at 24 h compared

to ~99% in the cells without auxin addition (Fig: 2B). This suggests a meiotic arrest induced by the Rfa1 depletion.

It was shown that pre-meiotic DNA replication occurs around 1-3 h after the induction of meiosis (Sollier, 2004). To check whether these cells show pre-meiotic DNA replication, FACS analysis was performed. The cells without auxin treatment showed 2C content at 0 h, prior to meiosis. After the induction of meiosis, cells with more than 2C content started appearing at 2 h and most of the cells showed 4 C content by 4 h. The cells with between 2C to 4C contents are in the pre-meiotic S phase (Fig: 2C). After depletion of Rfa1 at 2 h, the cells showed only 2C peaks at any time points and contained very less 4C peak (Fig: 2D) till 8 h. This indicates a defect in the lack of pre-meiotic DNA replication when Rfa1 was depleted, consistent with a critical role of RPA in pre-meiotic DNA replication as shown in mitotic DNA replication (Wold MS 1997).

### 3.18 Depletion of Rfa1 before S-phase affects axis formation:

Axial element formation is a crucial step in meiotic prophase I. Axial elements are proteinaceous structures with an array of chromatin loops that run along the lengths of chromosomes serving as a chromosome scaffold for alignment and pairing of homologous chromosomes (Klein F 1999). Rec8, a subunit of cohesin for sister chromatid cohesion, is a component of the axial element. Immunostaining of Rec8 on chromosome spreads from a synchronous meiotic culture provides information about the efficient formation of the axis. Rec8 on chromosomal spreads localize into distinct patterns such as dotty, short linear, and long linear staining (Fig: 3A) (Challa K 2019).

In the *RFA1-AID* control cells without auxin addition, line-like Rec8 staining started appearing from 5 h (11.89%$\pm$9.37, n=3), peaked at 6 h (41.78%$\pm$5.38, n=3), and gradually decreased at 8 h (32.66%$\pm$20.13, n=3) and 10 h (31.14%$\pm$11.44, n=3) (Fig: 3B, 3C). When

auxin was added at 2 h for Rfa1-depletion before pre-meiotic S-phase, very few line-like Rec8 staining was seen even at 10 h (7.96%±2.05, n=3) (Fig: 3B, 3D). Most of the cells sustained with short line-like staining till 10 h (78.82%±6.33, n=3). This suggested a defect in axis formation when Rfa1 was depleted before the pre-meiotic S-phase.

### 3.4 Depletion of Rfa1 before S-phase affects elongation of Synaptonemal Complex:

To analyze the role of RPA in SC elongation, immunostaining for Zip1 was done in chromosomal spreads from a synchronous meiotic culture. Zip1 is a transverse element protein of synaptonemal complex (SC). Zip1 staining shows three distinct patterns of staining such as dot, short line-like, and long line-like staining which corresponds to leptotene, zygotene, and pachytene stages of prophase I (Fig: 4A) (Newnham L 2010). In *RFA1-AID* control cells without Auxin, short line-like staining appeared from 4 h (7.23%±7.10, n=3)) and increased at 5 h (23.16%±10.04, n=3) and 6 h (28.90%±9.61, n=3) (Fig 4C). When Rfa1 was depleted from 2 h, substantial number of cells with short line like staining appeared from 6 h (19.9%±14.05, n=3) which was ~2 h delayed from the control suggesting a delay in the transition timing from dot-like to short line-like staining when Rfa1 was depleted from 2 h. In the control cells, Zip1 forms long line-like staining from 5 h (8.46%±7.06, n=3), which peaked at 6 h (31.07%±4.49, n=3) and gradually decreased at 8 h (22.31%±14.63, n=3) and 10 h (18.59%±4.62, n=3) (Fig 4B, 4C). When Auxin was added at 2 h for Rfa1 depletion, proper elongation of SCs was not seen. Very few cells showed long line-like staining at 8 h (0.66%±1.15, n=3) and 10 h (8.32%±7.75, n=3) and most of the cells remained with short line-like staining till 10 h (51.87%±13.28, n=3) (Fig 4B, 4D). This suggests a delay in transition from leptotene to zygotene and a defect in SC elongation when Rfa1 was depleted prior to pre-meiotic S-phase.

### 3.5 Depletion of RPA before S-phase affects loading of Rad51 on ssDNA:

*Saccharomyces cerevisiae* Rad51 is a homolog of RecA present in both mitotic and meiotic cells. Dmc1 is another RecA homolog but is expressed specifically in meiotic cells. Previous studies show that Dmc1 and Rad51 are crucial in meiotic recombination by promoting strand invasion and strand exchange through binding to the ssDNA overhang of meiotic DSBs (Bishop DK 1994). Previous *in vitro* studies show that, during meiotic recombination, Rad51 displaces RPA with the help of mediator proteins such as Rad52 and binds to ssDNA as the filament, which is followed by the binding of Dmc1 (Gasior SL 1998).

I checked the role of RPA in Rad51 filament formation by depleting Rfa1 in *RFA1-AID* cells and performing immunostaining of chromosomal spreads with anti-Rad51. Rad51 shows punctuate staining that corresponds with a site of ongoing recombination (Bishop DK 1994). In the control (without auxin), Rad51 foci started appearing at 2 h (12.89% $\pm$1.18, n=3), reaches a plateau at 5 h (50.9%$\pm$1.6, n=3) and 6 h (55.6%$\pm$5.8, n=3) and then started declining from 8 h (44.8%$\pm$17.2, n=3) and 10 h (31.2%$\pm$9.7, n=3) (Fig 5A, 5B). When Auxin was added for Rfa1 depletion at 2 h, before pre-meiotic S-phase, very few cells at 2 h, 4 h and 6 h (3.92%$\pm$4.00, n=3) had Rad51 foci. (Fig 5A, 5B). An increase in Rad51 focus-positive cells was observed at 8 h (12.6%$\pm$4.53, n=3) and 10 h (50.7%$\pm$10.51, n=3). The number of foci observed in the Rad51 positive cells at 8 h (~11%, N=20, n=3) and 10 h (~19%, N=63, n=3) is relatively lower than the focus number observed in the control at 5 h (~31%, N=75, n=3) and 6 h (~32%, N=75, n=3)) (Fig 5C, 5D). This data suggests that RPA is required for the timely formation of Rad51 foci.

### 3.6 Depletion of RPA after S-phase accumulates fragmented chromosomes.

RPA is essential in the pre-meiotic S-phase. To know the role of events after pre-meiotic S-phase, I depleted Rfa1 after the pre-meiotic S-phase by adding auxin from 4 h into SPM with a synchronous meiotic culture. FACS analysis was performed to ensure that these cells have completed pre-meiotic S-phase replication. A shift in peaks from 2C to 4C was observed when the auxin was depleted at 4 h like the control, suggesting completion of pre-meiotic DNA replication under the condition (Fig: 6C, 6D).

Samples were collected for DAPI analysis. The cells with depleted Rfa1 showed abnormal chromosomal segregation and fragmented chromosomal DNA with more than 4 DAPI bodies in most cells after 8h. (Fig: 6B). This made it difficult to quantify the meiosis progression. To analyze meiotic progression precisely, whole-cell immunostaining with tubulin was performed to check the spindle morphology of these cells. Immunostaining of whole cells with anti-tubulin showed spindle morphology specific to meiosis I and II such as prophase I, metaphase I, anaphase I, metaphase II, anaphase II and post-meiosis (Pablo-Hernando, M and Arnaiz-Pita 2008). In *RFA1-AID* cells without the addition of auxin, metaphase I cells with short spindles appeared from 6 h (~23%), which is followed with the appearance of MII morphology with two spindles. Post-meiotic cells with 4 dapi bodies and no spindles appeared from 8 h (~62%) and gradually increased at 10 h (~84%) and 24 h (~99%) (Fig: 8B, 8C). When Rfa1 was depleted, like the control, metaphase I cells appeared at 6 h (~15%). Post-meiotic cells appeared at 8 h (~54%) and increased at 10 h (~74%) and 24 h (~96%) following a similar trend to the control with a slight delay in progression (Fig: 8B, 8D). This indicates the Rfa1 depletion after pre-meiotic DNA replication did not affect the progression of meiosis.

To know the role of Rfa1 in meiotic DSB formation and its repair, clamped

homogenous electric field (CHEF) gel electrophoresis analysis was performed to check the presence of fragmented chromosomal DNAs, which are induced by the meiotic DSBs. In CHEF analysis, the whole genome of budding yeast can be resolved, and the presence of fragmented chromosomes with DSBs shows a smeared band because of random fragmentation (Chu, G.1986) and these smear bands disappear at late meiosis I by DSB repair. In *RFA1-AID* cells without auxin, full-length chromosomes appeared at 0 h (Fig: 6A). A slight reduction in a level of full-length chromosomes and smeared bands were observed at 4 h and 5 h which corresponds to the formation of DSBs. At 6 h the smeared bands disappeared, and full-length chromosomes were observed till 8 h, 10 h and 24 h, which indicates DSB repair. When Rfa1 was depleted from 4 h after induction of meiosis, the number of full-length chromosomes gradually reduced at 5 h, and fragmented chromosomes with reduced sizes of 0.3-0.5 Mb appeared at 6 h and accumulated till 24 h. This indicates that Rfa1 is essential for DSB repair. Combined with normal meiotic progression under the condition, it suggests that Rfa1 plays a critical role in coupling the DSB repair with meiosis progression, thus recombination checkpoint (see below).

### 3.7 Depletion of RPA after S-phase shows defective axis formation.

I next checked the effect of Rfa1 depletion after pre-meiotic DNA replication on axis formation. As described above, in control cells (without the treatment of auxin), long line-like Rec8 staining started appearing from 5 h (~23%), peaked at 6 h (~56%), and gradually reduced at 8 h (~13%) and 10 h (Fig: 9B, 9C). When Rfa1 was depleted at 4h, after pre-meiotic DNA replication, most of cells showed short line-like staining and sustained till 10 h with reduced long line staining (9B, 9D). This indicates abnormal axis formation when RPA was depleted after the pre-meiotic S-phase.

### 3.8 Depletion of RPA after pre-meiotic S-phase shows defect in elongation of the synaptonemal complex:

To analyze the role of RPA in SC elongation, immunostaining for Zip1 was done in chromosomal spreads from a synchronous meiotic culture. (Fig: 10A). In the control cells, long linear Zip1 staining was observed from 5 h (~19%), peaked at 6 h (~50%) and gradually disappeared after 8 h (~10%) (Fig 10B, 10C). When Rfa1 was depleted at 4h, very little long linear zip1 staining was observed in the cells (Fig: 10B, 10D). This suggests that the depletion of Rfa1 after pre-meiotic S-phase affects SC elongation.

### 3.9 Role of RPA in the maintenance of Rad51 and Dmc1 ssDNA filament:

Depletion of RPA before pre-meiotic S-phase showed a defect in the formation of Rad51 foci, probably due to impaired DSB formation. To see the effect of Rfa1 depletion on the Rad51 and Dmc1 assembly, 43mmune-staining analysis of chromosome spreads was performed. In the control cells (without auxin treatment), Rad51 foci appeared from 4 h and then started to disappear from 6 h. By depleting Rfa1 after the pre-meiotic S-phase from 4 h, the maintenance and/or turnover of Rad51 and Dmc1 foci can be analyzed.

Immunostaining of chromosomal spreads were performed with anti-Rad51and anti-Dmc1. When Rfa1 was depleted at 4 h, an immediate reduction in Rad51 foci was observed at 5 h and little Rad51 foci were detected at 6 h. At later time points at 8 h and 10 h, an increase in Rad51 foci was observed in ~72% and ~68% of cells respectively. This suggests the role of RPA in the maintenance of Rad51 after loading onto ssDNA. (Fig: 11A, 11B).

Similarly, I checked the localization of Dmc1 on chromosomes by immunostaining meiotic chromosomal spreads with anti-Dmc1. As shown previously (Bishop DK 1994), under the control, Dmc1 formed punctuate foci from 4h, peaked at 6h and reduced at 8h and 10h. When Rfa1 was depleted, the number of Dmc1-positive nuclei reduced at 5 h and 6 h compared to that at 4 h. An increase in the number of foci to ~29 % and ~70% was observed at 8 h and 10 h respectively (Fig: 11C, 11D). This suggests that Rfa1 plays a critical role in the maintenance of Dmc1 assembly on meiotic chromosomes as Rad51 assembly.

**3.10 RPA is necessary for meiotic DSB formation:**

RPA depletion before pre-meiotic S-phase showed the inefficient formation of meiotic DSBs. To rule out the rapid turnover of DSBs under the condition, I used *dmc1Δ*, which stalls meiotic DSB repair without any turnover (Bishop DK 1992). CHEF analysis was performed by using a *dmc1Δ-RFA1-AID* to analyze chromosomal breaks. Without auxin treatment, in *dmc1Δ-Rfa1-AID* cells, full-length chromosomes can be seen till 3 h. At 3 h, smeared bands that correspond to fragmented chromosomes started to appear with a reduction in full-length chromosomes. In further incubation with SPM, fragmented chromosomes accumulated till 24 h in *dmc1Δ-Rfa1-AID* cells. When Rfa1 was depleted from 2 h, the accumulation of DSBs were relatively less compared to the control. At 4 h, some smeared bands were detected with clear full-length chromosomes. These full-length chromosomes were observed till later time points such as at 9 h. At 24 h, full-length chromosome bands disappeared. These indicate reduced and delayed DSB formation, suggesting that Rfa1 promotes efficient DSB formation, rather than rapid turnover (Fig: 12A).

### 3.11 Meiotic arrest in dmc1*Δ* is rescued by Rfa1 depletion:

In previous studies, it was reported that the absence of Dmc1 in budding yeast causes the accumulation of DSBs, which induced an arrest in mid-prophase I (Bishop DK 1992) This arrest induced by meiotic DSBs is called the recombination checkpoint or pachytene checkpoint (Chu S 1998). This arrest activates Mec1/ATR kinase, which in turn phosphorylates various proteins including an axis protein, Hop1. Phosphorylation of Hop1 by Mec1 kinase was indeed a response to double stranded breaks in cells (Roeder, Bailis 2000). Mek1/Mre4 is a meiosis-specific kinase which gets activated by phosphorylated Hop1 (Carballo JA 2008). Mek1/Mre4 mediate the phosphorylation of the downstream target, Ndt80. The Ndt80-phosphorylation inactivates Ndt80, which is the transcriptional activator essential for the exit of mid-prophase I (pachytene stage). Previous studies (Zou L 2003) suggest a critical role of RPA for the ATR activation, but this idea has not experimentally address. Since the robust arrest by Dmc1 deletion provides a system to confirm the idea, I depleted Rfa1, RPA, after DSB formation in the *dmc1Δ* strain to address whether Rfa1 depletion affects recombination checkpoint activation.

Rfa1 was depleted at 4 h after induction of meiosis is *RFA1-AID-dmc1Δ.* Samples were collected and fixed using 70% ethanol and DAPI analysis was performed in these samples. In the *dmc1Δ-Rfa1-AID* strain, most of the cells prevailed with a single nucleus in a cell, confirming no nuclear division due to prophase I arrest. However, nuclear division was observed with cells having more 4 or more DAPI bodies when Rfa1 was depleted suggesting checkpoint alleviation (Fig: 13F).

Furthermore, to confirm the meiotic arrest bypass, spindle elongation was analyzed in these cells by whole cell staining as shown above, when Rfa1 was depleted. Rfa1 depletion from 2 h, i.e., before pre-meiotic S-phase showed very less spindle elongation. Almost all the

cells retained spindle morphology seen in prophase I till 24 h (Fig: 14). This is a bit surprising since it suggests that meiosis arrest induced by Rfa1-depletion prior to pre-meiotic DNA replication is independent of Rfa1 function.

However, Rfa1 depletion from 4 h showed spindle elongation (Fig: 15A). At 6 h, ~18% of cells were in metaphase I with short spindles and ~25% of cells in anaphase I with long spindles whereas in control without auxin addition, ~99% of cells remained in prophase I with no spindle elongation. At 8 h, ~40% of Rfa1-depleted cells started progressing to post-meiosis II which was increased to ~90% at 10 h. On the other hand, more than 99% of control cells sustained in prophase I till 24 h (Fig: 15B, 15C, 15D). This confirms the role of Rfa1 in the maintenance of recombination checkpoint.

**3.12 RPA depletion does not affect DSB accumulation in *dmc1Δ*:**

To check the DSB status of *dmc1* deletion cells when Rfa1 was depleted at 4 h, samples were collected for CHEF analysis. Due to the defect in DSB repair in the absence of Dmc1, *dmc1Δ-RFA1-AID* cells accumulated DSBs in the presence of auxin (Bishop DK 1992). In *dmc1Δ-Rfa1-AID* cells, bands of full-length chromosomes were observed till 3 h. After 3 h there was a reduction in bands of full-length chromosomes and an accumulation of smeared bands which corresponds to DSBs from 4 h till 24 h. When Rfa1 was depleted, DSBs started appearing from 3 h or 4 h, and accumulated till 24 h (Fig: 12B) even when meiotic division was observed as mentioned above.

Rad51-focus formation was analyzed by immunostaining chromosomal spreads from *dmc1Δ-RFA1-AID* cells. Rad51 forms a punctuate foci in the nucleus which refers to a

recombination event (Bishop DK 1994). In *dmc1-Rfa1-AID* cells without auxin, Rad51 foci started appearing from 4 h (~83%) and persisted with a similar number of Rad51-positive cells at 5 h (~91%), 6 h (~91%), 8 h (~91%) and 10 h (~91%) (Fig:16A, 16B). When auxin was added at 4 h, the percentage of Rad51-focus positive cells reduced drastically to ~4% at 5 h. The number of Rad51-focus positive cells didn't exceed ~10% till 10 h when Rfa1 was depleted (Fig:16A, 16B). The Focus number per nucleus was counted in spreads having at least 5 foci. In the control, an average of ~40 foci per nuclei was observed at 6 h (Fig: 16C). When Rfa1 was depleted from 4 h, almost no nuclei had more than 5 foci at 6 h (Fig: 16D). This suggests that Rfa1 is critical for the maintenance of Rad51 foci on meiotic chromosomes.

**3.13 Defect in recombination checkpoint when Rfa1 was depleted:**

To further study the role of RPA in the recombination checkpoint, I checked the expression of some of the key regulators in this pathway. In *dmc1Δ* DSB accumulation prolonged Mek1 activation (Wan L 2004). This was demonstrated by western blotting for histone H3 (H3)-T11 phosphorylation (H3-pT11) which is a target of Mek1. In *dmc1Δ-RFA1-AID* cells without auxin, H3-pT11 bands appear at 4 h and persisted till 10h. When Rfa1 was depleted from 2 h, very little H3-pT11 bands were seen till 10 h which suggests weak activation of Mek1. (Fig: 17A). When Rfa1 was depleted from 4 h, H3-T11 phosphorylation disappeared from 5 h, suggesting inactivation of Mek1 (Fig: 13A).

Exit from prophase was also confirmed by western blot with Cdc5, whose expression depends on Ndt80 activation (Fig: 13A). Cdc5 expression was not observed in the control of the absence of Dmc1, suggesting prophase arrest. When Rfa1 was depleted from 4 h, cells

showed expression of Cdc5 from 5 h which intensified at 6 h and later reduced at 8 h and 10 h.

Further in *dmc1Δ-RFA1-AID* cells, slow migrating Hop1 bands which correspond with the phosphorylation were seen from 4 h till 10 h (Fig: 16A). When Rfa1 was depleted from 2 h, very little slow migrating bands of Hop1 were observed, consistent with little DSB formation under the condition. Hop1 phosphorylation was very less compared to the control till 10 h (Fig: 17A). When Rfa1 was depleted from 4 h a gradual reduction in the slow migrating bands of Hop1 can be observed from 6 h. This was confirmed by checking the localization of Hop1 on chromosomes. In *dmc1Δ-RFA1-AID* control cells, Hop1-positive cells appeared at 2 h and persisted with ~93% in further incubation. When Rfa1 was depleted from 4 h, a gradual reduction in Hop1-positive cells was observed from 5 h (~83%) and continued decreasing at 6 h (~38%), 8 h (~18%), and 10 h (~17%) (Fig: 18B, 18C). . These results suggest checkpoint alleviation.

### 3.14 Bypass of *dmc1Δ* arrest is dependent on Ndt80:

From previous results, pachytene exit of *dmc1* cells was observed when RPA was depleted. To further analyze the role of Ndt80 in this checkpoint bypass, a *ndt80Δ* mutation was introduced into *Rfa1-AID-dmc1Δ.* After induction of meiosis, RPA was depleted from 4 h in *Rfa1-AID, dmc1Δ, ndt80Δ* cells. The depletion of Rfa1 was confirmed by western blotting with Rfa1-myc (Fig: 20A). Immunostaining of chromosomal spreads with Rfa2 showed a big reduction in Rfa2 foci after 4 h which confirms depletion of RPA in these cells

(Fig:27B, 27C). Whole-cell staining of tubulin showed that *RFA1-AID-dmc1Δ-ndt80Δ* cells both without and with auxin treatment showed no spindle elongation; ~100% of *ndt80Δ-Rfa1-AID-dmc1Δ* cells remained in prophase I at 24 h and ~97% of cells remained in prophase I when Rfa1 was depleted (Fig: 19B, 19C). Further expression of Hop1 was checked by western blotting with anti-Hop1 Hop1 bands started appearing from 2 h and slower migrating Hop1 bands which corresponds to phosphorylated Hop1 started appearing from 4 h in both control and Rfa1 depleted cells (Fig: 20A). These phosphorylated bands were seen till 10 h in both control and Rfa1 depleted cells. So, to check localization of Hop1 on chromosomes, immunostaining with Hop1 was performed on chromosomal spreads. No reduction in Hop1 foci was observed throughout the time course. Both control and Rfa1 depleted cells showed similar Hop1 kinetics (Fig 21A, 21B). These results suggest that the checkpoint alleviation in *dmc1Δ* cells when Rfa1 was depleted was still dependent on Ndt80.

**3.15 Checkpoint recovery in *dmc1Δ* meiosis:**

To analyze the extent of this checkpoint alleviation in *dmc1Δ* deletion cells, Rfa1 was depleted after 24 h of induction of meiosis (Fig: 17C). To check progression of meiosis, samples were collected for western blotting. Expression of Cdc5 was checked. In *dmc1Δ-RFA1-AID* cells without auxin, Cdc5 bands were not seen till 30 h. In Rfa1 depleted cells, Cdc5 bands appeared at 26 h and persisted till 30 h (Fig: 22A). Expression of Hop1 was also analyzed using western blotting with anti-Hop1. In *dmc1Δ-RFA1-AID* cells, phosphorylated Hop1 bands can be seen from 24 h till 30 h without any reduction in the slow migrating bands suggesting persistent phosphorylation of Hop1 till 30 h. When Rfa1 was depleted, Hop1

phosphorylation bands started to disappear from 26 h and gradually reduced till 30 h (Fig: 17A).

DSB status was checked when Rfa1 was depleted after 24 h in *dmc1Δ-RFA1-AID* cells. Both control and Rfa1 depleted samples accumulated DSBs from 24 h till 30 h similar to previous result where meiotic arrest in *dmc1Δ* was bypassed despite the accumulation of DSBs (Fig: 22B).

### 3.16 Role of RPA in zip1Δ induced meiotic progression delay:

The existence and significance of a synapsis checkpoint in meiosis remains a topic of debate. While some studies suggest that a checkpoint monitors proper synapsis between homologous chromosomes, others propose that it is a consequence of defects in meiotic recombination or chromosome structure rather than an independent checkpoint (Borner GV 2004). I analyzed the role of RPA in *zip1Δ* induced meiotic progression delay by using an *RFA1-AID-zip1Δ* strain.

RPA was depleted at 4h in *RFA1-AID-zip1Δ* strain after inducing synchronous meiosis. Depletion of RPA was confirmed using western blot with Rfa1-myc where a decrease in expression of Rfa1 was observed from 5 h when auxin was added at 4 h (Fig: 23A). Further immunostaining with Rfa2 a subunit of RPA showed reduction in chromosome bound RPA at 5 h (~0%) which was maintained at 6 h (~0.5%), 8 h (~3%) and 10 h (~8%) when Rfa1 was depleted. In the control at 5 h ~85% of Rfa2 was observed and ~86%, ~16% and ~12% of chromosome bound Rfa2 was observed at 6 h, 8 h and 10 h respectively (Fig: 25C, 25D).

Tubulin whole cell staining was performed on *RFA1-AID-zip1Δ* cells to analyze meiotic progression. In the control without addition of auxin, metaphase I cells were first observed at 8 h (~14%) and later completed meiosis by accumulating ~99% of post meiotic cells in 24 h (Fig:24B, 24C). When Rfa1 was depleted, an earlier progression through meiosis was observed. Metaphase I cell started appearing from 6 h (~24%) (Fig: 24B, 24D). Cdc5 expression was checked by western blotting with anti-Cdc5 which also supports the previous result where Cdc5 bands appeared from 5 h when Rfa1 was depleted. In control, Cdc5 expression was observed from 8 h (Fig: 23A).

Hop1 localization was observed on chromosomal spreads in *RFA1-AID-zip1Δ* cells. In the control the number of Hop1 positive cells started appearing from 2 h (~51%), reached a plateau at 4 h (~97%) and maintained at 5 h (~92%) and 6 h (~91%), and started reducing at 8 h (~59%) and 10 h (~20%) (Fig: 26B, 26C). When Rfa1 was depleted at 4 h number of Hop1 positive cells reduced to ~56% at 5 h. Hop1 positive cells further reduced at 6 h (39%), 8 h (~17%) and 10 h (~20%) (Fig: 26B, 26D). Western blotting with anti-Hop1 showed appearance of Hop1 bands from 2 h. Phospho-Hop1 bands started appearing from 4 h and sustained till 8 h and disappeared at 10 h in the control. When Rfa1 was depleted at 4 h, reduction in slower migrating Hop1 phosphorylated bands from 8h was observed which was earlier than the control (Fig: 26A).

H3-T11 phosphorylation was checked which was a target of Mek1 which gets phosphorylated by Hop1. In the control, H3-pT11 bands started appearing from 4 h and showed persistent expression till 8 h and disappeared at 10 h. When Rfa1 was depleted at 4 h, H3-pT11 bands started disappearing from 5 h suggesting earlier inactivation of Mek1 in Rfa1 depleted cells (Fig: 23A).

Immunostaining for Rad51 was performed in *RFA1-AID-zip1Δ* cells. When Rfa1 was depleted at 4 h, the amount of chromosome bound Rad51 reduced to ~2% at 5 h when compared to ~86% at 5 h in the control. Rad51 localization on chromosomes maintained at a minimal level at 6 h (~6%), 8 h (~9%) and 10 h (~7%) (Fig: 25A, 25B).

**3.17 Depletion of RPA dissociates Pch2 from chromosomes.**

Pch2 is a meiosis specific AAA+ ATPase which was found to be involved in checkpoint during aberrant meiosis. It plays a regulatory role in recombination checkpoint in response to unprocessed DSBs through interaction with Xrs2 which leads to activation of Hop1 as well as other downstream kinases such as Mek1 (Kerr 2012) (Roeder and Bailis 2000) (Usui 2001). It was also known that Pch2 is required for timely removal of Hop1 from chromosomes (Borner 2008).

To check the effect of RPA depletion in localization of Pch2, immunostaining was performed on chromosomal spreads from *dmc1Δ-RFA1-AID* and *zip1Δ-RFA1-AID* cells. Previous studies on Pch2 shows that Pch2 localizes in the nucleus with small amounts of Pch2 detected in a punctuate pattern on chromosomes (Segundo S 1999). In *dmc1-RFA1-AID* cells Pch2 foci started appearing from 2 h (~9%), reached a plateau at 5 h (~93%), 6 h (~88%), 8 h (~91%) and 10 h (~88%). When RPA was depleted in these cells, Pch2 positive cells started reducing from 6 h (~21%) to 10 h (~3%) (Fig: 27A, 27B).

Similarly, in *zip1-RFA1-AID* cells Pch2 positive cells appeared from 2 h (~8 h) and peaked at 6 h (~93%) and gradually decreased at 8 h (~74%) and 10 h (~22%). When RPA was depleted, number of Pch2 positive cells started reducing from 5 h (~62%) and continued decreasing at 6 h (~7%) much earlier than the control (Fig: 27C, 27D).

### 3.18 Depletion of Rfa1 does not affect the checkpoint delay caused by Rad50S:

Rad50 is a component of the MRX complex which plays a crucial role in removal of Spo11 from the double stranded breaks (Manfrini 2010). This is followed by resection of the double stranded DNA break into a 3' ssDNA overhang which is a substrate for RPA. Rad50S is a separation of function mutant of Rad50 which shows a defect in removal of Spo11 thus leaving Spo11 covalently attached to the double stranded break (Usui 2006).

Rfa1 was depleted at 4 h in *RFA1-AID-rad50S* strain. The depletion was confirmed by western blotting with anti-myc-Rfa1 where a reduction in Rfa1-myc was observed from 5 h when auxin was added (Fig: 28A). Further immunostaining with Rfa2, a subunit of RPA was performed. Both the control and Rfa1 depleted cells showed similar kinetics for chromosome bound Rfa2 with very few positive cells (Fig: 28B, 28C) since rad50S cells does not generate ssDNAs.

To check meiotic progression in cells, samples were collected for whole cell immunostaining and was stained with tubulin to analyze morphology of spindles. In *rad50S-RFA1-AID* cells, metaphase I cells started appearing at 6 h (~3%) and progressed through meiosis II where ~42% of cells completed meiosis II at 24 h. When Rfa1 was depleted, like the control, metaphase I cells started appearing at 6 h (~7%) and progressed through meiosis II with ~32% cells completing meiosis II at 24 h (Fig: 29C, 29D).

Western blotting with anti-Hop1 showed no difference in expression of Hop1 between the control and the cells with auxin. Very less expression of H3-pT11 was observed in the control and in the cells with depleted Rfa1. (Fig 28A)

Further localization of Hop1 was checked in *rad50S-RFA1-AID* cells, Hop1 positive cells started appearing from 4 h (~32%) and gradually increased at 5 h (~47%), 6 h (~67%), 8 h (~80%) and 10 h (~77%). When Rfa1 was depleted a similar trend in Hop1 kinetics was observed. Hop1 positive cells started appearing at 4 h (~32%) and gradually increased at 5 h (~47), 6 h (~53%), 8 h (~86%) and 10 h (~79%) (Fig: 30A, 30B). As expected, since rad50S doesn't form ssDNAs which is a substrate for RPA, depletion of RPA had almost no effect in meiotic progression delay caused by rad50S.

# Discussion

## 4.1 Role of RPA in budding yeast meiosis

Replication Protein A (RPA) stands out as a pivotal eukaryotic single-stranded DNA (ssDNA) binding protein, yet its comprehensive role in meiotic recombination remains underexplored. This study elucidates the diverse functions of RPA in crucial regulatory processes, including axis formation and maintenance, synaptonemal complex elongation, and Rad51 nucleoprotein filament dynamics during meiosis.

This study demonstrated that depletion of RPA disrupts the aforementioned processes, underscoring its indispensable role in orchestrating key events in meiotic recombination. Notably, the absence of RPA impairs axis formation, compromises synaptonemal complex elongation, and hampers the formation and maintenance of Rad51 nucleoprotein filaments, thereby emphasizing the multifaceted involvement of RPA in these critical regulatory pathways.

Interestingly, depleting Rfa1, a subunit of RPA, after the initiation of meiosis at 4 hours did not disturb cell division or meiotic progression. This intriguing observation highlights a crucial aspect of RPA function - its necessity for the activation of a checkpoint mechanism. Our results provide compelling evidence that RPA serves as a sensor for double-stranded DNA breaks, triggering a checkpoint mechanism that effectively halts meiotic progression, ensuring the fidelity of the recombination process.

## 4.2 RPA was a positive regulator for Rad51 ssDNA filament assembly.

During homologous recombination, RPA indeed plays a crucial role in the formation of the Rad51 single-stranded DNA (ssDNA) filament. RPA binds tightly and specifically to

exposed single-stranded DNA regions at the site of DNA damage, such as those generated during the processing of DNA double-strand breaks (DSBs). From previous studies the displacement of RPA from ssDNA is a critical step for the assembly of the Rad51 filament. Several factors, including Rad52 and Rad55-Rad57 complexes, assist in removing RPA and promoting Rad51 filament formation. This suggested an inhibitory effect of RPA on Rad51 ssDNA filament formation. However, from this study it was observed that when RPA was depleted, the maintenance of Rad51 on ssDNA was highly inefficient. The presence of RPA on the ssDNA creates a platform for the recruitment and loading of Rad51 recombinase and it was also observed when RPA was depleted after Rad51 assembly, Rad51 was removed from chromosomes suggesting a role in maintenance of Rad51 ssDNA filament. This can be attributed to spontaneous dissociation Rad51 filaments where Rad51 can spontaneously dissociate from ssDNA over time, especially in the absence of stabilizing factors like RPA. The dynamic nature of the Rad51 filament may lead to its disassembly without active regulation. Secondly, in the absence of RPA, certain DNA helicases such as Srs2 could also play a role in dismantling Rad51 filaments from ssDNA. It's essential to note that the absence of RPA can significantly impact the dynamics of Rad51 filament formation and stability, leading to altered behavior during meiosis. The specific mechanism by which Rad51 dissociates from ssDNA in the absence of RPA would require further investigation and experimentation to be fully elucidated.

**4.3 RPA plays a role in recombination checkpoint.**

Mec1/Tel1 checkpoint pathway, is a crucial DNA damage response mechanism in eukaryotic cells. Mec1 and Tel1 are kinases that function as transducers of DNA damage signals, initiating a signaling cascade to promote cell cycle arrest and DNA repair upon

encountering DNA damage, particularly during replication stress and during the cell cycle phases when DNA is most vulnerable, such as S phase and meiosis.

In the Mec1/Tel1 checkpoint pathway, RPA acts as a sensor of DNA damage. RPA binds to single-stranded DNA (ssDNA) regions that are exposed upon DSB formation. This binding is facilitated by the affinity of RPA for ssDNA, making it an essential component for detecting and stabilizing these damaged DNA structures. Although there are previous invitro studies which has discussed the interaction between Ddc2 and RPA and thus in activation of Mec1, there are no in vivo evidence suggesting this role of RPA in DDR.

Upon binding to ssDNA, RPA promotes the recruitment and activation of Mec1 kinase. This kinase is then able to phosphorylate various downstream targets involved in the recombination checkpoint such as meiosis specific kinase Mek1, Hop1. One of the critical targets of Mec1 and Tel1 kinases is the effector kinase Rad53 (in budding yeast) or Chk2 (in mammals), which plays a central role in propagating the DNA damage signal and enforcing cell cycle arrest.

In dmc1 cells when Rfa1 was depleted, it induced pachytene exit in cells thus bypassing the checkpoint. Mek1 was inactivated in Rfa1 depleted cells which resulted in dephosphorylation of Hop1 and expression of Cdc5. Interestingly CHEF analysis revealed that this pachytene exit does not involve DSB repair. DSB accumulation was still observed in Rfa1 depleted dmc1 cells.

RPA plays a critical role as a DNA damage sensor in the Mec1/Tel1 checkpoint pathway. By binding to ssDNA at sites of DNA damage, RPA facilitates the activation of Mec1 and Tel1 kinases, leading to the initiation of a signaling cascade that triggers cell cycle arrest and promotes DNA repair to maintain genome integrity and cell survival.

**4.4 RPA plays a role in synapsis checkpoint.**

The synapsis checkpoint is an important regulatory mechanism during meiosis that ensures proper chromosome pairing and synapsis before proceeding to the next stages of meiotic recombination. RPA (Replication Protein A) plays a critical role in the synapsis checkpoint by sensing the presence of unpaired or partially synapsed chromosomes and activating the checkpoint response to delay cell cycle progression until proper synapsis is achieved.

During meiosis, RPA binds to single-stranded DNA (ssDNA) regions, and its presence is essential for the recruitment and stabilization of the recombinase protein Rad51. Rad51 forms nucleoprotein filaments on ssDNA, facilitating the homology search and strand exchange required for homologous recombination and synapsis. Proper synapsis involves the formation of the synaptonemal complex (SC), a protein structure that physically connects homologous chromosomes.

From this study it was observed that the synapsis checkpoint relies on RPA's ability to recognize and bind to ssDNA gaps or unpaired regions in unsynapsed chromosomes. This was demonstrated using *RFA1-AID-zip1* strain where the delay in meiotic progression due to abnormal SC formation was abolished. This was done by a similar mechanism to the recombination checkpoint which involves in inactivation of Mek1 and its downstream targets such as Hop1 and expression of Cdc5. This can suggest when synapsis is incomplete or delayed, RPA continues to coat these unpaired regions, preventing the formation of a fully functional SC. This prolonged association of RPA with unpaired DNA triggers the activation of the checkpoint.

The activated checkpoint signals inhibit cell cycle progression, leading to the arrest of meiotic recombination and the delay of further meiotic events until the synapsis is completed. Once the SC is properly formed, RPA is displaced from the synapsed DNA, and the checkpoint is relieved, allowing the cell to proceed with meiosis.

In summary, RPA plays a crucial role in the recombination checkpoint by sensing unpaired DNA regions during meiosis. Its presence at unrepaired sites activates the checkpoint response, delaying cell cycle progression until proper chromosome synapsis is achieved, ensuring accurate chromosome segregation and faithful transmission of genetic information to the progeny.

# Figures:

## Figure 1:

A)

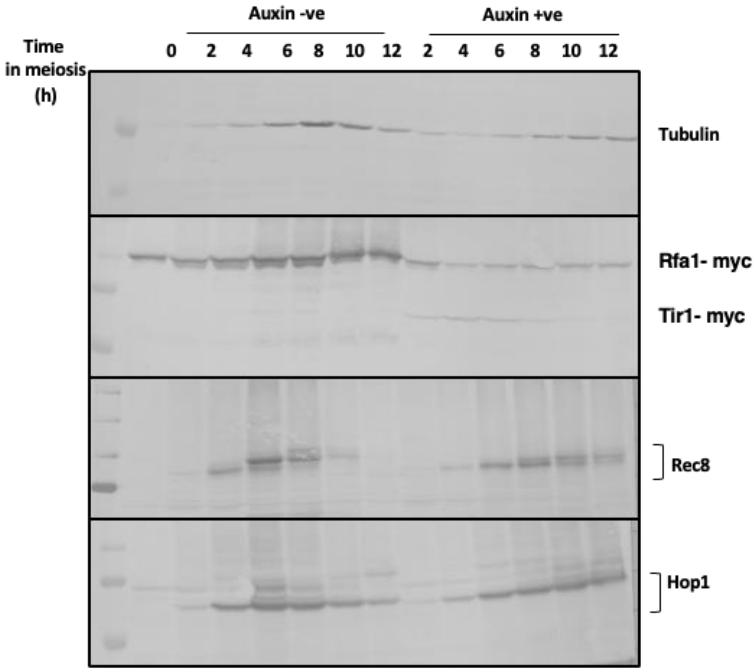


B)

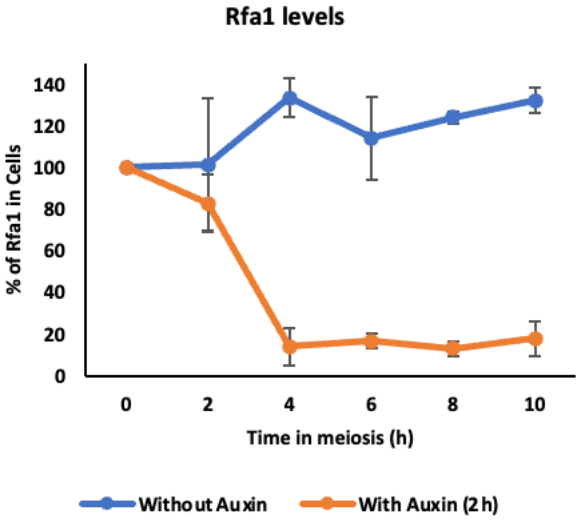


C)

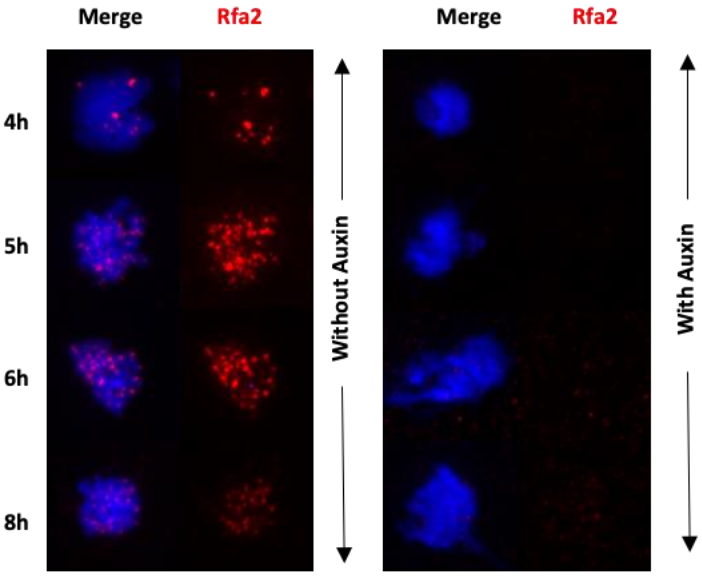


D)

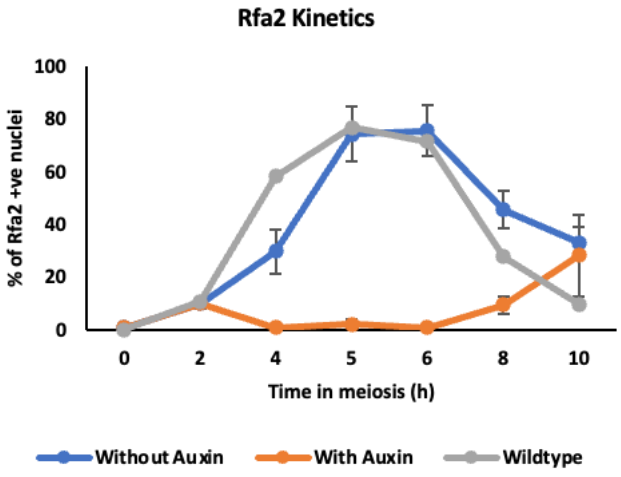


E)

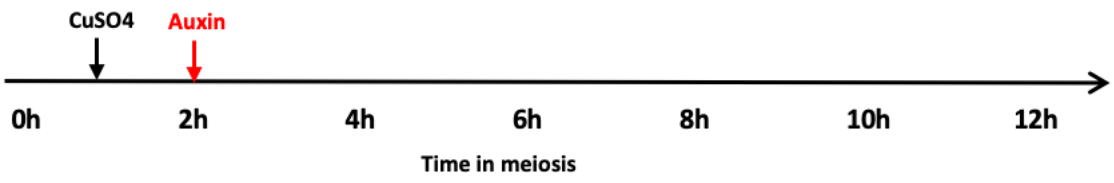

**Figure 1:**

A. Western Blot analysis with the indicated antibodies with lysates obtained from *RFA1-AID* (SAY15/16) cells at various time points during meiosis with or without addition of Auxin at 2h.

B. ImageJ quantification of expression of Rfa1 from western blot using anti-myc antibody.

C. Rfa2 staining. Nuclear spreads from *RFA1-AID* (SAY15/16) with or without addition of Auxin at 2h were stained with anti-Rfa2 (Red) and DAPI (Blue). Representative images at each time point under the two conditions are shown.

D. Rfa2 kinetics. The number of Rfa2 positive cells (more than 5 foci) were counted at each time point. At each time point more than 50 cells were counted. (n=3)

E. A schematic representation of timeline for addition of auxin and $CuSO_4$.

**Figure 2:**

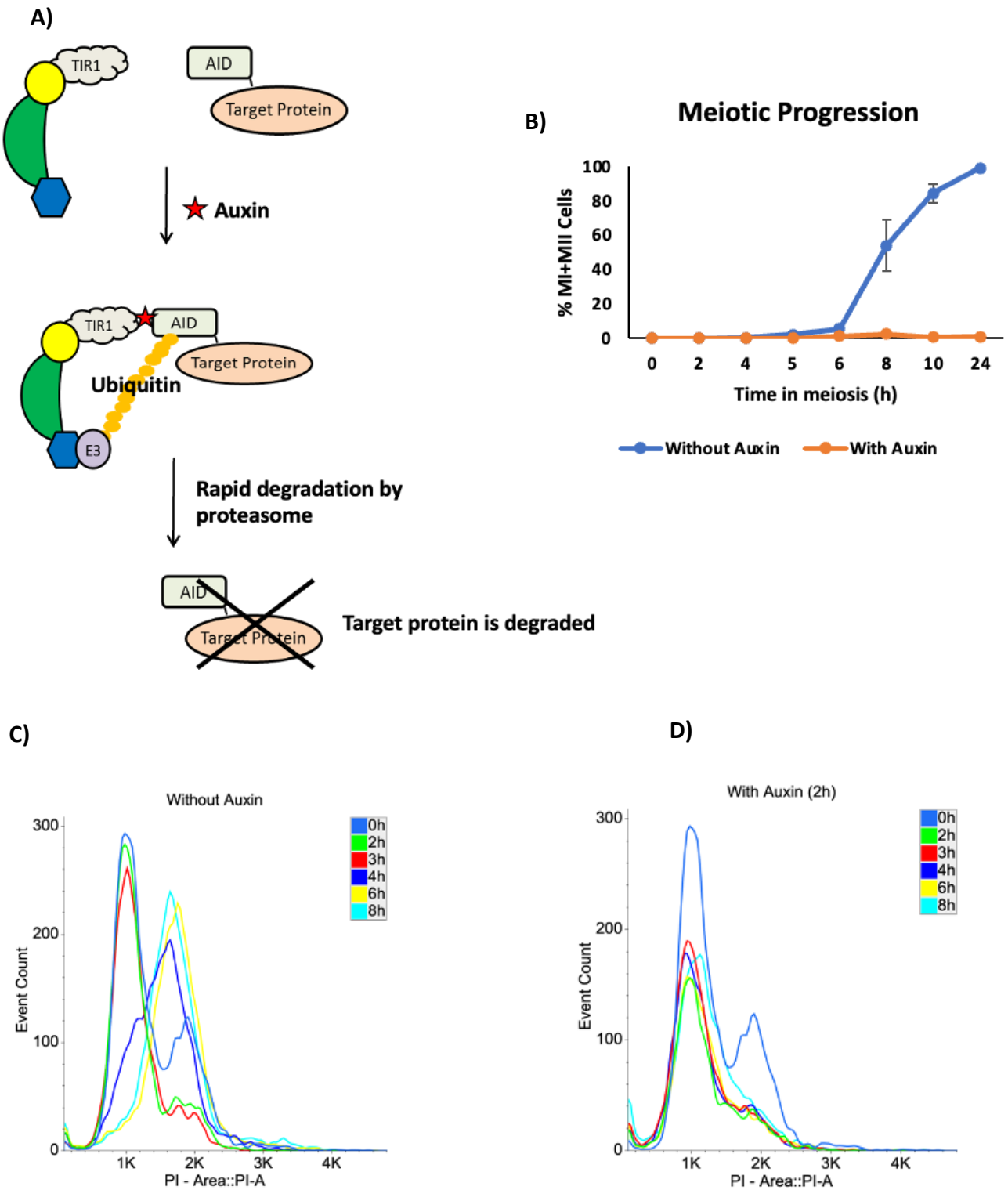
A)
TIR1
AID
Target Protein
Auxin
TIR1
AID
Target Protein
Ubiquitin
E3
Rapid degradation by proteasome
AID
Target Protein
Target protein is degraded
B)
Meiotic Progression
% MI+MII Cells
100
80
60
40
20
0
0
2
4
5
6
8
10
24
Time in meiosis (h)
Without Auxin
With Auxin
C)
Without Auxin
300
200
100
0
Event Count
1K
2K
3K
4K
PI - Area::PI-A
0h
2h
3h
4h
6h
8h
D)
With Auxin (2h)
300
200
100
0
Event Count
1K
2K
3K
4K
PI - Area::PI-A
0h
2h
3h
4h
6h
8h

**Figure 2:**

A. Schematic representation of Auxin inducible degron.

B. Meiotic Cell cycle progression. The entry into meiosis I and II by *RFA1-AID* (SAY 15/16) cells with and without auxin were analyzed using DAPI staining. More than 100 cells were counted from each time point. (n=3)

C. FACS profile of *RFA1-AID* (SAY 15/16) cells without addition of auxin at 2h. Fixed cells were stained with PI and analyzed using cell sorter.

D. FACS profile of *RFA1-AID* (SAY 15/16) cells with addition of auxin at 2h. Fixed cells were stained with PI and analyzed using cell sorter.

**Figure 3:**

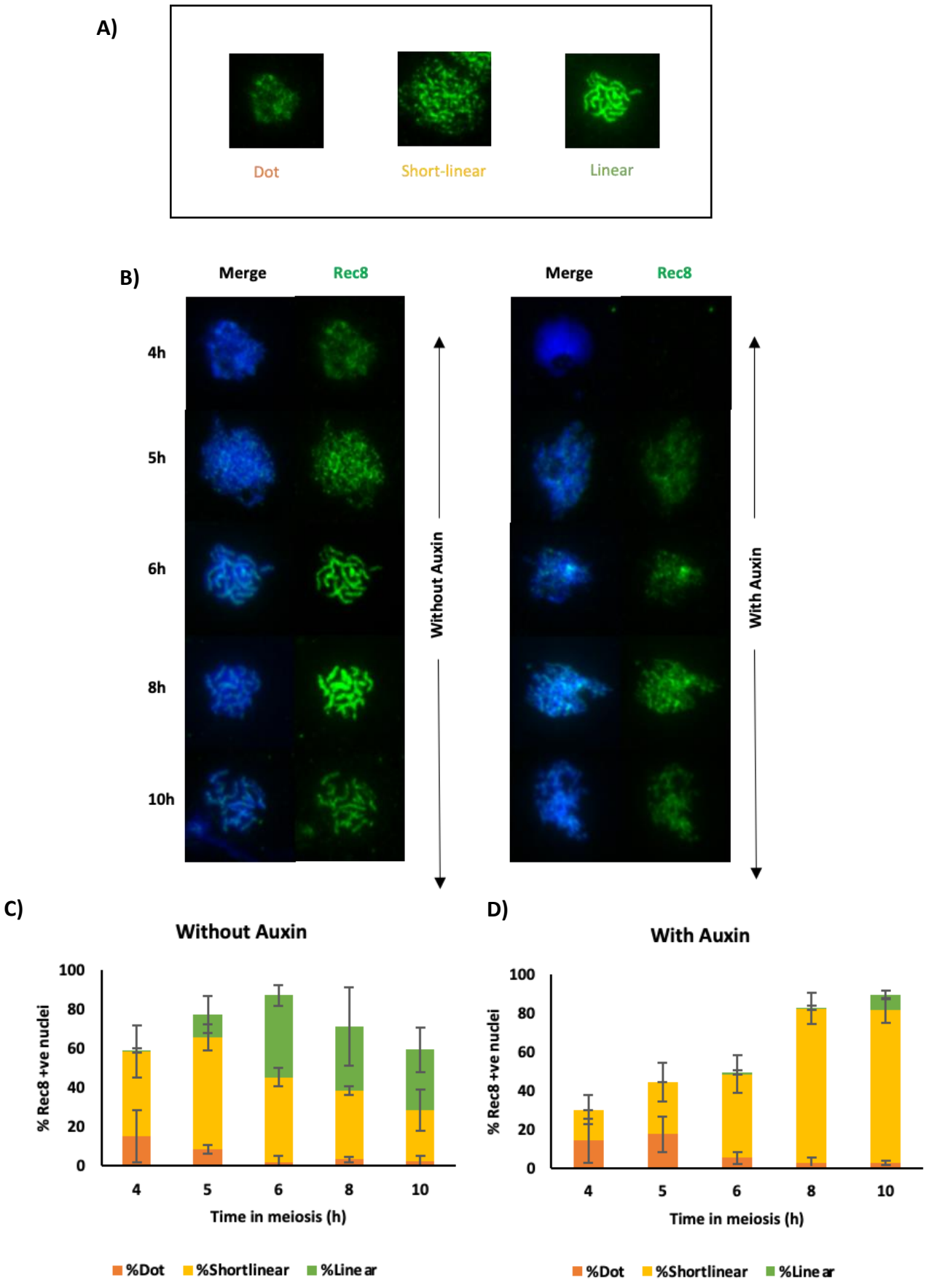
A)
Dot
Short-linear
Linear
B)
Merge
Rec8
Merge
Rec8
4h
5h
6h
8h
10h
Without Auxin
With Auxin
C)
Without Auxin
% Rec8 +ve nuclei
100
80
60
40
20
0
4
5
6
8
10
Time in meiosis (h)
%Dot
%Shortlinear
%Linear
D)
With Auxin
% Rec8 +ve nuclei
100
80
60
40
20
0
4
5
6
8
10
Time in meiosis (h)
%Dot
%Shortlinear
%Linear

**Figure 3:**

A. Representative images showing different classes of Rec8 staining during budding yeast meiotic recombination.

B. Rec8 staining. Nuclear spreads from *RFA1-AID* (SAY15/16) with or without addition of Auxin at 2h were stained with anti-Rec8 (green) and DAPI (Blue). Representative images at each time point under the two conditions are shown.

C. Rec8 kinetics without Auxin. Different classes of Rec8 staining were quantified from each time point. More than 50 cells were counted at each time point. (n=3)

D. Rec8 kinetics with Auxin. Different classes of Rec8 staining were quantified from each time point. More than 50 cells were counted at each time point. (n=3)

**Figure 4:**

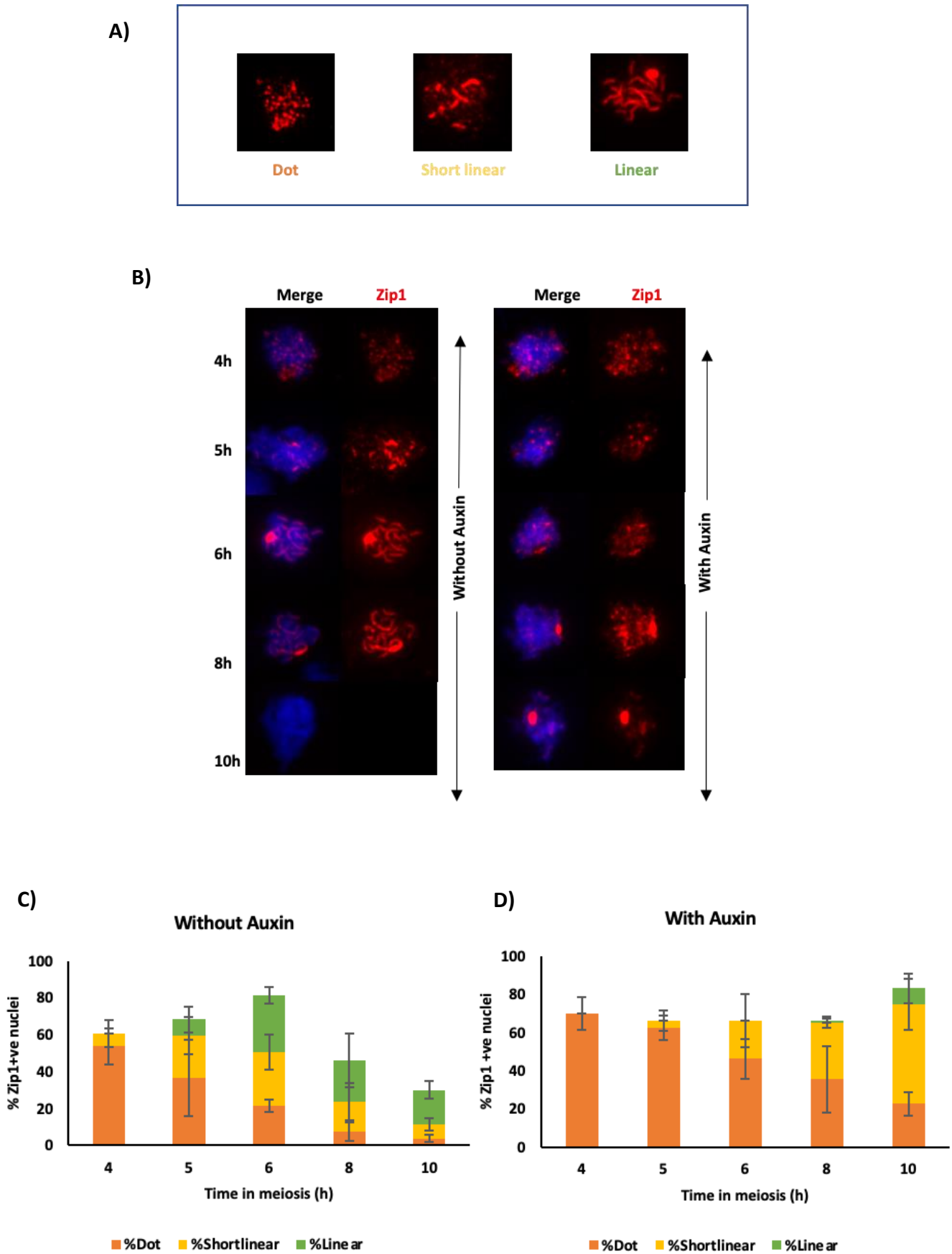
A)
Dot
Short linear
Linear
B)
Merge
Zip1
Merge
Zip1
4h
5h
6h
8h
10h
Without Auxin
With Auxin
C)
Without Auxin
% Zip1+ve nuclei
100
80
60
40
20
0
4
5
6
8
10
Time in meiosis (h)
%Dot
%Shortlinear
%Linear
D)
With Auxin
% Zip1 +ve nuclei
100
80
60
40
20
0
4
5
6
8
10
Time in meiosis (h)
%Dot
%Shortlinear
%Linear

**Figure 4:**

A. Representative images showing different classes of Zip1 staining during budding yeast meiotic recombination.

B. Zip1 staining. Nuclear spreads from *RFA1-AID* (SAY15/16) with or without addition of Auxin at 2h were stained with anti-Zip1 (Red) and DAPI (Blue). Representative images at each time point under the two conditions are shown.

C. Zip1 kinetics without Auxin. Different classes of Zip1 staining were quantified from each time point. More than 50 cells were counted at each time point. (n=3)

D. Zip1 kinetics with Auxin. Different classes of Zip1 staining were quantified from each time point. More than 50 cells were counted at each time point. (n=3)

**Figure 5:**

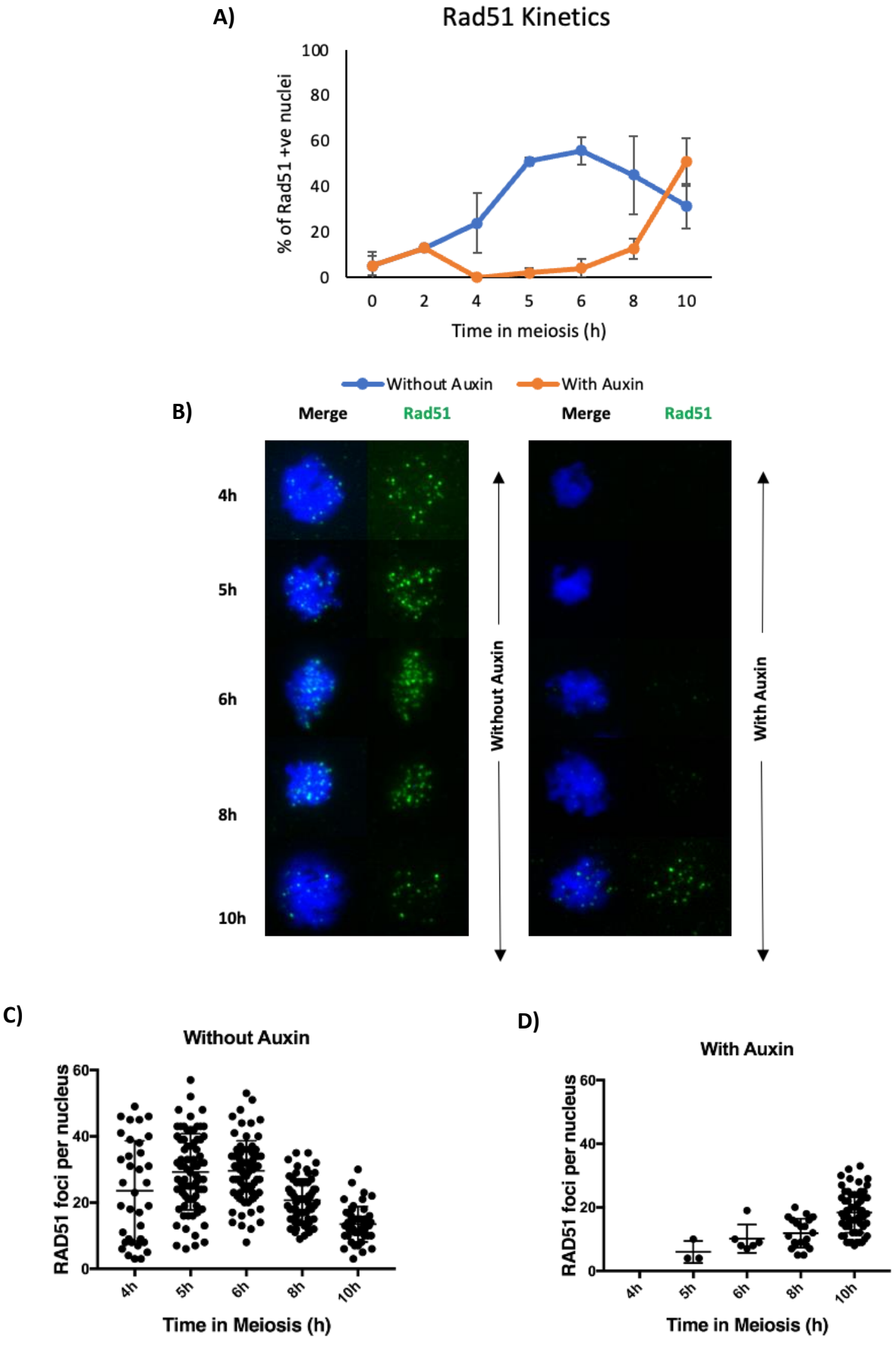
A)
Rad51 Kinetics
% of Rad51 +ve nuclei
100
80
60
40
20
0
0
2
4
5
6
8
10
Time in meiosis (h)
B)
Without Auxin
With Auxin
Merge
Rad51
Merge
Rad51
4h
5h
6h
8h
10h
Without Auxin
With Auxin
C)
Without Auxin
RAD51 foci per nucleus
60
40
20
0
4h
5h
6h
8h
10h
Time in Meiosis (h)
D)
With Auxin
RAD51 foci per nucleus
60
40
20
0
4h
5h
6h
8h
10h
Time in Meiosis (h)

**Figure 5:**

A. Rad51 kinetics. The number of Rad51 positive cells (more than 5 foci) were counted at each time point. At each time point more than 50 cells were counted. (n=3)

B. Rad51 staining. Nuclear spreads from *RFA1-AID* (SAY15/16) with or without addition of Auxin at 2h were stained with anti-Rad51 (Green) and DAPI (Blue). Representative images at each time point under the two conditions are shown.

C. Rad51 foci count without Auxin. Number of foci in each cell were counted at each time point. At each time point more than 75 cells or all Rad51 positive cells were counted.

D. Rad51 foci count with Auxin. Number of foci in each cell were counted at each time point. At each time point more than 75 cells or all Rad51 positive cells were counted.

**Figure 6:**

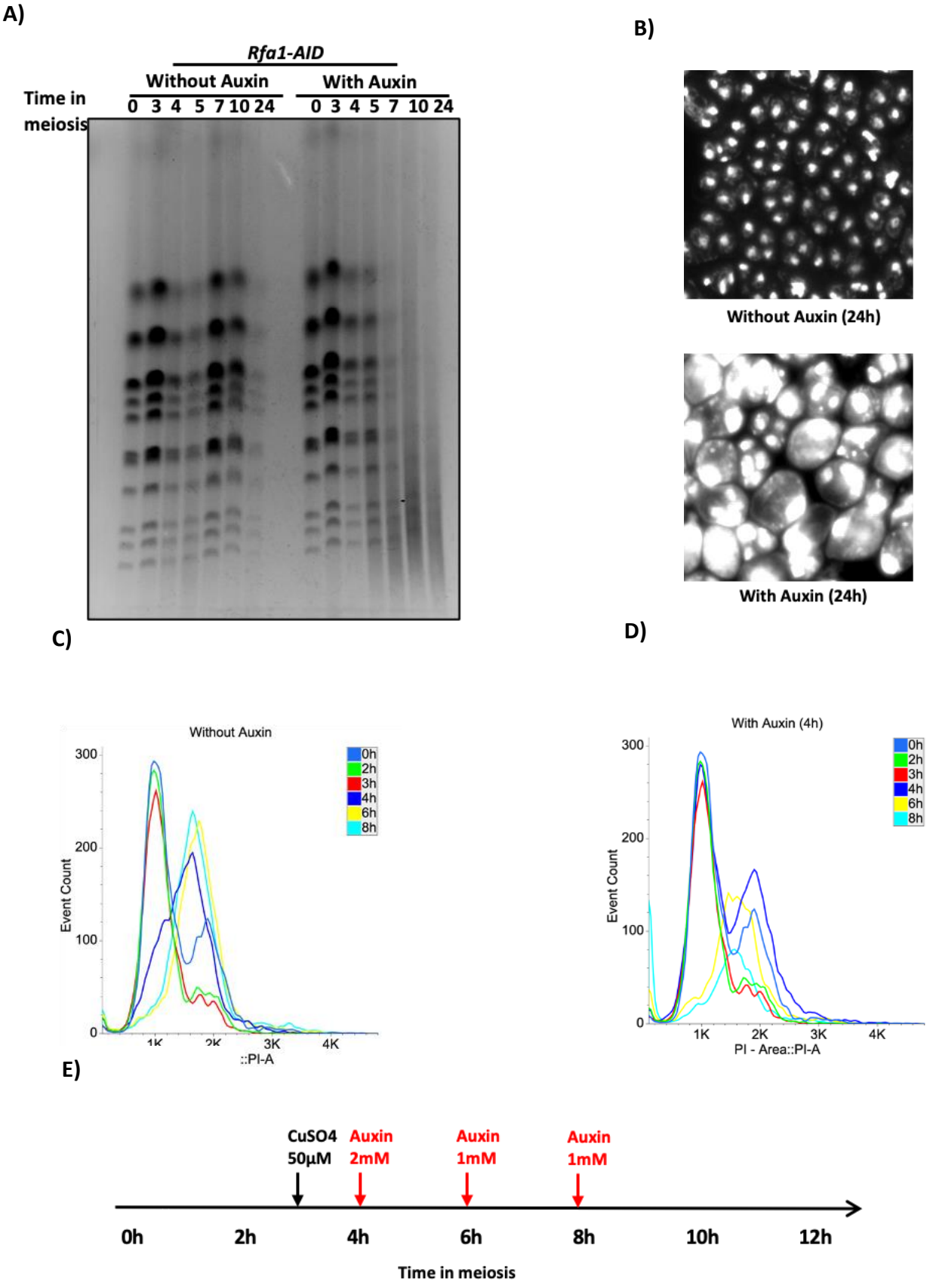
A)
Rfa1-AID
Without Auxin
With Auxin
Time in meiosis
0 3 4 5 7 10 24
0 3 4 5 7 10 24
B)
Without Auxin (24h)
With Auxin (24h)
C)
Without Auxin
Event Count
::PI-A
0h
2h
3h
4h
6h
8h
D)
With Auxin (4h)
Event Count
PI - Area::PI-A
E)
CuSO4 50µM
Auxin 2mM
Auxin 1mM
Auxin 1mM
0h
2h
4h
6h
8h
10h
12h
Time in meiosis

**Figure 6:**

A. CHEF analysis. Chromosomal DNA from *RFA1-AID* (SAY 15/16) were analyzed using Clamped homogenous electric field Gel electrophoresis with or without addition of Auxin at 4h.

B. DAPI Staining showing abnormal chromosome segregation after addition of Auxin at 4h. Representative images of *RFA1-AID* (SAY15/ 16) cells at 24h with or without Auxin at 4h using DAPI staining.

C. FACS profile of *RFA1-AID* (SAY 15/16) cells without addition of auxin at 4h. Fixed cells were stained with PI and analyzed using cell sorter.

D. FACS profile of *RFA1-AID* (SAY 15/16) cells with addition of auxin at 4h. Fixed cells were stained with PI and analyzed using cell sorter.

E. A schematic representation of timeline for addition of auxin and $CuSO_4$.

**Figure 7:**

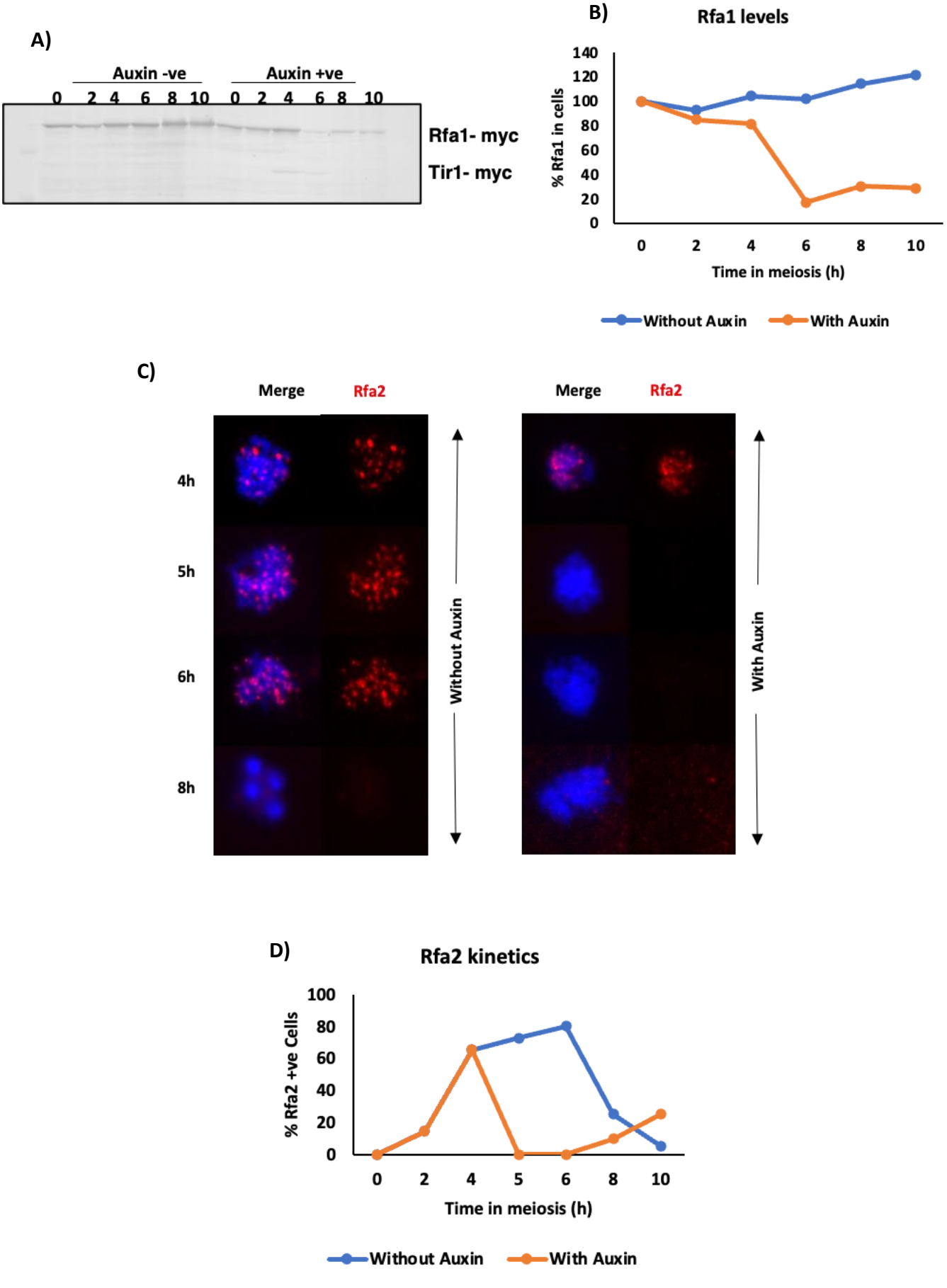
A)
Auxin -ve
Auxin +ve
0 2 4 6 8 10 0 2 4 6 8 10
Rfa1- myc
Tir1- myc
B)
Rfa1 levels
% Rfa1 in cells
140
120
100
80
60
40
20
0
0 2 4 6 8 10
Time in meiosis (h)
Without Auxin
With Auxin
C)
Merge
Rfa2
Merge
Rfa2
4h
5h
6h
8h
Without Auxin
With Auxin
D)
Rfa2 kinetics
% Rfa2 +ve Cells
100
80
60
40
20
0
0 2 4 5 6 8 10
Time in meiosis (h)
Without Auxin
With Auxin

**Figure 7:**

A. Western Blot analysis with anti-myc antibody with lysates obtained from *RFA1-AID* (SAY15/16) cells at various time points during meiosis with or without addition of Auxin at 4h.

B. ImageJ quantification of expression of Rfa1 from western blot using anti-myc antibody with or without auxin at 4h.

C. Rfa2 staining. Nuclear spreads from *RFA1-AID* (SAY15/16) with or without addition of Auxin at 4h were stained with anti-Rfa2 (Red) and DAPI (Blue). Representative images at each time point under the two conditions are shown.

D. Rfa2 kinetics. The number of Rfa2 positive cells (more than 5 foci) were counted at each time point with or without addition of auxin at 4h. At each time point more than 50 cells were counted.

**Figure 8:**

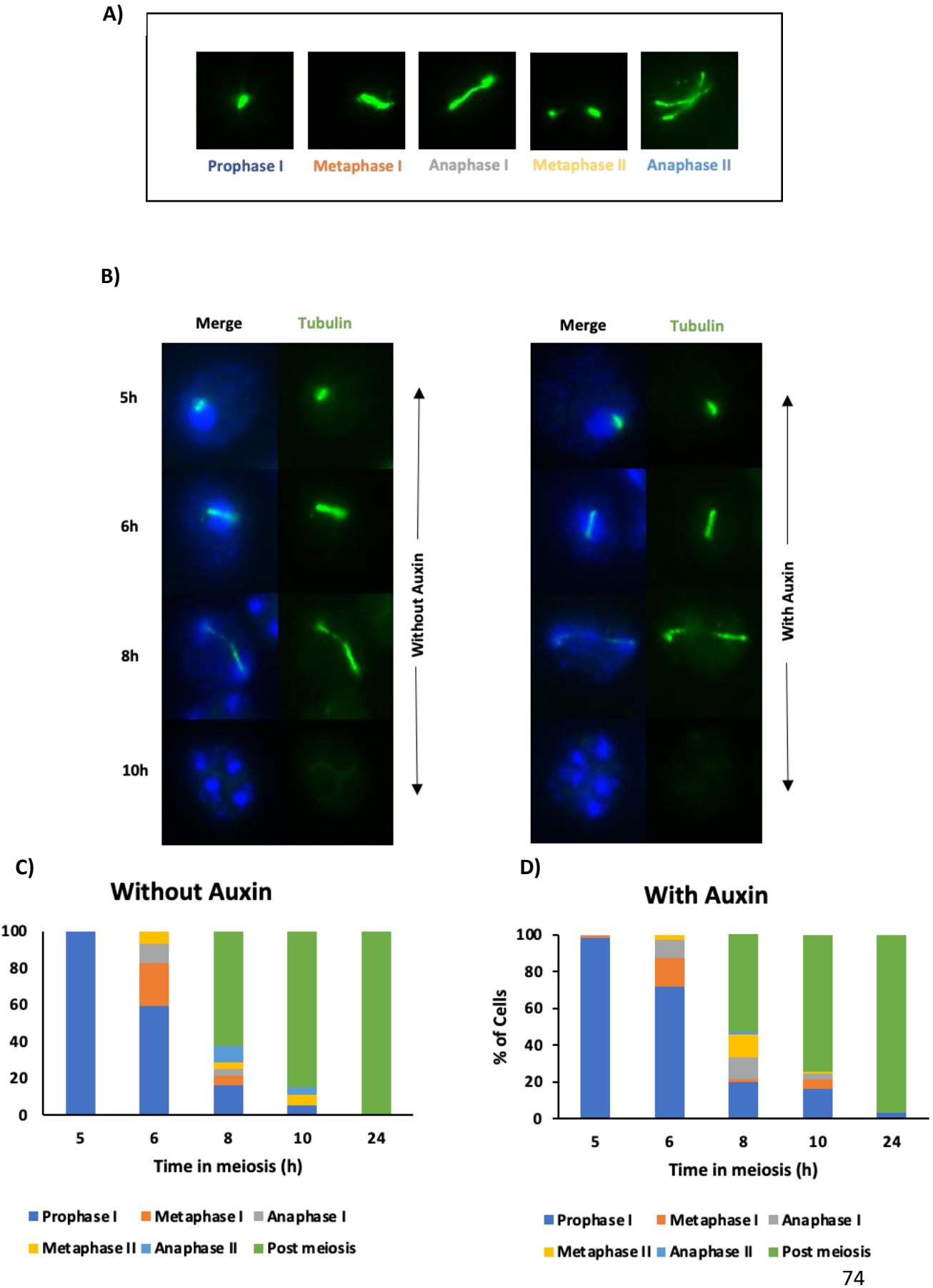
A)
Prophase I
Metaphase I
Anaphase I
Metaphase II
Anaphase II
B)
Merge
Tubulin
5h
6h
8h
10h
Without Auxin
Merge
Tubulin
With Auxin
C)
Without Auxin
% of Cells
100
80
60
40
20
0
5
6
8
10
24
Time in meiosis (h)
Prophase I
Metaphase I
Anaphase I
Metaphase II
Anaphase II
Post meiosis
D)
With Auxin
% of Cells
100
80
60
40
20
0
5
6
8
10
24
Time in meiosis (h)
Prophase I
Metaphase I
Anaphase I
Metaphase II
Anaphase II
Post meiosis

**Figure 8:**

A. Representative images of classes of tubulin staining during meiosis showing spindle elongation at different stages of meiosis.

B. Tubulin whole cell staining. *RFA1-AID* (SAY15/16) cells with or without addition of Auxin at 4h were stained with anti-Tubulin (Green) and DAPI (Blue). Representative images at each time point under the two conditions are shown.

C. Meiotic progression without Auxin. Different classes of Tubulin staining were quantified from each time point. More than 100 cells were counted at each time point.

D. Meiotic progression with Auxin. Different classes of Tubulin staining were quantified from each time point. More than 100 cells were counted at each time point.

**Figure 9:**

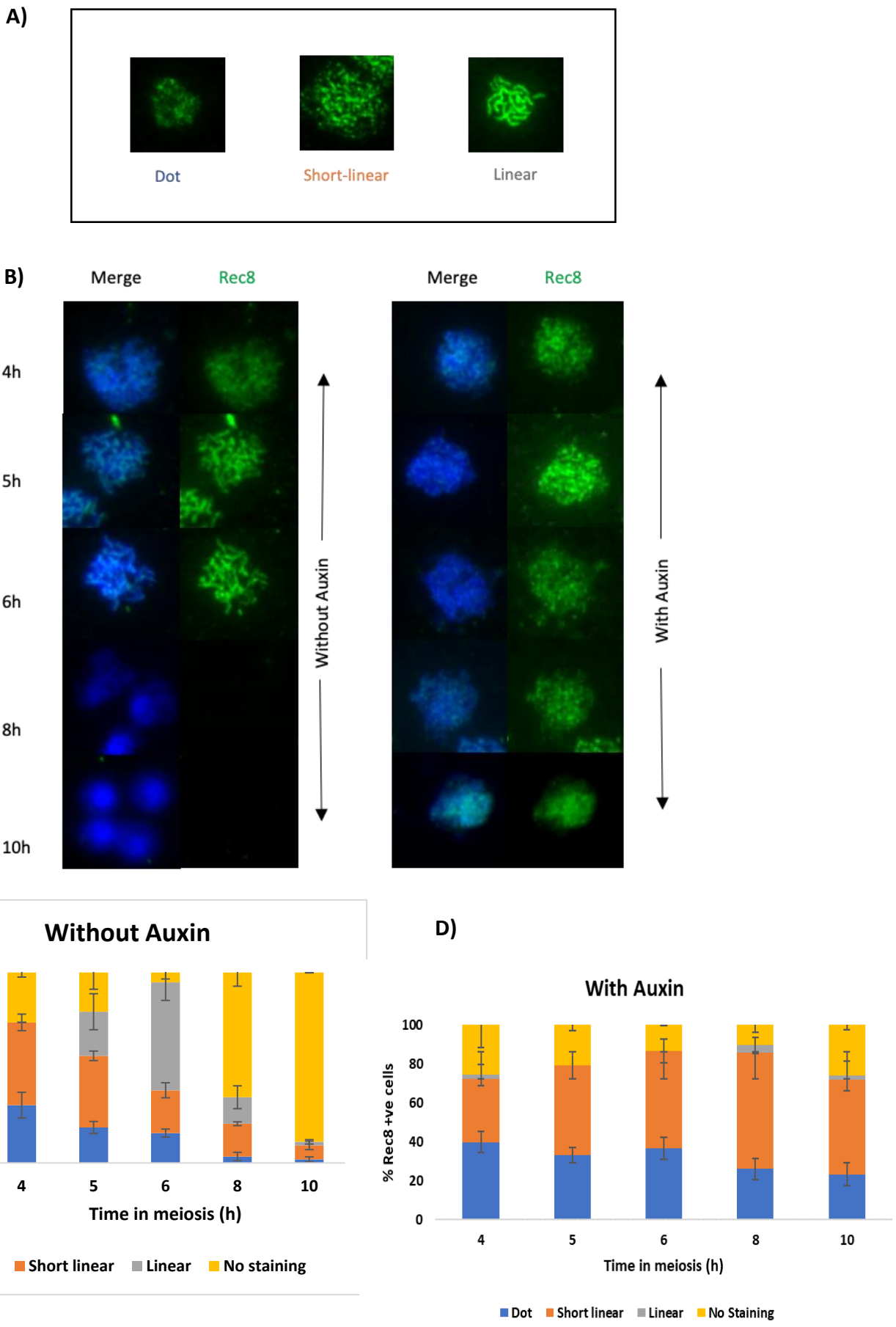
A)
Dot
Short-linear
Linear
B)
Merge
Rec8
Merge
Rec8
4h
5h
6h
8h
10h
Without Auxin
With Auxin
Without Auxin
% REc8 +ve cells
100
80
60
40
20
0
4
5
6
8
10
Time in meiosis (h)
Dot
Short linear
Linear
No staining
D)
With Auxin
% Rec8 +ve cells
100
80
60
40
20
0
4
5
6
8
10
Time in meiosis (h)
Dot
Short linear
Linear
No Staining

**Figure 9:**

A. Representative images showing different classes of Rec8 staining during meiosis.

B. Rec8 staining. Nuclear spreads from *RFA1-AID* (SAY15/16) with or without addition of Auxin at 4h were stained with anti-Rec8 (green) and DAPI (Blue). Representative images at each time point under the two conditions are shown.

C. Rec8 kinetics without Auxin. Different classes of Rec8 staining were quantified from each time point. More than 50 cells were counted at each time point.

D. Rec8 kinetics with Auxin. Different classes of Rec8 staining were quantified from each time point. More than 50 cells were counted at each time point.

**Figure 10:**

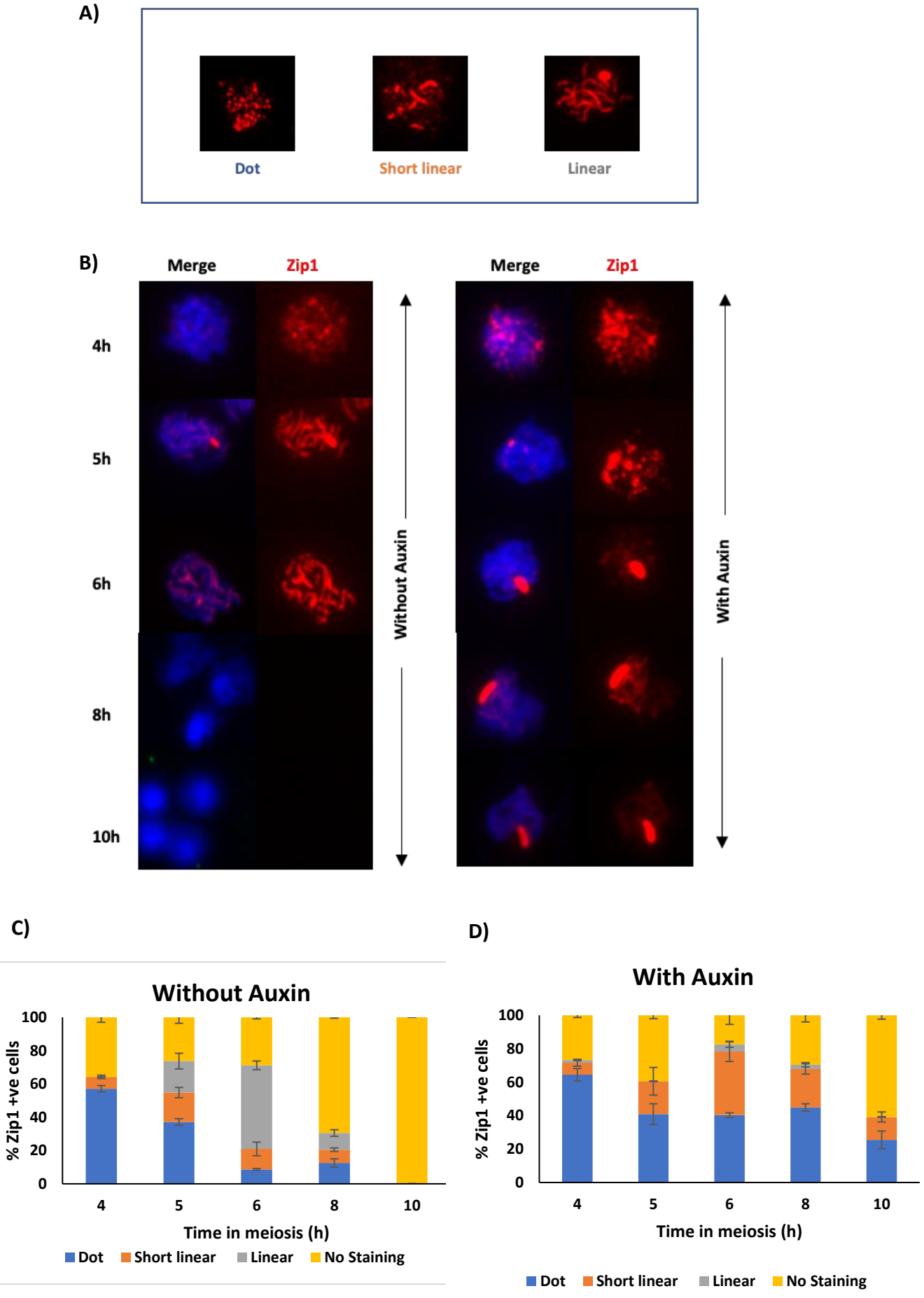
A)
Dot
Short linear
Linear
B)
Merge
Zip1
Merge
Zip1
4h
5h
6h
8h
10h
Without Auxin
With Auxin
C)
Without Auxin
% Zip1 +ve cells
100
80
60
40
20
0
4
5
6
8
10
Time in meiosis (h)
Dot
Short linear
Linear
No Staining
D)
With Auxin
% Zip1 +ve cells
100
80
60
40
20
0
4
5
6
8
10
Time in meiosis (h)
Dot
Short linear
Linear
No Staining

**Figure 10:**

A. Representative images showing different classes of Zip1 staining during meiosis.

B. Zip1 staining. Nuclear spreads from *RFA1-AID* (SAY15/16) with or without addition of Auxin at 4h were stained with anti-Zip1 (Red) and DAPI (Blue). Representative images at each time point under the two conditions are shown.

C. Zip1 kinetics without Auxin. Different classes of Zip1 staining were quantified from each time point. More than 50 cells were counted at each time point.

D. Zip1 kinetics with Auxin. Different classes of Zip1 staining were quantified from each time point. More than 50 cells were counted at each time point.

**Figure 11:**

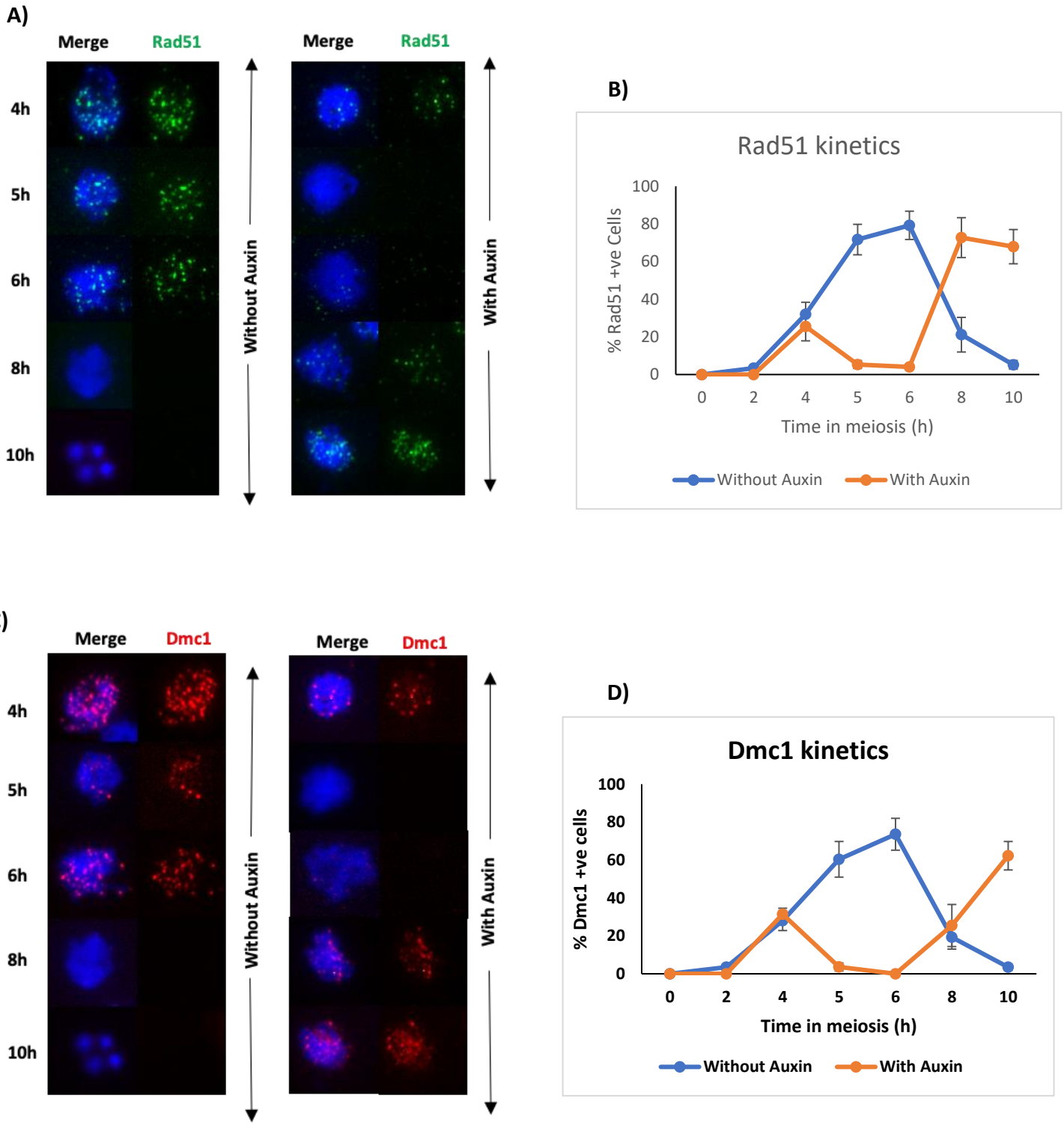
A)
Merge
Rad51
Merge
Rad51
4h
5h
6h
8h
10h
Without Auxin
With Auxin
B)
Rad51 kinetics
% Rad51 +ve Cells
100
80
60
40
20
0
0
2
4
5
6
8
10
Time in meiosis (h)
Without Auxin
With Auxin
C)
Merge
Dmc1
Merge
Dmc1
4h
5h
6h
8h
10h
Without Auxin
With Auxin
D)
Dmc1 kinetics
% Dmc1 +ve cells
100
80
60
40
20
0
0
2
4
5
6
8
10
Time in meiosis (h)
Without Auxin
With Auxin

**Figure 11:**

A. Rad51 staining. Nuclear spreads from *RFA1-AID* (SAY15/16) with or without addition of Auxin at 4h were stained with anti-Rad51 (Green) and DAPI (Blue). Representative images at each time point under the two conditions are shown.

B. Rad51 kinetics. The number of Rad51 positive cells (more than 5 foci) were counted at each time point. At each time point more than 50 cells were counted.

C. Dmc1 staining. Nuclear spreads from *RFA1-AID* (SAY15/16) with or without addition of Auxin at 4h were stained with anti-Dmc1 (Red) and DAPI (Blue). Representative images at each time point under the two conditions are shown.

D. Dmc1 kinetics. The number of Dmc1 positive cells (more than 5 foci) were counted at each time point. At each time point more than 50 cells were counted.

**Figure 12:**

A)

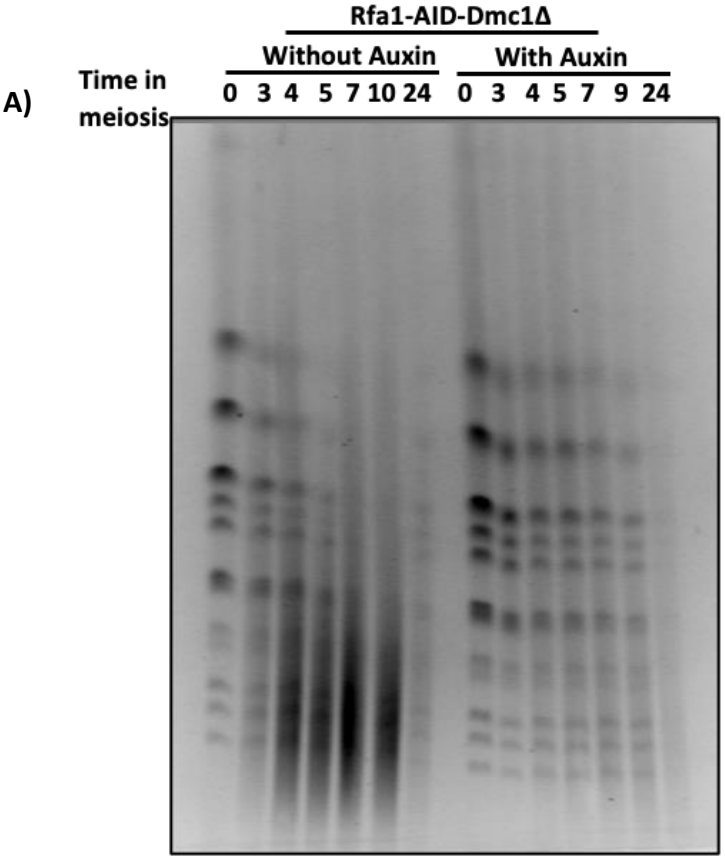
Rfa1-AID-Dmc1Δ
Without Auxin
With Auxin
Time in meiosis
0 3 4 5 7 10 24
0 3 4 5 7 9 24

B)

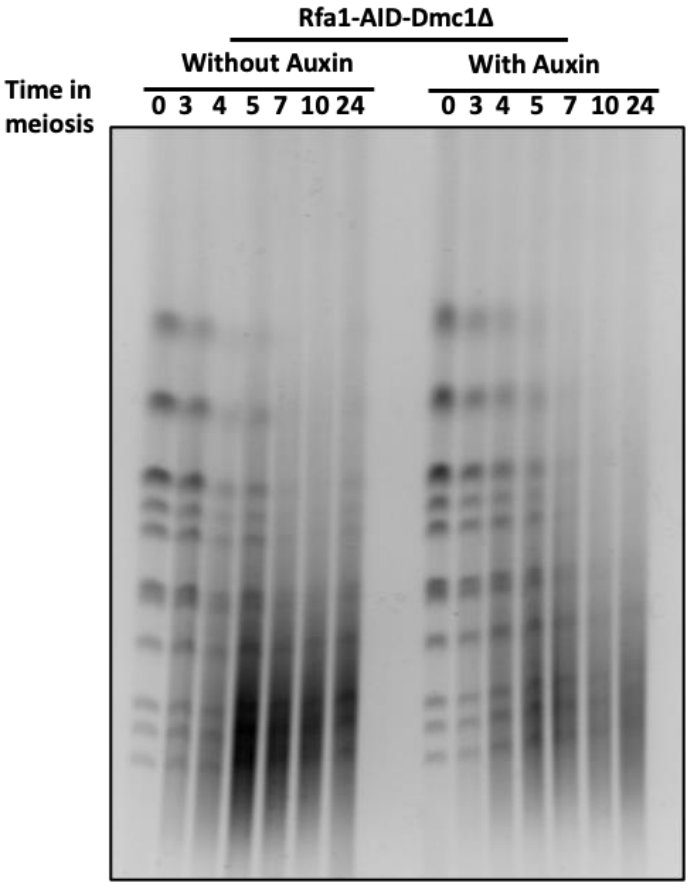
Rfa1-AID-Dmc1Δ
Without Auxin
With Auxin
Time in meiosis
0 3 4 5 7 10 24
0 3 4 5 7 10 24

**Figure 12:**

A. CHEF analysis. Chromosomal DNA from *dmc1Δ -RFA1-AID* (SAY 62/63) were analyzed using Clamped homogenous electric field Gel electrophoresis with or without addition of Auxin at 2h.

B. CHEF analysis. Chromosomal DNA from *dmc1Δ-RFA1-AID* (SAY 62/63) were analyzed using Clamped homogenous electric field Gel electrophoresis with or without addition of Auxin at 4h.

Figure 13:

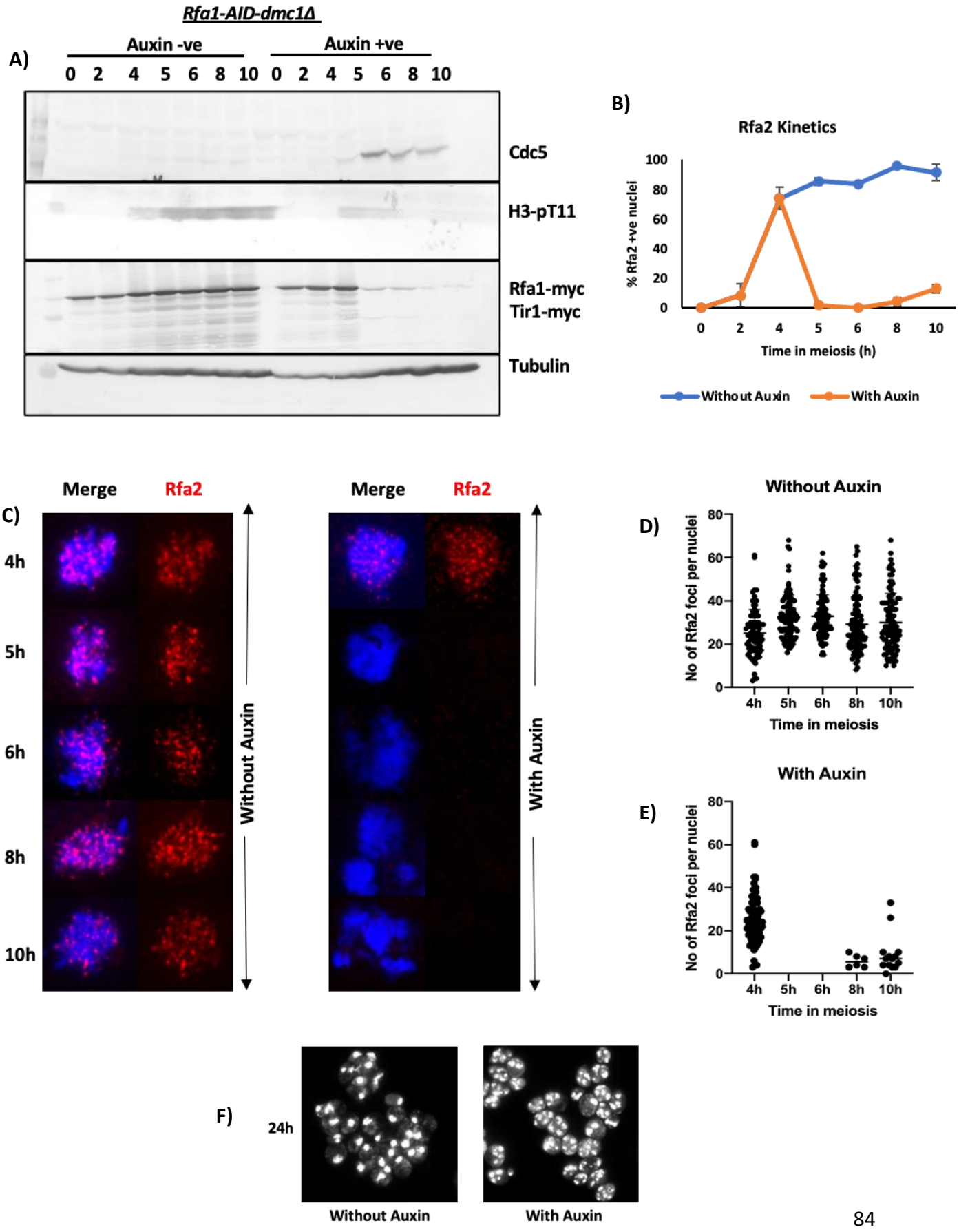
A)
Rfa1-AID-dmc1Δ
Auxin -ve
Auxin +ve
0 2 4 5 6 8 10 0 2 4 5 6 8 10
Cdc5
H3-pT11
Rfa1-myc
Tir1-myc
Tubulin
B)
Rfa2 Kinetics
% Rfa2 +ve nuclei
Time in meiosis (h)
Without Auxin
With Auxin
C)
Merge
Rfa2
4h
5h
6h
8h
10h
Without Auxin
With Auxin
D)
Without Auxin
No of Rfa2 foci per nuclei
Time in meiosis
E)
With Auxin
F)
24h
Without Auxin
With Auxin

**Figure 13:**

A. Western Blot analysis with the indicated antibodies with lysates obtained from *dmc1Δ -RFA1-AID* (SAY62/63) cells at various time points during meiosis with or without addition of Auxin at 4h.

B. Rfa2 kinetics. The number of Rfa2 positive cells (more than 5 foci) were counted at each time point for *dmc1Δ -RFA1-AID* (SAY62/63) cells with or without addition of auxin at 4h. At each time point more than 50 cells were counted. (n=3)

C. Rfa2 staining. Nuclear spreads from *dmc1Δ -RFA1-AID* (SAY62/63) with or without addition of Auxin at 4h were stained with anti-Rfa2 (Red) and DAPI (Blue). Representative images at each time point under the two conditions are shown.

D. Rfa2 foci count without Auxin. Number of foci in each *dmc1Δ -RFA1-AID* (SAY62/63) cells were counted at each time point. At each time point more than 75 cells or all Rfa2 positive cells were counted.

E. Rfa2 foci count with Auxin. Number of foci in each *dmc1Δ -RFA1-AID* (SAY62/63) cells were counted at each time point. At each time point more than 75 cells or all Rfa2 positive cells were counted.

F. DAPI Staining showing chromosome segregation after addition of Auxin at 4h in *dmc1Δ -RFA1-AID* cells. Representative images of *dmc1Δ -RFA1-AID* (SAY62/63) cells at 24h with or without Auxin at 4h using DAPI staining.

**Figure 14:**

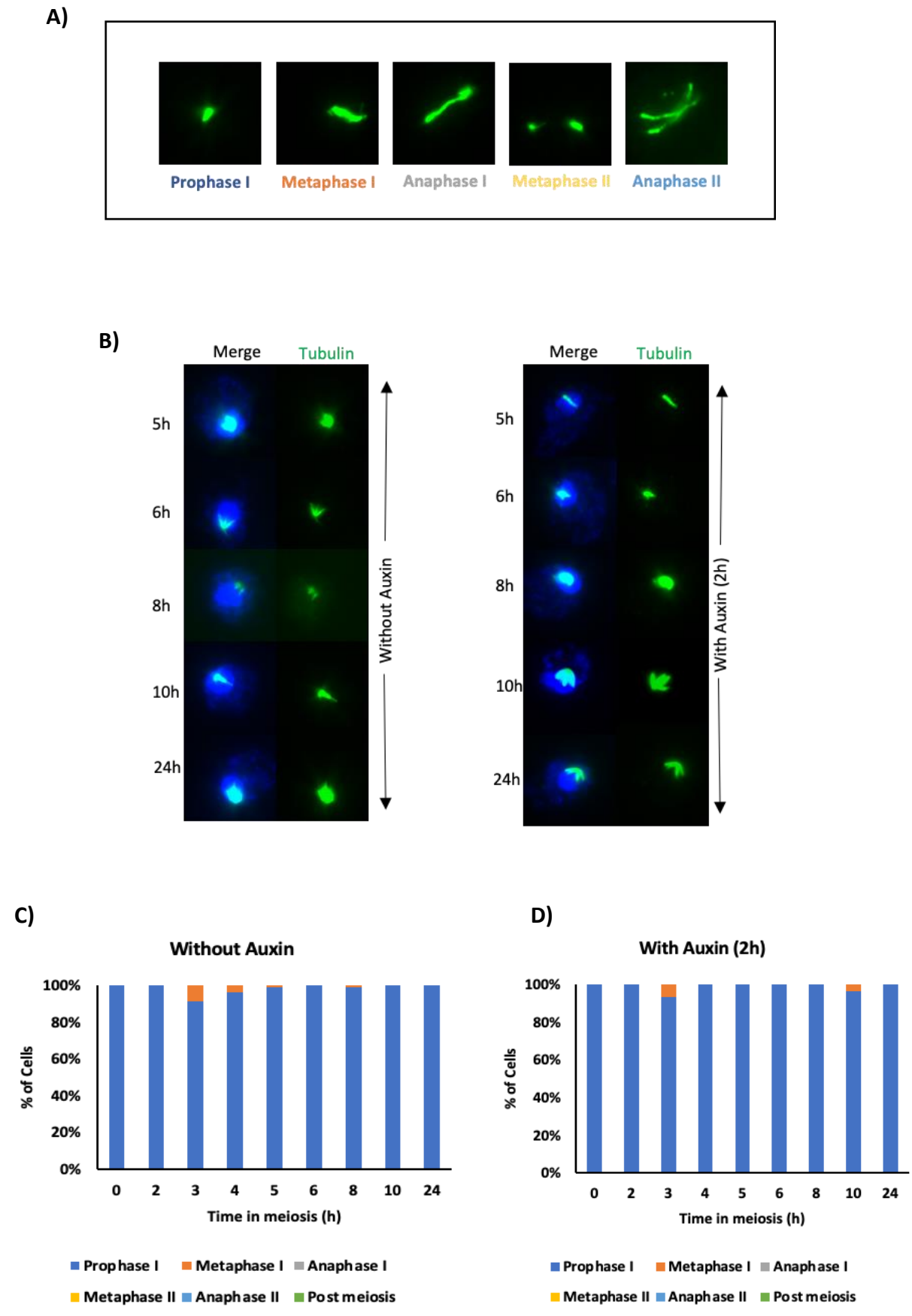
A)
Prophase I
Metaphase I
Anaphase I
Metaphase II
Anaphase II
B)
Merge
Tubulin
5h
6h
8h
10h
24h
Without Auxin
Merge
Tubulin
5h
6h
8h
10h
24h
With Auxin (2h)
C)
Without Auxin
100%
80%
60%
40%
20%
0%
% of Cells
0
2
3
4
5
6
8
10
24
Time in meiosis (h)
Prophase I
Metaphase I
Anaphase I
Metaphase II
Anaphase II
Post meiosis
D)
With Auxin (2h)
100%
80%
60%
40%
20%
0%
% of Cells
0
2
3
4
5
6
8
10
24
Time in meiosis (h)
Prophase I
Metaphase I
Anaphase I
Metaphase II
Anaphase II
Post meiosis

**Figure 14:**

A. Representative images of classes of tubulin staining during meiosis showing spindle elongation at different stages of meiosis.

B. Tubulin whole cell staining. *dmc1Δ-RFA1-AID* (SAY62/63) cells with or without addition of Auxin at 2h were stained with anti-Tubulin (Green) and DAPI (Blue). Representative images at each time point under the two conditions are shown.

C. Meiotic progression without Auxin. Different classes of Tubulin staining were quantified from each time point. More than 100 cells were counted at each time point.

D. Meiotic progression with Auxin. Different classes of Tubulin staining were quantified from each time point. More than 100 cells were counted at each time point.

**Figure 15:**

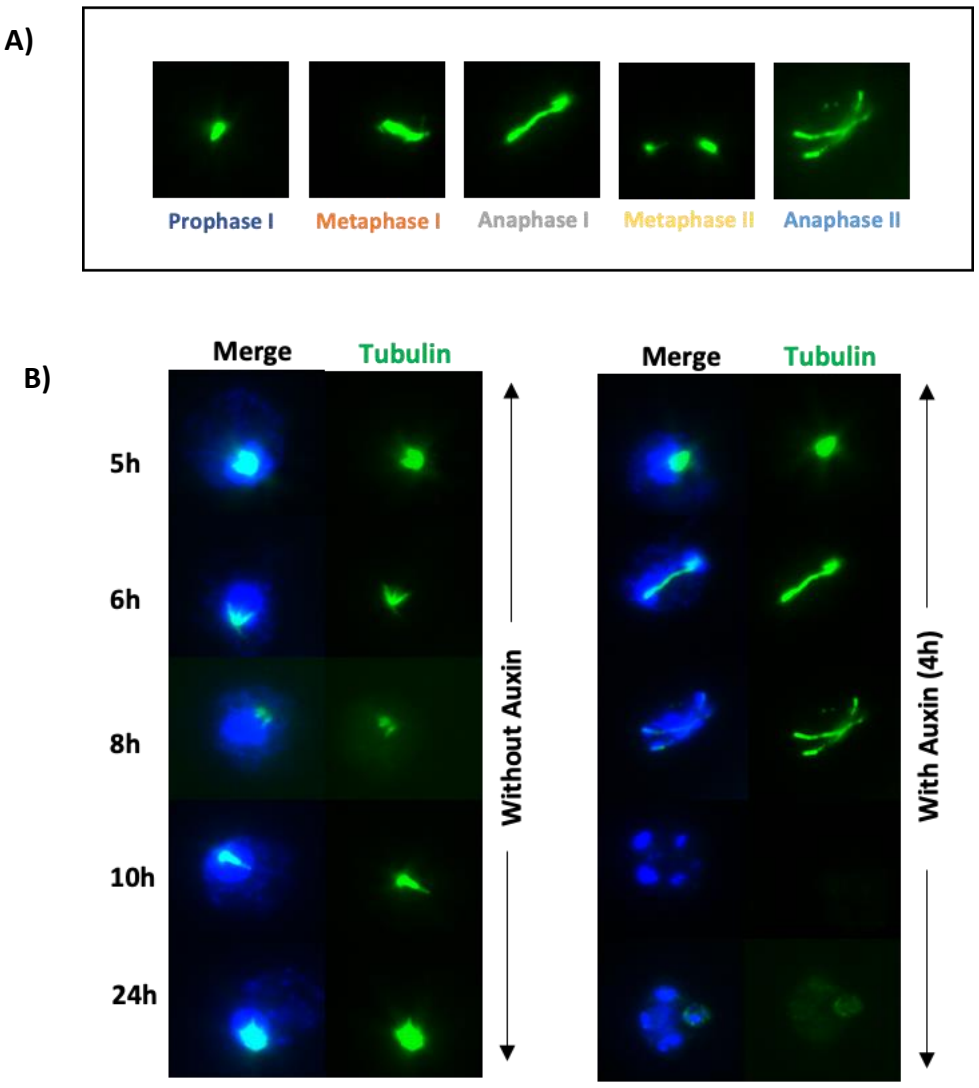
A)
Prophase I
Metaphase I
Anaphase I
Metaphase II
Anaphase II
B)
Merge
Tubulin
Merge
Tubulin
5h
6h
8h
10h
24h
Without Auxin
With Auxin (4h)
C)
Without Auxin
% of cells
100
80
60
40
20
0
0
2
4
5
6
8
10
24
Time in meiosis (h)
Prophase I
Metaphase I
Anaphase I
Metaphase II
Anaphase II
Post meiosis
D)
With Auxin
% of Cells
100
80
60
40
20
0
0
2
4
5
6
8
10
24
Time in meiosis (h)
Prophase I
Metaphase I
Anaphase I
Metaphase II
Anaphase II
Post meiosis

**Figure 15:**

A. Representative images of classes of tubulin staining during meiosis showing spindle elongation at different stages of meiosis.

B. Tubulin whole cell staining. *dmc1Δ-RFA1-AID* (SAY62/63) cells with or without addition of Auxin at 4h were stained with anti-Tubulin (Green) and DAPI (Blue). Representative images at each time point under the two conditions are shown.

C. Meiotic progression without Auxin. Different classes of Tubulin staining were quantified from each time point. More than 100 cells were counted at each time point. (n=3)

D. Meiotic progression with Auxin. Different classes of Tubulin staining were quantified from each time point. More than 100 cells were counted at each time point. (n=3)

**Figure 16:**

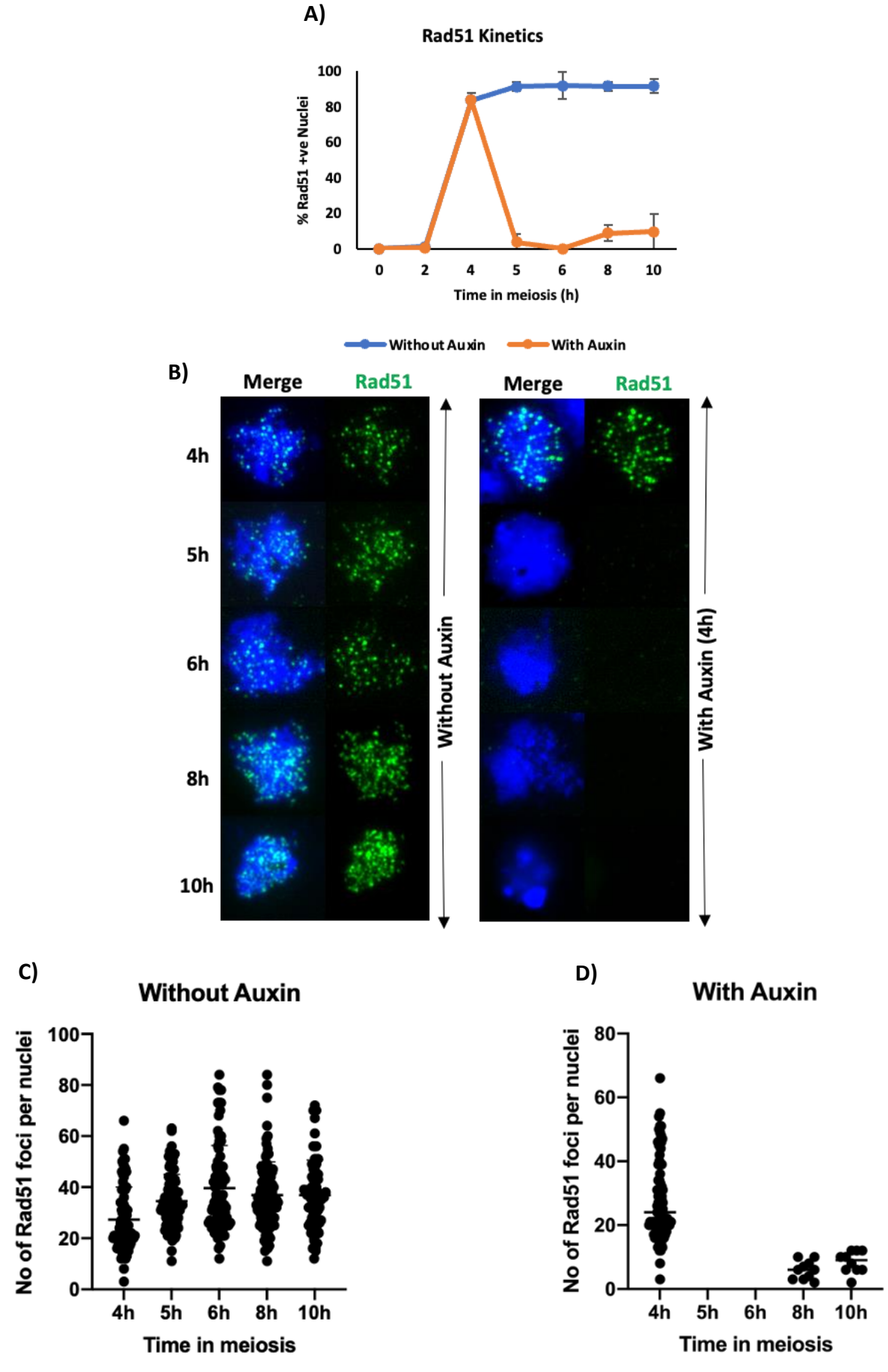
A)
Rad51 Kinetics
% Rad51 +ve Nuclei
100
80
60
40
20
0
0
2
4
5
6
8
10
Time in meiosis (h)
Without Auxin
With Auxin
B)
Merge
Rad51
Merge
Rad51
4h
5h
6h
8h
10h
Without Auxin
With Auxin (4h)
C)
Without Auxin
No of Rad51 foci per nuclei
100
80
60
40
20
0
4h
5h
6h
8h
10h
Time in meiosis
D)
With Auxin
No of Rad51 foci per nuclei
80
60
40
20
0
4h
5h
6h
8h
10h
Time in meiosis

**Figure 16:**

A. Rad51 kinetics. The number of Rad51 positive cells (more than 5 foci) in *dmc1Δ-RFA1-AID* (SAY62/63) with or without addition of Auxin at 4h were counted at each time point. At each time point more than 50 cells were counted. (n=3)

B. Rad51 staining. Nuclear spreads from *dmc1Δ-RFA1-AID* (SAY62/63) with or without addition of Auxin at 4h were stained with anti-Rad51 (Green) and DAPI (Blue). Representative images at each time point under the two conditions are shown.

C. Rad51 foci count without Auxin. Number of foci in each cell were counted at each time point. At each time point more than 75 cells or all Rad51 positive cells were counted.

D. Rad51 foci count with Auxin. Number of foci in each cell were counted at each time point. At each time point more than 75 cells or all Rad51 positive cells were counted.

**Figure 17:**

**A)**

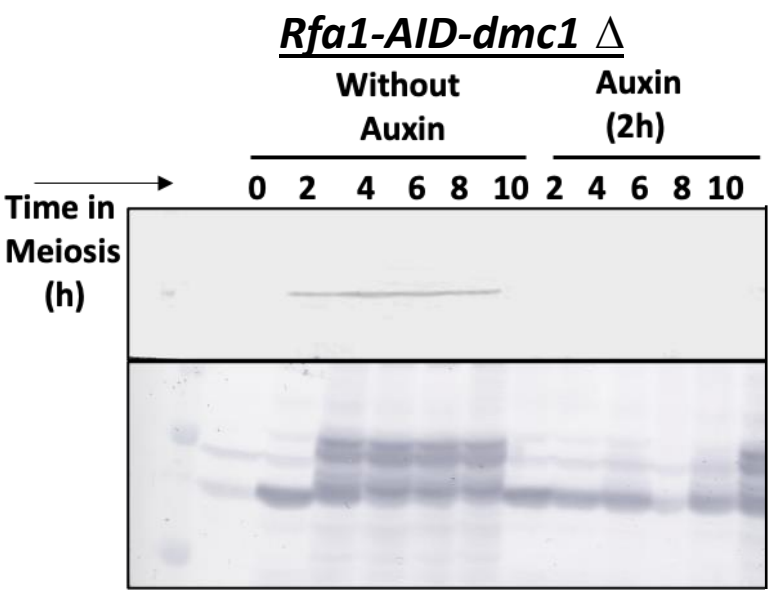
Rfa1-AID-dmc1 Δ
Without Auxin
Auxin (2h)
Time in Meiosis (h)
0 2 4 6 8 10 2 4 6 8 10

**Figure 17:**

A. Western Blot analysis with anti-H3-pT11 and anti-Hop1 with lysates obtained from *dmc1Δ -RFA1-AID* (SAY15/16) cells at various time points during meiosis with or without addition of Auxin at 2h and 4h.

**Figure 18:**

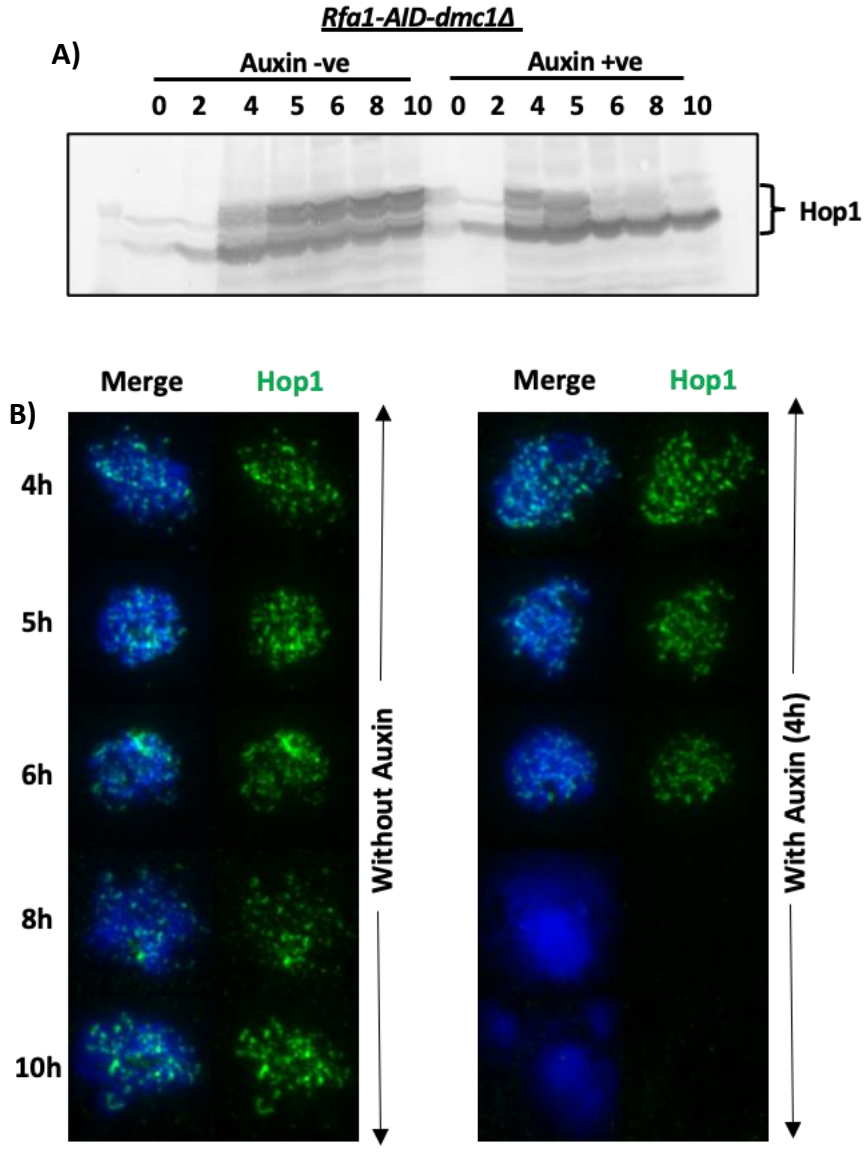
Rfa1-AID-dmc1Δ
A)
Auxin -ve
Auxin +ve
0 2 4 5 6 8 10 0 2 4 5 6 8 10
Hop1
B)
Merge
Hop1
Merge
Hop1
4h
5h
6h
8h
10h
Without Auxin
With Auxin (4h)

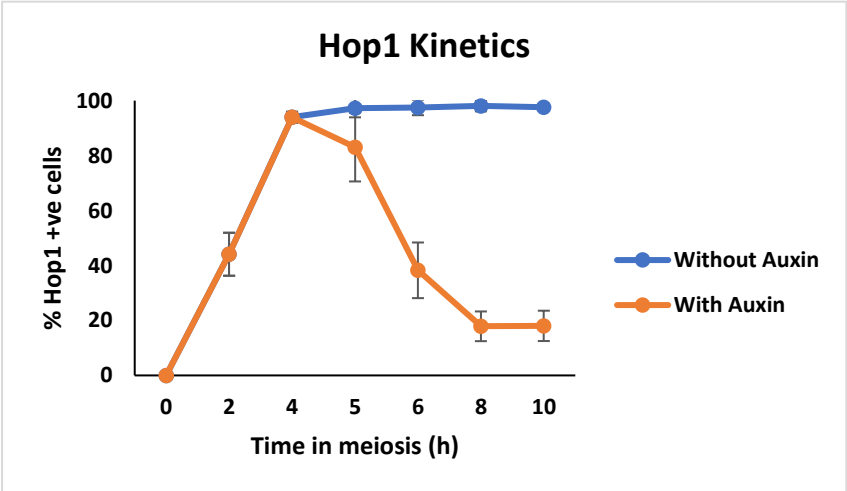
Hop1 Kinetics
% Hop1 +ve cells
100
80
60
40
20
0
0 2 4 5 6 8 10
Time in meiosis (h)
Without Auxin
With Auxin

**Figure 18:**

A. Western Blot analysis with anti-Hop1 with lysates obtained from *dmc1Δ -Rfa1-AID* (SAY62/63) cells at various time points during meiosis with or without addition of Auxin at 4h.

B. Hop1 staining. Nuclear spreads from *dmc1Δ -RFA1-AID* (SAY62/63) with or without addition of Auxin at 4h were stained with anti-Hop1 (Green) and DAPI (Blue). Representative images at each time point under the two conditions are shown.

C. Hop11 kinetics. The number of Hop11 positive cells (more than 5 foci) in *dmc1Δ -RFA1-AID* (SAY62/63) with or without addition of Auxin at 4h were counted at each time point. At each time point more than 50 cells were counted. (n=3)

**Figure 19:**

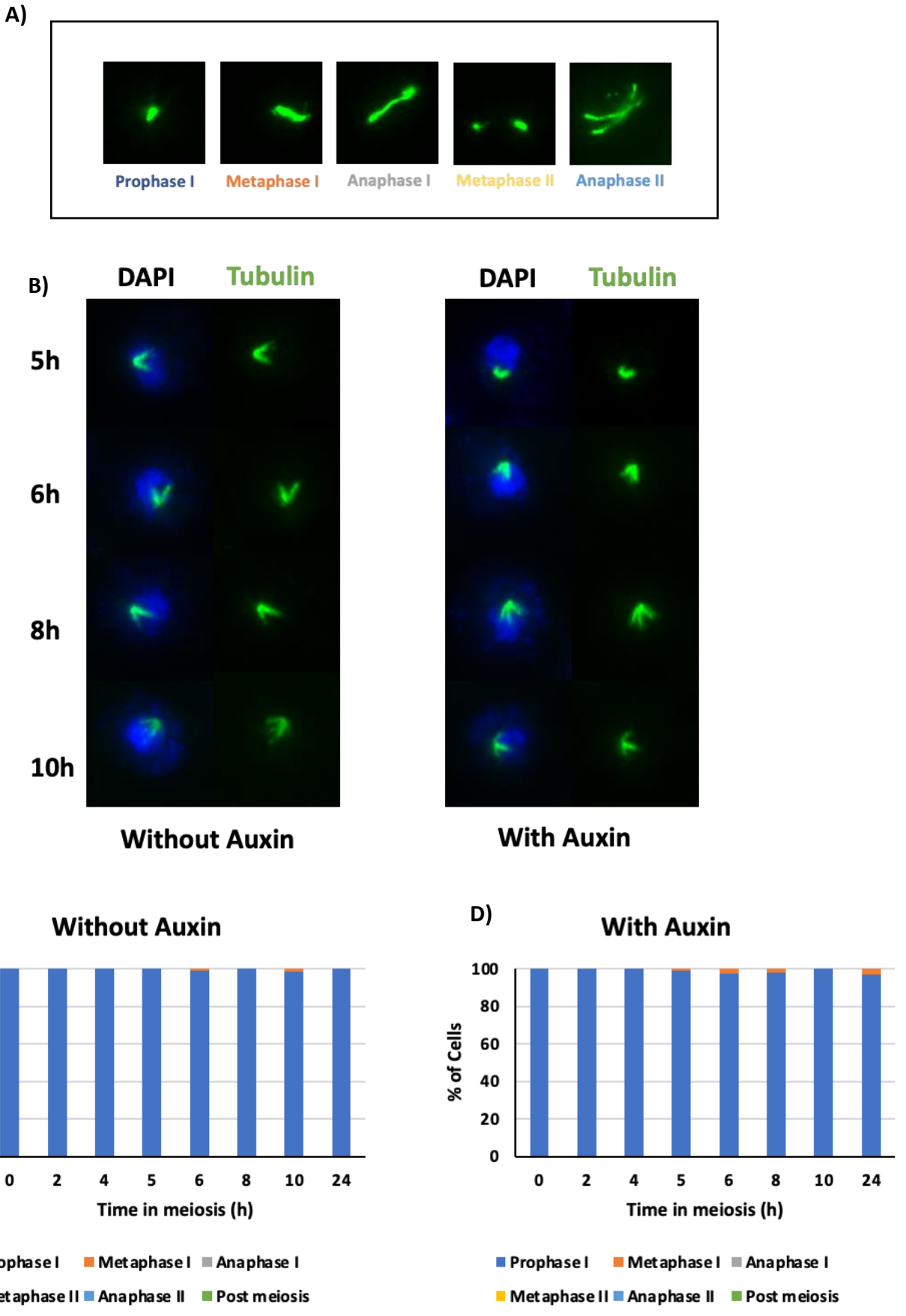
A)
Prophase I
Metaphase I
Anaphase I
Metaphase II
Anaphase II
B)
DAPI
Tubulin
DAPI
Tubulin
5h
6h
8h
10h
Without Auxin
With Auxin
C)
Without Auxin
% of Cells
100
80
60
40
20
0
0
2
4
5
6
8
10
24
Time in meiosis (h)
Prophase I
Metaphase I
Anaphase I
Metaphase II
Anaphase II
Post meiosis
D)
With Auxin
% of Cells
100
80
60
40
20
0
0
2
4
5
6
8
10
24
Time in meiosis (h)
Prophase I
Metaphase I
Anaphase I
Metaphase II
Anaphase II
Post meiosis

**Figure 19:**

A. Representative images of classes of tubulin staining during meiosis showing spindle elongation at different stages of meiosis.

B. Tubulin whole cell staining. *ndt80Δ -dmc1Δ -RFA1-AID* (SAY 80/81) cells with or without addition of Auxin at 4h were stained with anti-Tubulin (Green) and DAPI (Blue). Representative images at each time point under the two conditions are shown.

C. Meiotic progression without Auxin. Different classes of Tubulin staining were quantified from each time point. More than 100 cells were counted at each time point.

D. Meiotic progression with Auxin. Different classes of Tubulin staining were quantified from each time point. More than 100 cells were counted at each time point.

**Figure 20:**

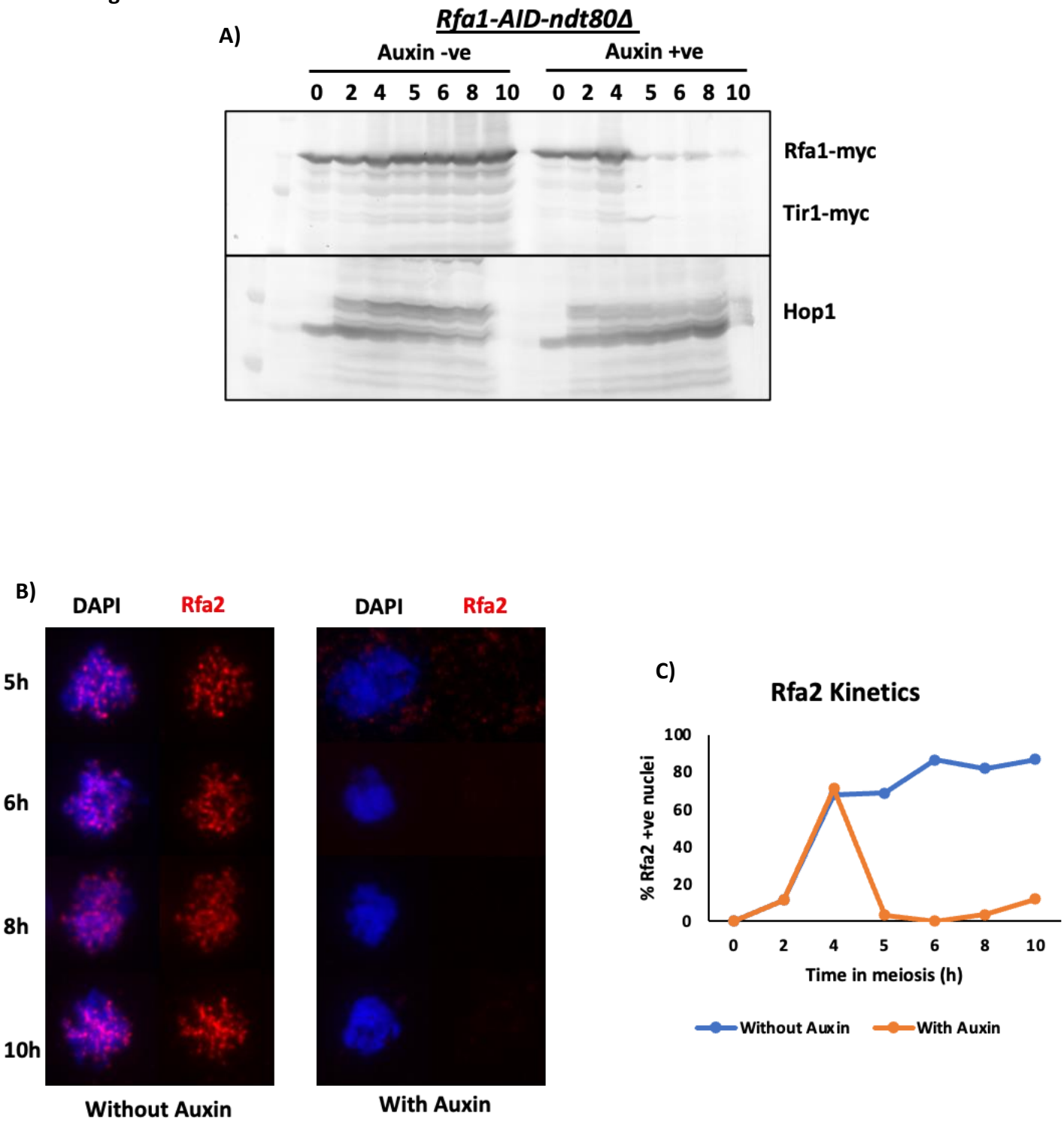
A)
Rfa1-AID-ndt80Δ
Auxin -ve
Auxin +ve
0 2 4 5 6 8 10 0 2 4 5 6 8 10
Rfa1-myc
Tir1-myc
Hop1
B)
DAPI
Rfa2
DAPI
Rfa2
5h
6h
8h
10h
Without Auxin
With Auxin
C)
Rfa2 Kinetics
% Rfa2 +ve nuclei
100
80
60
40
20
0
0 2 4 5 6 8 10
Time in meiosis (h)
Without Auxin
With Auxin

**Figure 20:**

A. Western Blot analysis with anti-myc and anti-Hop1 with lysates obtained from *ndt80Δ -dmc1Δ -RFA1-AID* (SAY 80/81) cells at various time points during meiosis with or without addition of Auxin at 4h.

B. Rfa2 staining. Nuclear spreads from *ndt80Δ -dmc1Δ -RFA1-AID* (SAY 80/81) with or without addition of Auxin at 4h were stained with anti-Rfa2 (Red) and DAPI (Blue). Representative images at each time point under the two conditions are shown.

C. Rfa2 kinetics. The number of Rfa2 positive cells (more than 5 foci) in *ndt80Δ -dmc1Δ -RFA1-AID* (SAY 80/81) with or without addition of Auxin at 4h were counted at each time point. At each time point more than 50 cells were counted.

**Figure 21:**

A)

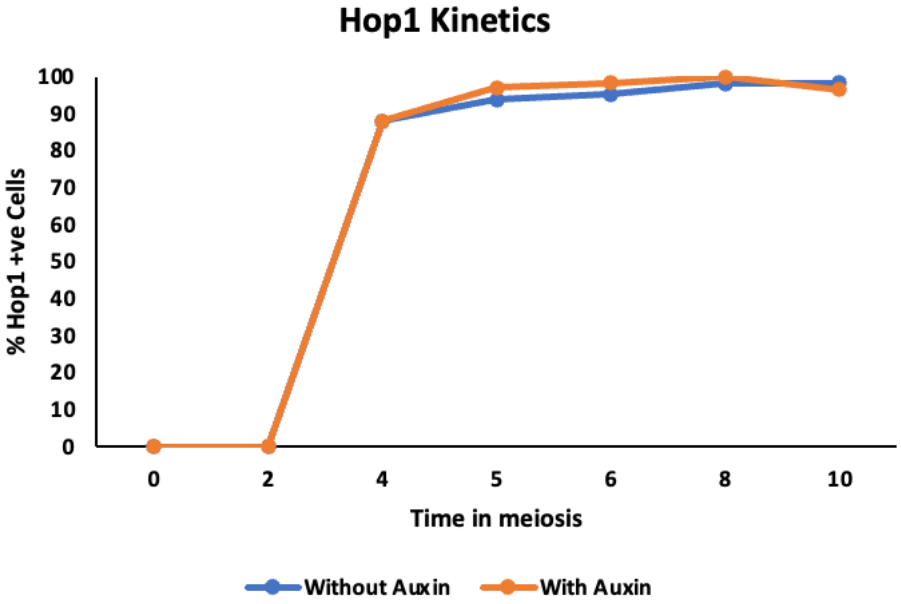
Hop1 Kinetics
% Hop1 +ve Cells
100
90
80
70
60
50
40
30
20
10
0
0
2
4
5
6
8
10
Time in meiosis
Without Auxin
With Auxin

B)

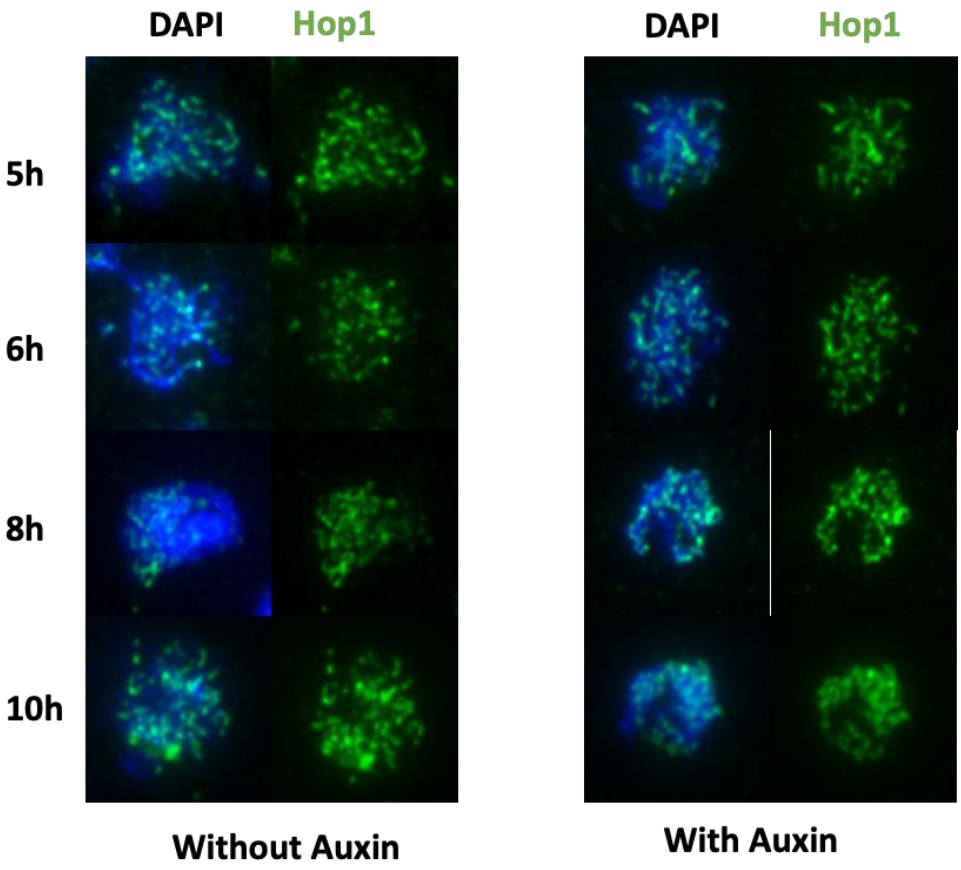
DAPI
Hop1
DAPI
Hop1
5h
6h
8h
10h
Without Auxin
With Auxin

**Figure 21:**

A. Hop1 kinetics. The number of Hop1 positive cells (more than 5 foci) in *ndt80Δ -dmc1Δ -RFA1-AID* (SAY 80/81) with or without addition of Auxin at 4h were counted at each time point. At each time point more than 50 cells were counted.

B. Hop1 staining. Nuclear spreads from *ndt80Δ -dmc1Δ -RFA1-AID* (SAY 80/81) with or without addition of Auxin at 4h were stained with anti-Hop1 (Green) and DAPI (Blue). Representative images at each time point under the two conditions are shown.

**Figure 22:**

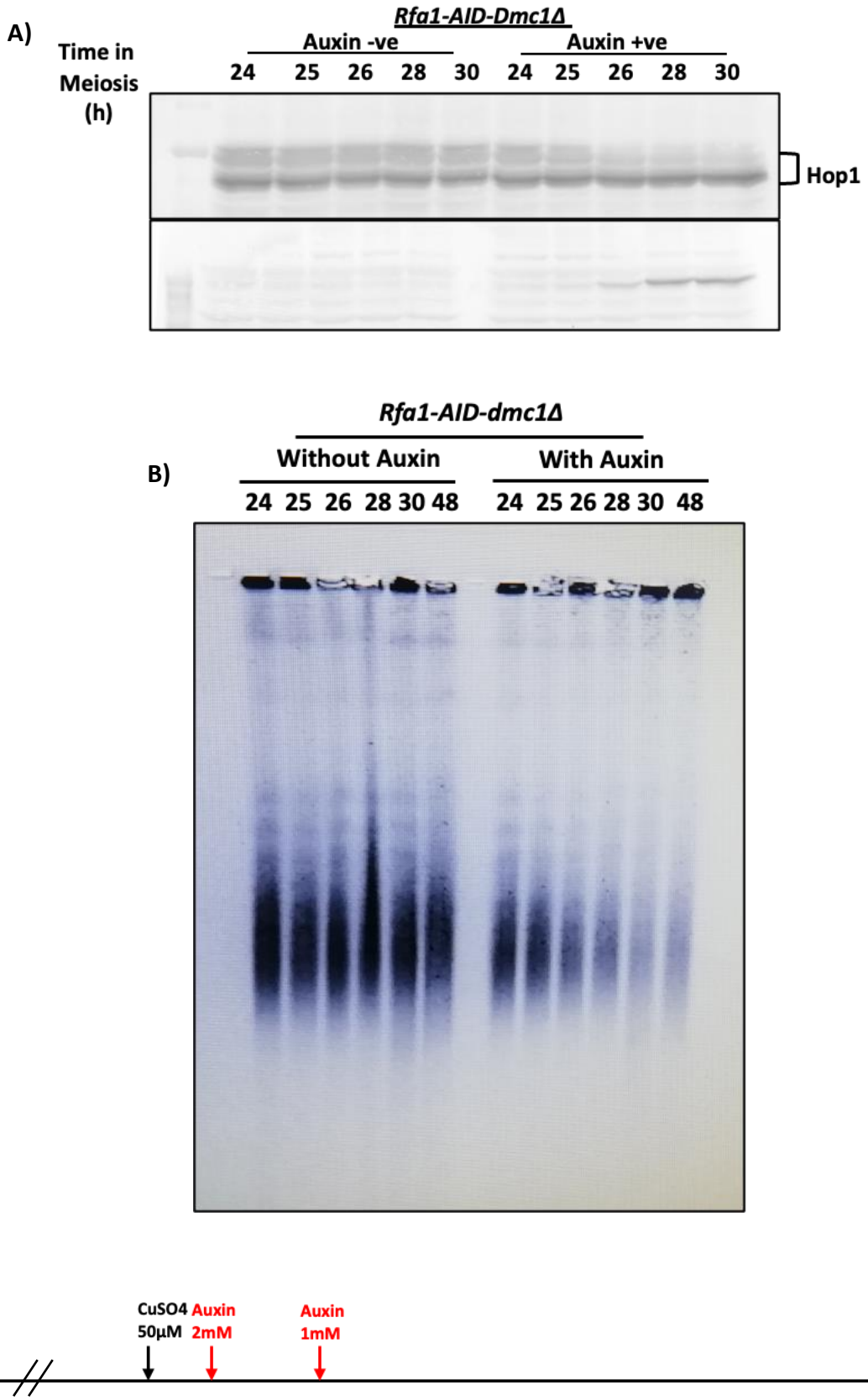
A)
Rfa1-AID-Dmc1Δ
Time in Meiosis (h)
Auxin -ve
Auxin +ve
24 25 26 28 30 24 25 26 28 30
Hop1
B)
Rfa1-AID-dmc1Δ
Without Auxin
With Auxin
24 25 26 28 30 48 24 25 26 28 30 48
C)
CuSO4 50µM
Auxin 2mM
Auxin 1mM
0h
23h
24h
26h
28h
30h
48h
Time in meiosis

**Figure 22:**

A. Western Blot analysis with anti-Hop1 with lysates obtained from *dmc1Δ -RFA1-AID* (SAY62/63) cells at various time points during meiosis with or without addition of Auxin at 24h.

B. CHEF analysis. Chromosomal DNA from *dmc1Δ -RFA1-AID* (SAY62/63) were analyzed using Clamped homogenous electric field Gel electrophoresis with or without addition of Auxin at 24h.

C. A schematic representation of timeline for addition of auxin and $CuSO_4$.

**Figure 23:**

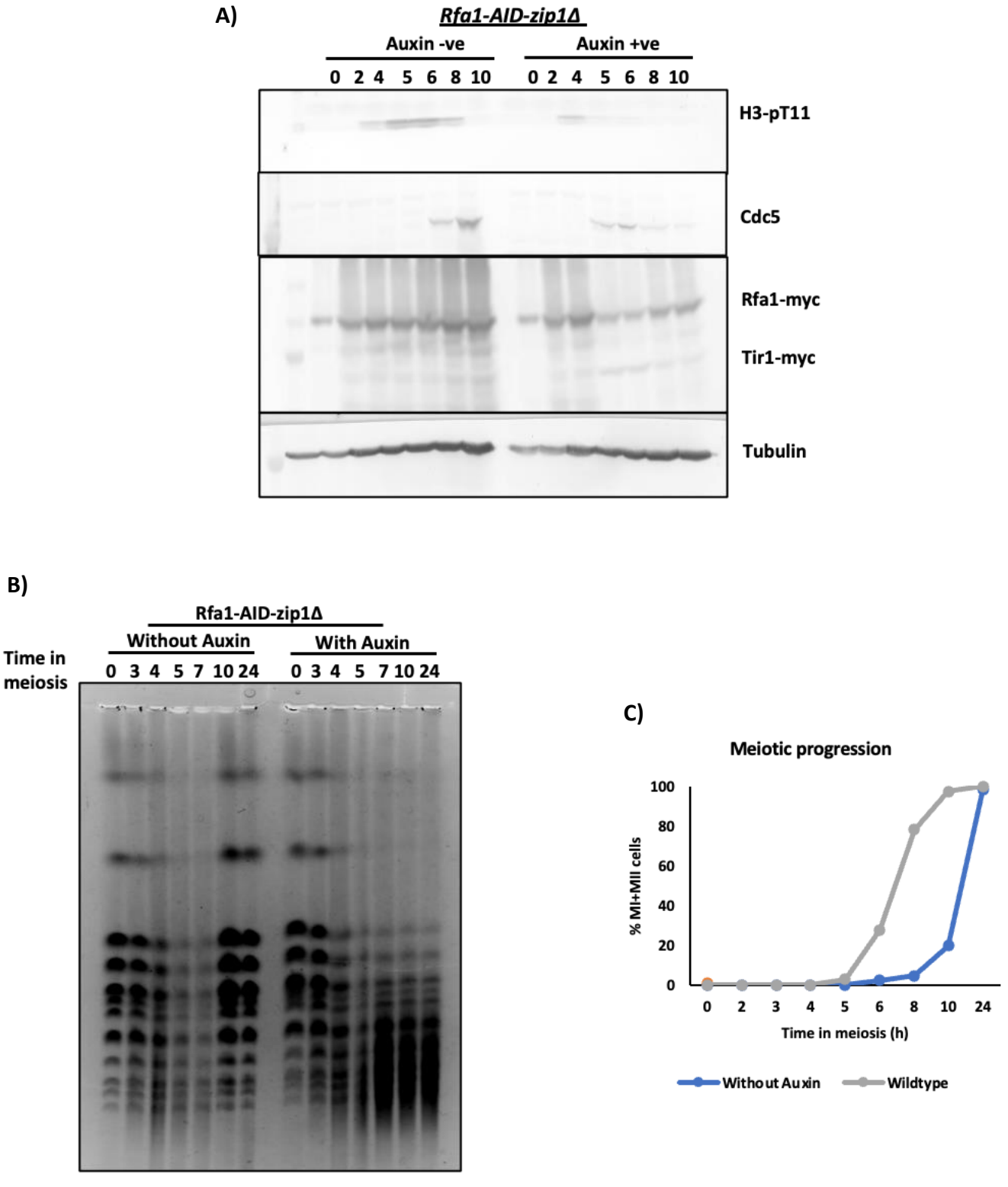
A)
Rfa1-AID-zip1Δ
Auxin -ve
Auxin +ve
0 2 4 5 6 8 10
0 2 4 5 6 8 10
H3-pT11
Cdc5
Rfa1-myc
Tir1-myc
Tubulin
B)
Rfa1-AID-zip1Δ
Without Auxin
With Auxin
Time in meiosis
0 3 4 5 7 10 24
0 3 4 5 7 10 24
C)
Meiotic progression
% MI+MII cells
100
80
60
40
20
0
0 2 3 4 5 6 8 10 24
Time in meiosis (h)
Without Auxin
Wildtype

**Figure 23:**

A. Western Blot analysis with anti-H3-pT11, anti-Cdc5, anti-myc and anti-tubulin with lysates obtained from *zip1Δ -RFA1-AID* (SAY 72/73) cells at various time points during meiosis with or without addition of Auxin at 4h.

B. CHEF analysis. Chromosomal DNA from *zip1Δ -RFA1-AID* (SAY 72/73) were analyzed using Clamped homogenous electric field Gel electrophoresis with or without addition of Auxin at 4h.

C. Meiotic Cell cycle progression. The entry into meiosis I and II by *zip1Δ -RFA1-AID* (SAY 72/73) cells and Wildtype (SAY 1/2) cells were analyzed using DAPI staining. More than 100 cells were counted from each time point. (n=3)

**Figure 24:**

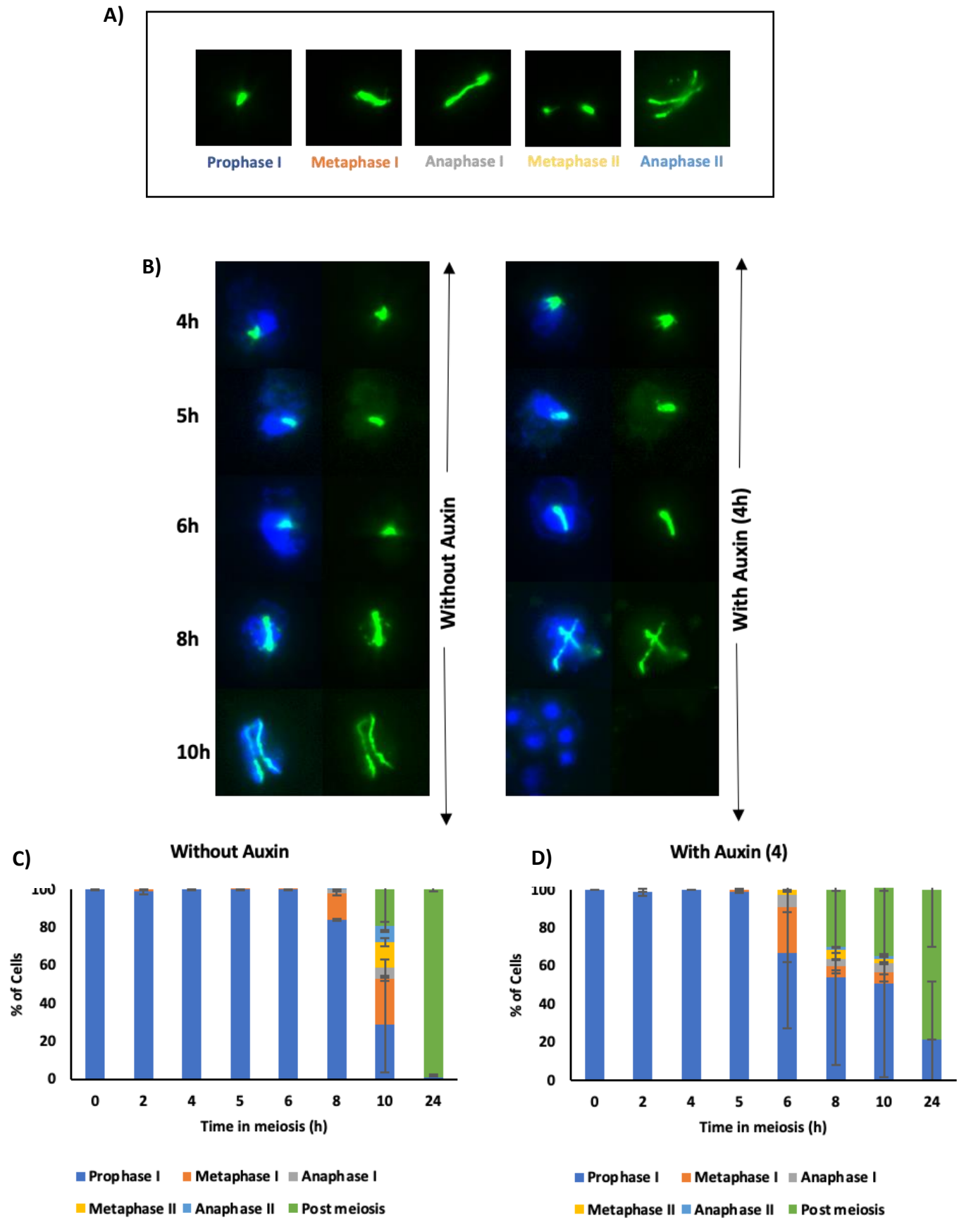
A)
Prophase I
Metaphase I
Anaphase I
Metaphase II
Anaphase II
B)
4h
5h
6h
8h
10h
Without Auxin
With Auxin (4h)
C)
Without Auxin
% of Cells
Time in meiosis (h)
Prophase I
Metaphase I
Anaphase I
Metaphase II
Anaphase II
Post meiosis
D)
With Auxin (4)
% of Cells
Time in meiosis (h)
Prophase I
Metaphase I
Anaphase I
Metaphase II
Anaphase II
Post meiosis

**Figure 24:**

A. Representative images of classes of tubulin staining during meiosis showing spindle elongation at different stages of meiosis.

B. Tubulin whole cell staining. *zip1Δ -RFA1-AID* (SAY 72/73) cells with or without addition of Auxin at 4h were stained with anti-Tubulin (Green) and DAPI (Blue). Representative images at each time point under the two conditions are shown.

C. Meiotic progression without Auxin. Different classes of Tubulin staining were quantified from each time point. More than 100 cells were counted at each time point. (n=3)

D. Meiotic progression with Auxin. Different classes of Tubulin staining were quantified from each time point. More than 100 cells were counted at each time point. (n=3)

**Figure 25:**

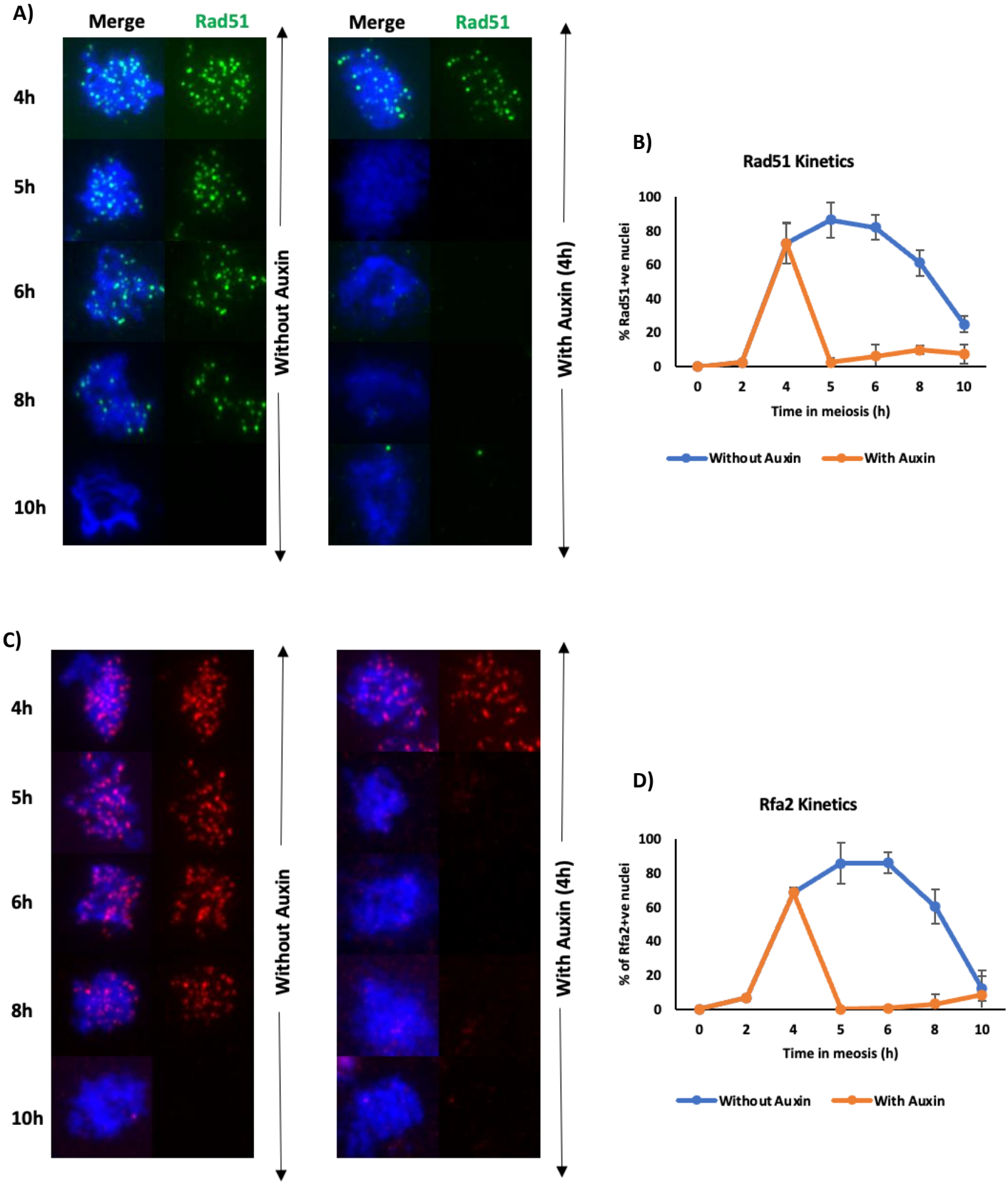
A)
Merge
Rad51
Merge
Rad51
4h
5h
6h
8h
10h
Without Auxin
With Auxin (4h)
B)
Rad51 Kinetics
% Rad51+ve nuclei
100
80
60
40
20
0
0
2
4
5
6
8
10
Time in meiosis (h)
Without Auxin
With Auxin
C)
4h
5h
6h
8h
10h
Without Auxin
With Auxin (4h)
D)
Rfa2 Kinetics
% of Rfa2+ve nuclei
100
80
60
40
20
0
0
2
4
5
6
8
10
Time in meosis (h)
Without Auxin
With Auxin

**Figure 25:**

A. Rad51 staining. Nuclear spreads from *zip1Δ -RFA1-AID* (SAY 72/73) with or without addition of Auxin at 4h were stained with anti-Rad51 (Green) and DAPI (Blue). Representative images at each time point under the two conditions are shown.

B. Rad51 kinetics. The number of Rad51 positive cells (more than 5 foci) were counted at each time point. At each time point more than 50 cells were counted. (n=3)

C. Rfa2 staining. Nuclear spreads from *zip1Δ -RFA1-AID* (SAY 72/73) with or without addition of Auxin at 4h were stained with anti-Rfa2 (Red) and DAPI (Blue). Representative images at each time point under the two conditions are shown.

D. Rfa2 kinetics. The number of Rfa2 positive cells (more than 5 foci) were counted at each time point. At each time point more than 50 cells were counted. (n=3)

**Figure 26:**

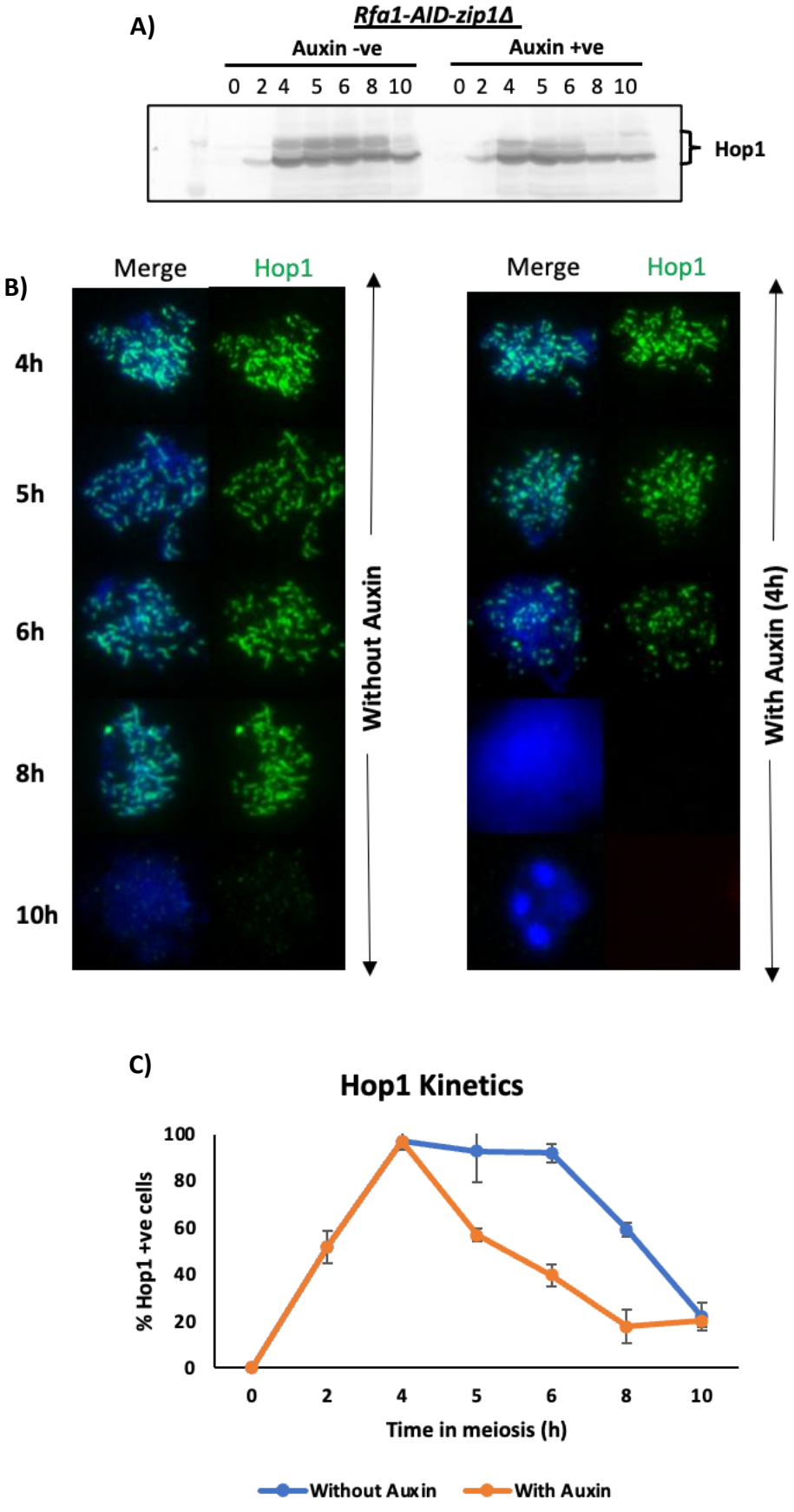
A)
Rfa1-AID-zip1Δ
Auxin -ve
Auxin +ve
0 2 4 5 6 8 10
0 2 4 5 6 8 10
Hop1
B)
Merge
Hop1
Merge
Hop1
4h
5h
6h
8h
10h
Without Auxin
With Auxin (4h)
C)
Hop1 Kinetics
% Hop1 +ve cells
100
80
60
40
20
0
0
2
4
5
6
8
10
Time in meiosis (h)
Without Auxin
With Auxin

**Figure 26:**

A. Western Blot analysis with anti-Hop1 with lysates obtained from *zip1Δ -RFA1-AID* (SAY 72/73) cells at various time points during meiosis with or without addition of Auxin at 4h.

B. Hop1 staining. Nuclear spreads from *zip1Δ -RFA1-AID* (SAY 72/73) with or without addition of Auxin at 4h were stained with anti-Hop1 (Green) and DAPI (Blue). Representative images at each time point under the two conditions are shown.

C. Hop1 kinetics. The number of Hop1 positive cells (more than 5 foci) in *zip1Δ -RFA1-AID* (SAY 72/73) with or without addition of Auxin at 4h were counted at each time point. At each time point more than 50 cells were counted. (n=3)

**Figure 27:**

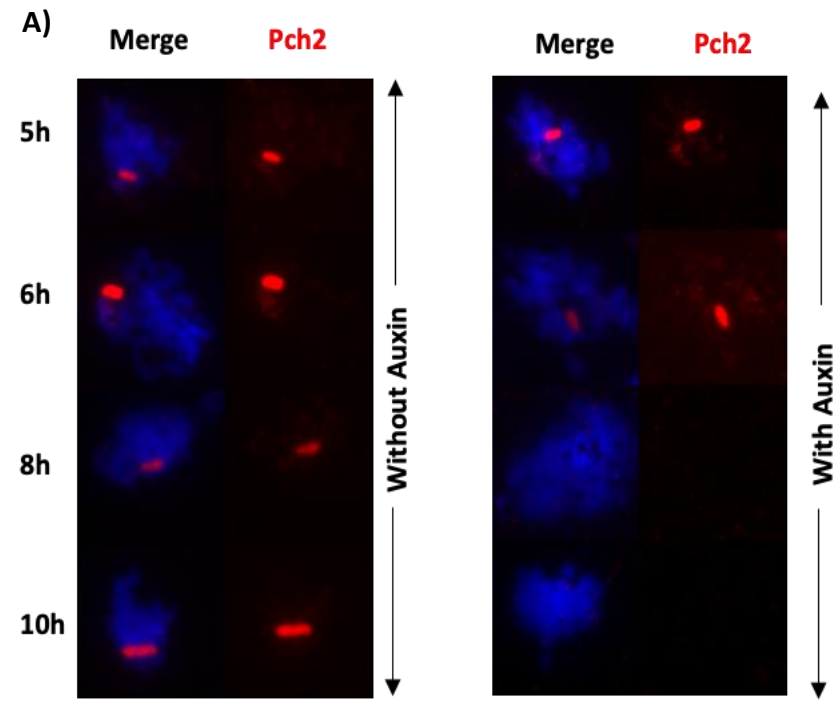
A)
Merge
Pch2
Merge
Pch2
5h
6h
8h
10h
Without Auxin
With Auxin

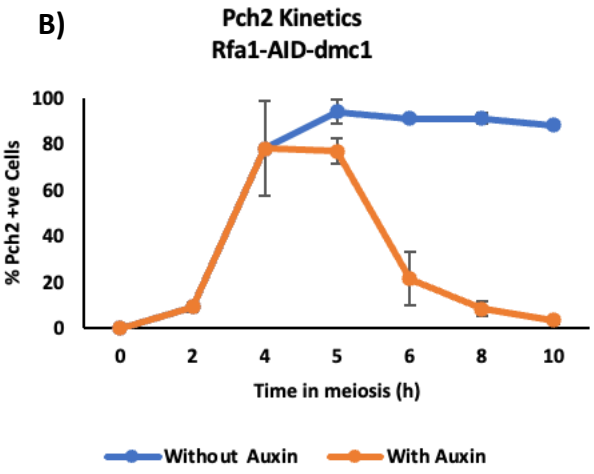
B)
Pch2 Kinetics
Rfa1-AID-dmc1
% Pch2 +ve Cells
100
80
60
40
20
0
0
2
4
5
6
8
10
Time in meiosis (h)
Without Auxin
With Auxin

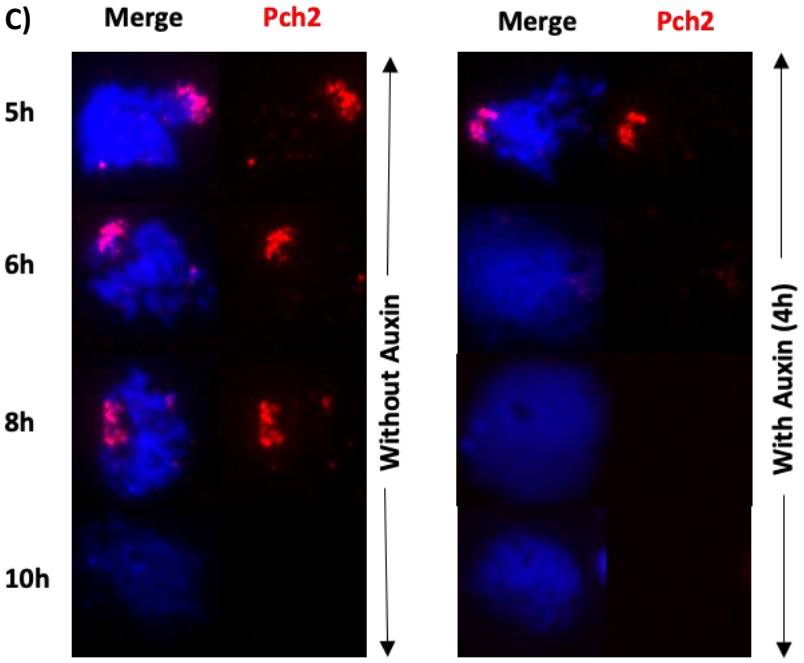
C)
Merge
Pch2
Merge
Pch2
5h
6h
8h
10h
Without Auxin
With Auxin (4h)

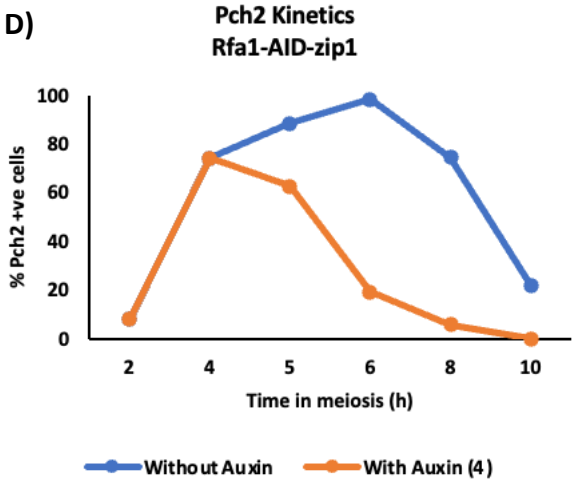
D)
Pch2 Kinetics
Rfa1-AID-zip1
% Pch2 +ve cells
100
80
60
40
20
0
2
4
5
6
8
10
Time in meiosis (h)
Without Auxin
With Auxin (4)

**Figure 27:**

A. Pch2 staining. Nuclear spreads from *dmc1Δ -RFA1-AID* (SAY62/63) with or without addition of Auxin at 4h were stained with anti-Pch2 (Red) and DAPI (Blue). Representative images at each time point under the two conditions are shown.

B. Pch2 kinetics. The number of Pch2 positive cells were counted at each time point. At each time point more than 50 cells were counted. (n=3)

C. Pch2 staining. Nuclear spreads from *zip1Δ -RFA1-AID* (SAY 72/73) with or without addition of Auxin at 4h were stained with anti-Pch2 (Red) and DAPI (Blue). Representative images at each time point under the two conditions are shown.

D. Pch2 kinetics. The number of Pch2 positive cells were counted at each time point. At each time point more than 50 cells were counted.

**Figure 28:**

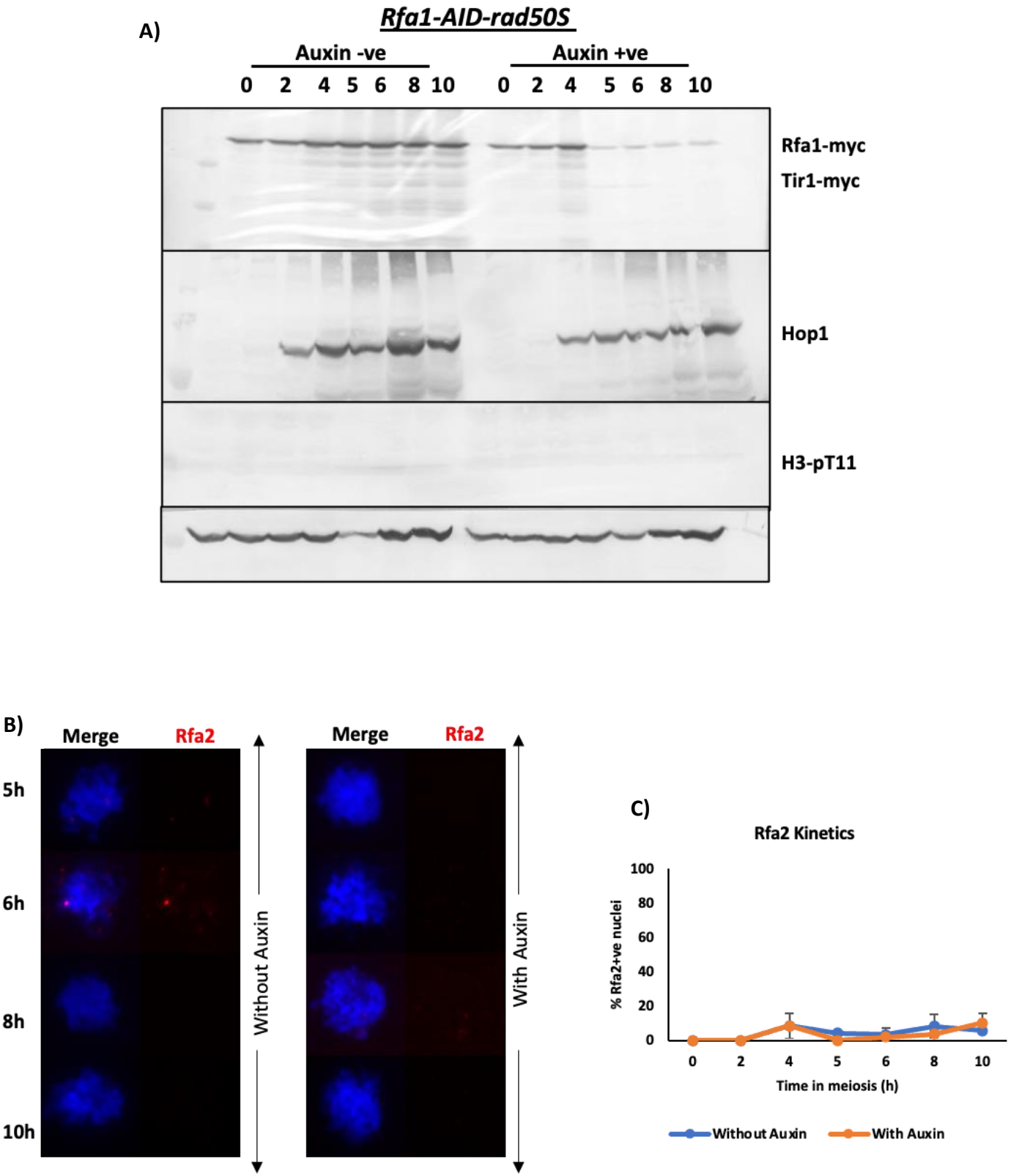
A)
Rfa1-AID-rad50S
Auxin -ve
Auxin +ve
0 2 4 5 6 8 10
0 2 4 5 6 8 10
Rfa1-myc
Tir1-myc
Hop1
H3-pT11
B)
Merge
Rfa2
Merge
Rfa2
5h
6h
8h
10h
Without Auxin
With Auxin
C)
Rfa2 Kinetics
% Rfa2+ve nuclei
100
80
60
40
20
0
0 2 4 5 6 8 10
Time in meiosis (h)
Without Auxin
With Auxin

**Figure 28:**

A. Western Blot analysis with anti-H3-pT11, anti-Hop1, anti-myc and anti-tubulin with lysates obtained from *rad50S-RFA1-AID* (SAY68/69) cells at various time points during meiosis with or without addition of Auxin at 4h.

B. Rfa2 staining. Nuclear spreads from *rad50S-RFA1-AID* (SAY68/69) with or without addition of Auxin at 4h were stained with anti-Rfa2 (Red) and DAPI (Blue). Representative images at each time point under the two conditions are shown.

C. Rfa2 kinetics. The number of Rfa2 positive cells (more than 5 foci) were counted at each time point. At each time point more than 50 cells were counted. (n=3)

**Figure 29:**

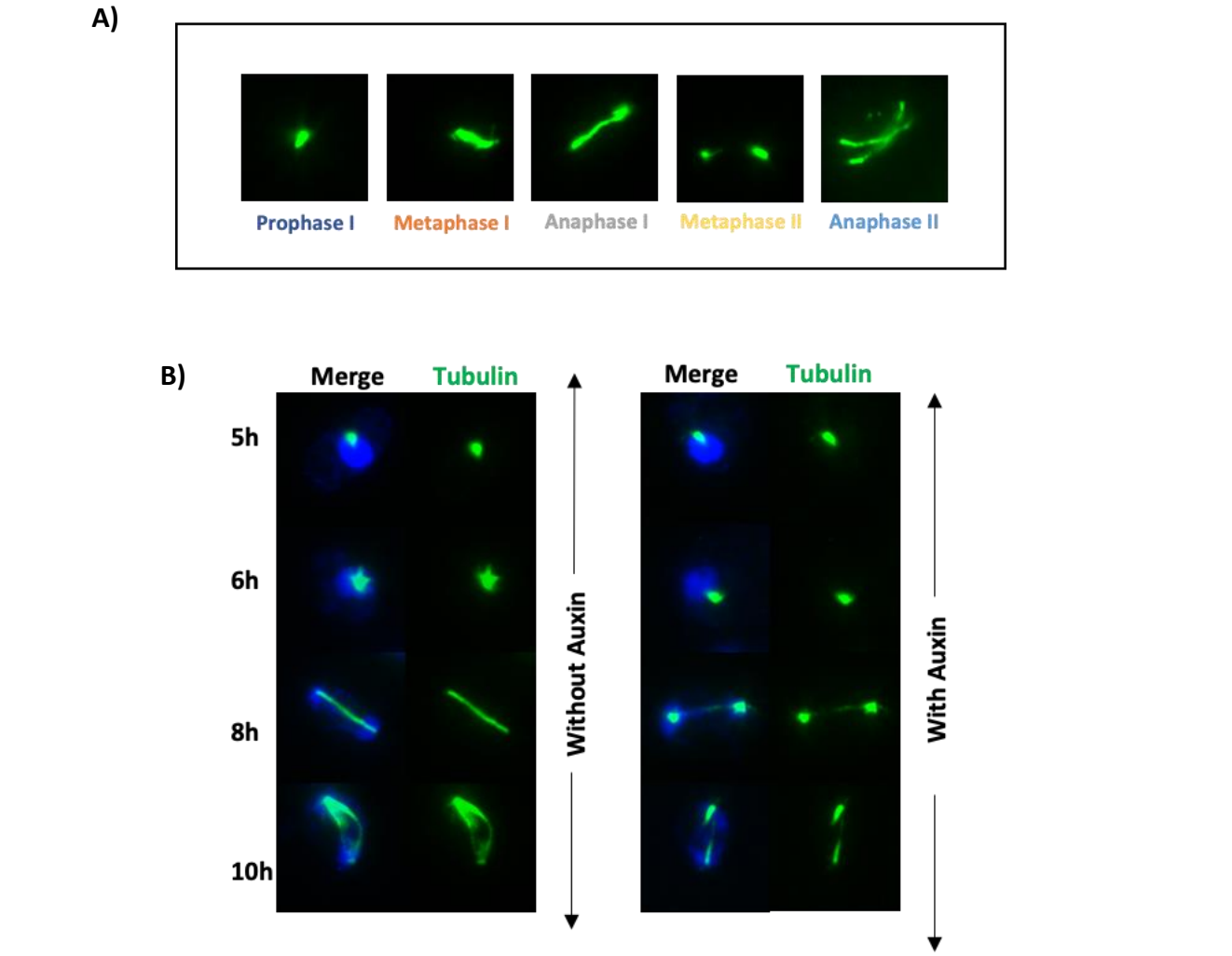
A)
Prophase I
Metaphase I
Anaphase I
Metaphase II
Anaphase II
B)
Merge
Tubulin
Merge
Tubulin
5h
6h
8h
10h
Without Auxin
With Auxin
C)
Without Auxin
% of Cells
100
90
80
70
60
50
40
30
20
10
0
0
2
3
4
5
6
8
10
24
Time in meiosis (h)
Prophase I
Metaphase I
Anaphase I
Metaphase II
Anaphase II
Post meiosis II
D)
With Auxin (4h)
% of Cells
100
90
80
70
60
50
40
30
20
10
0
0
2
3
4
5
6
8
10
24
Time in meiosis (h)
Prophase I
Metaphase I
Anaphase I
Metaphase II
Anaphase II
Post meiosis

**Figure 29:**

A. Representative images of classes of tubulin staining during meiosis showing spindle elongation at different stages of meiosis.

B. Tubulin whole cell staining. *rad50S-RFA1-AID* (SAY68/69) cells with or without addition of Auxin at 4h were stained with anti-Tubulin (Green) and DAPI (Blue). Representative images at each time point under the two conditions are shown.

C. Meiotic progression without Auxin. Different classes of Tubulin staining were quantified from each time point. More than 100 cells were counted at each time point.

D. Meiotic progression with Auxin. Different classes of Tubulin staining were quantified from each time point. More than 100 cells were counted at each time point.

**Figure 30:**

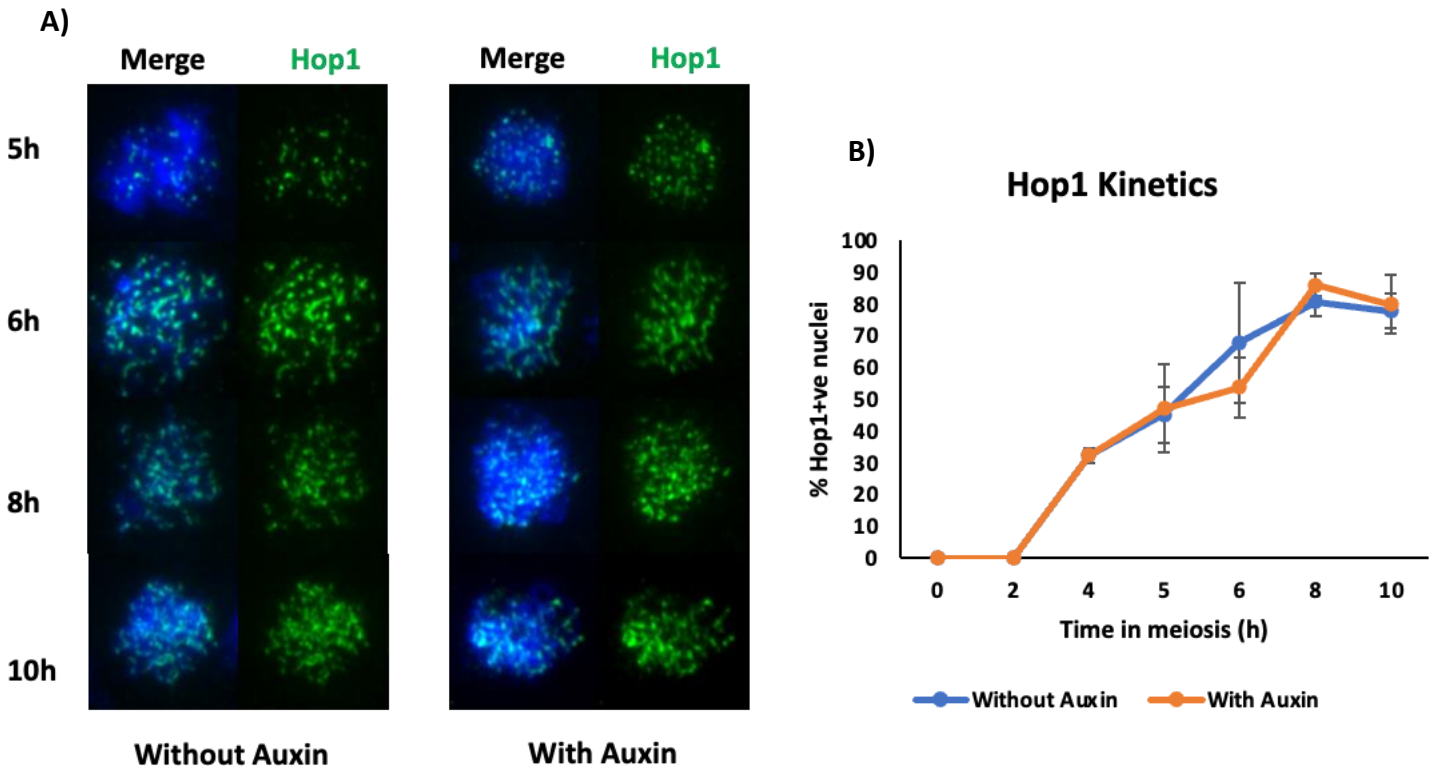
A)
Merge
Hop1
Merge
Hop1
5h
6h
8h
10h
Without Auxin
With Auxin
B)
Hop1 Kinetics
% Hop1+ve nuclei
100
90
80
70
60
50
40
30
20
10
0
0
2
4
5
6
8
10
Time in meiosis (h)
Without Auxin
With Auxin

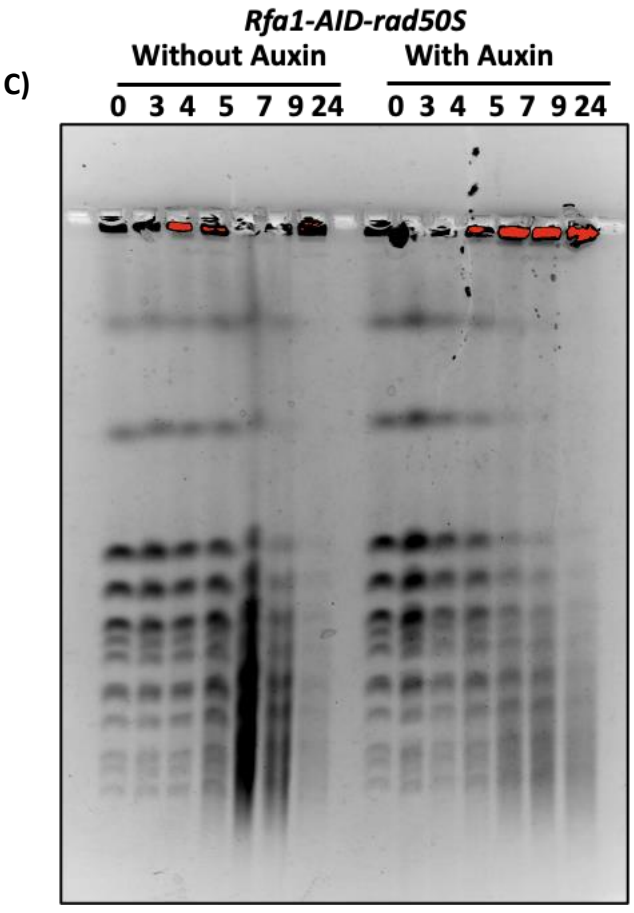
C)
Rfa1-AID-rad50S
Without Auxin
With Auxin
0 3 4 5 7 9 24
0 3 4 5 7 9 24

**Figure 30:**

A. Hop1 staining. Nuclear spreads from *rad50S-RFA1-AID* (SAY68/69) with or without addition of Auxin at 4h were stained with anti-Hop1 (Green) and DAPI (Blue). Representative images at each time point under the two conditions are shown.

B. Hop1 kinetics. The number of Hop1 positive cells (more than 5 foci) were counted at each time point. At each time point more than 50 cells were counted. (n=3)

C. CHEF analysis. Chromosomal DNA from *rad50S-RFA1-AID* (SAY68/69) were analyzed using Clamped homogenous electric field Gel electrophoresis with or without addition of Auxin at 4h.

# Roles of RPA during Meiosis

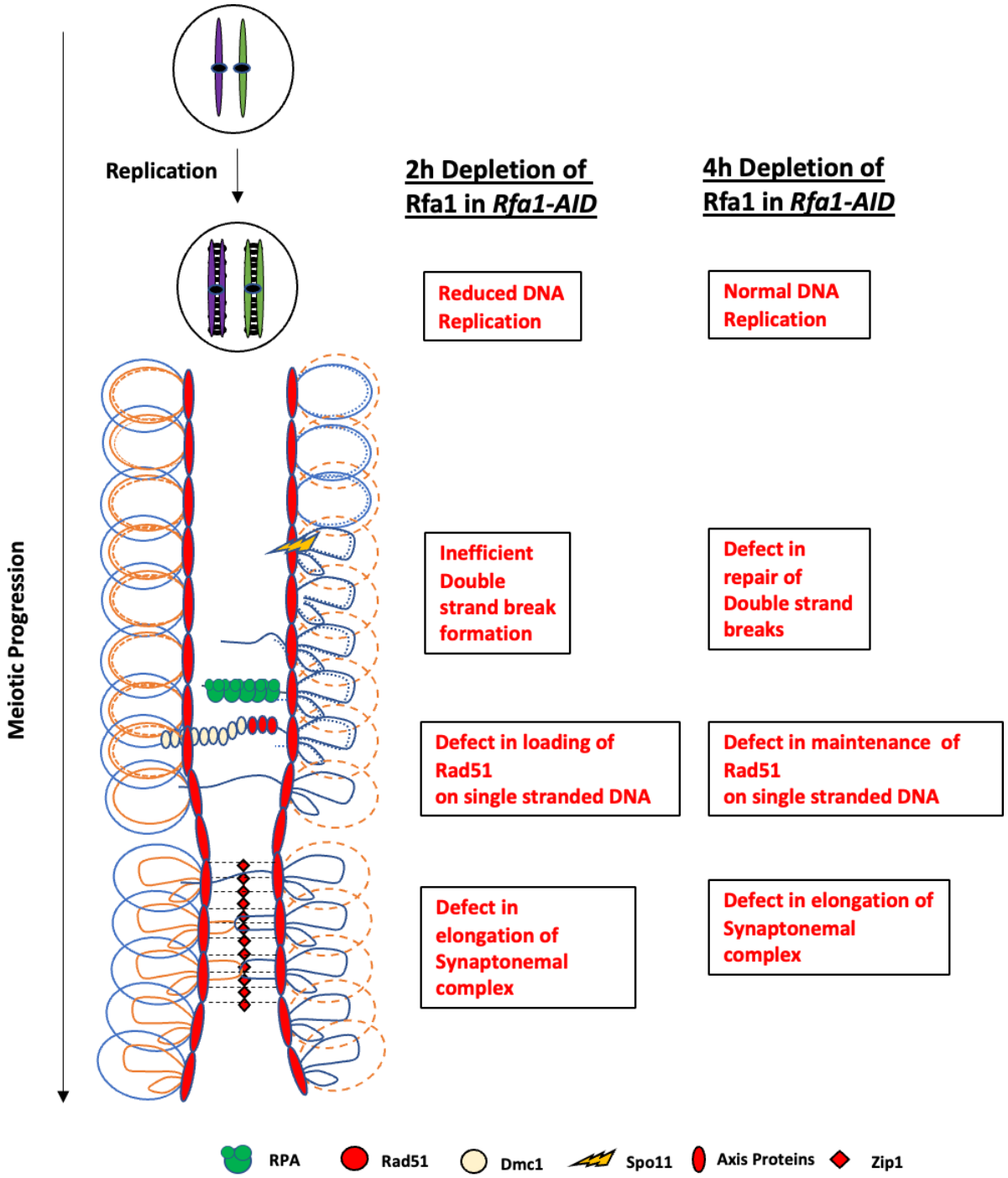


## Roles of RPA during Meiosis:

- Premeiotic S-phase replication
- Formation and repair of double stranded breaks
- Loading and maintenance of Rad51 recombinase on single stranded DNA
- Elongation of synaptonemal complex.

## Role of RPA during recombination checkpoint in dmc1 _ cells

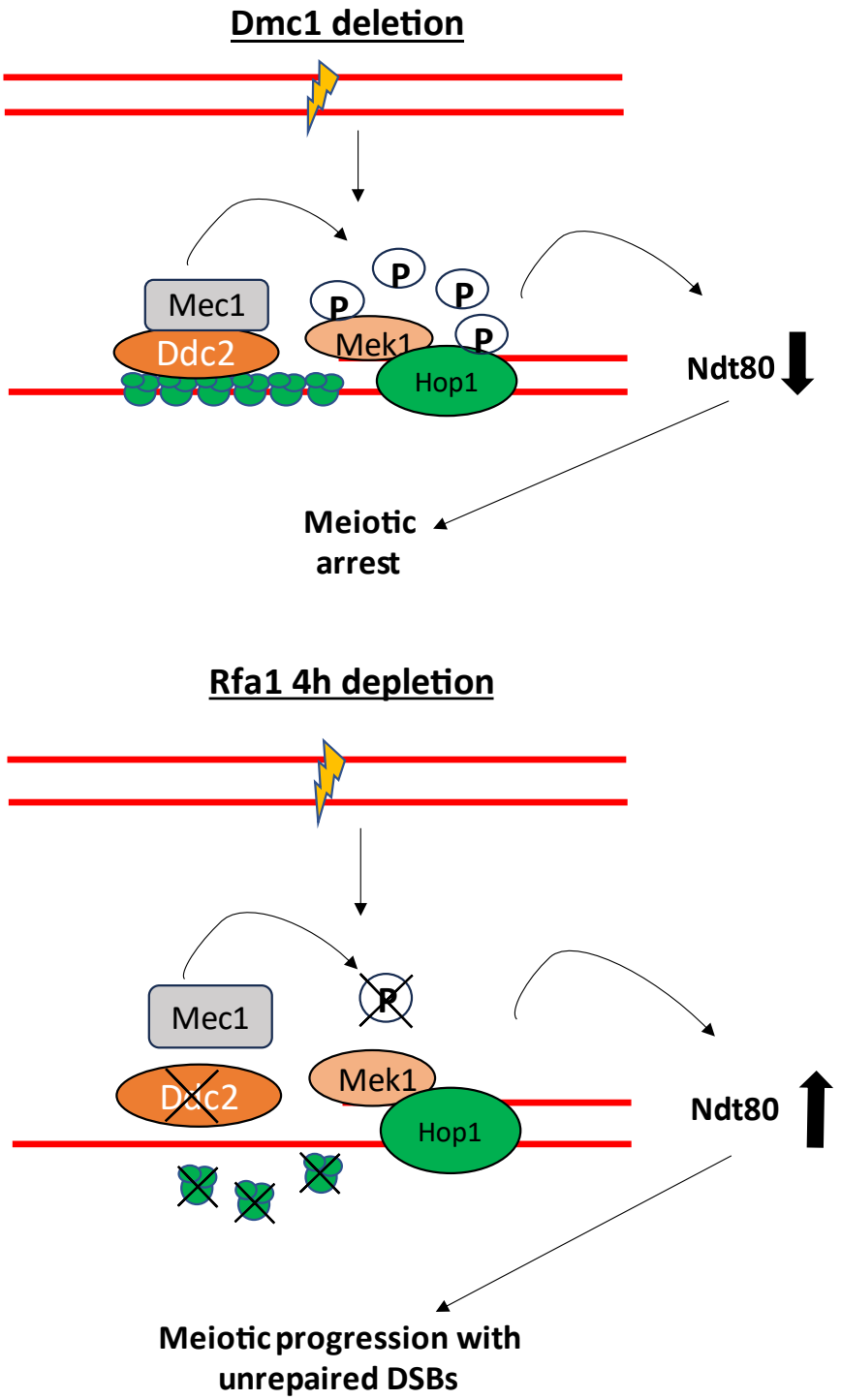


- RPA acts as a sensor for accumulation of ssDNA to activate the recombination checkpoint.

- Unlike most other checkpoint mutants RPA alleviates the checkpoint response while accumulating double stranded breaks which leads to improper segregation of chromosomes.

## References

**Agarwal S, Roeder GS**. Zip3 provides a link between recombination enzymes and synaptonemal complex proteins. Cell. 2000 Jul 21;102(2):245-55. doi: 10.1016/s0092-8674(00)00029-5. PMID: 10943844.

**Bailis JM, Roeder GS.** Pachytene exit controlled by reversal of Mek1-dependent phosphorylation. Cell. 2000 Apr 14;101(2):211-21. doi: 10.1016/S0092-8674(00)80831-4. PMID: 10786836.

**Bishop DK, Park D, Xu L, Kleckner N.** DMC1: a meiosis-specific yeast homolog of E. coli recA required for recombination, synaptonemal complex formation, and cell cycle progression. Cell. 1992 May 1;69(3):439-56. doi: 10.1016/0092-8674(92)90446-j. PMID: 1581960.

**Bishop DK.** RecA homologs Dmc1 and Rad51 interact to form multiple nuclear complexes prior to meiotic chromosome synapsis. Cell. 1994 Dec 16;79(6):1081-92. doi: 10.1016/0092-8674(94)90038-8. PMID: 7528104.

**Blackford AN, Jackson SP.** ATM, ATR, and DNA-PK: The Trinity at the Heart of the DNA Damage Response. Mol Cell. 2017 Jun 15;66(6):801-817. doi: 10.1016/j.molcel.2017.05.015. PMID: 28622525.

**Börner GV, Barot A, Kleckner N.** Yeast Pch2 promotes domainal axis organization, timely recombination progression, and arrest of defective recombinosomes during

meiosis. Proc Natl Acad Sci U S A. 2008 Mar 4;105(9):3327-32. doi: 10.1073/pnas.0711864105. Epub 2008 Feb 27. PMID: 18305165; PMCID: PMC2265181.

**Börner GV, Kleckner N, Hunter N.** Crossover/noncrossover differentiation, synaptonemal complex formation, and regulatory surveillance at the leptotene/zygotene transition of meiosis. Cell. 2004 Apr 2;117(1):29-45. doi: 10.1016/s0092-8674(04)00292-2. PMID: 15066280.

**Carballo JA, Panizza S, Serrentino ME, Johnson AL, Geymonat M, Borde V, Klein F, Cha RS.** Budding yeast ATM/ATR control meiotic double-strand break (DSB) levels by down-regulating Rec114, an essential component of the DSB-machinery. PLoS Genet. 2013 Jun;9(6):e1003545. doi: 10.1371/journal.pgen.1003545. Epub 2013 Jun 27. PMID: 23825959; PMCID: PMC3694840.

**Challa K, Fajish V G, Shinohara M, Klein F, Gasser SM, Shinohara A.** Meiosis-specific prophase-like pathway controls cleavage-independent release of cohesin by Wapl phosphorylation. PLoS Genet. 2019 Jan 3;15(1):e1007851. doi: 10.1371/journal.pgen.1007851. PMID: 30605471; PMCID: PMC6317811.

**Chu G.** Pulsed field electrophoresis in contour-clamped homogeneous electric fields for the resolution of DNA by size or topology. Electrophoresis. 1989 May-Jun;10(5-6):290-5. doi: 10.1002/elps.1150100504. PMID: 2670544.

**Chu S, Herskowitz I.** Gametogenesis in yeast is regulated by a transcriptional cascade dependent on Ndt80. Mol Cell. 1998 Apr;1(5):685-96. doi: 10.1016/s1097-2765(00)80068-4. PMID: 9660952.

**Chua PR, Roeder GS.** Zip2, a meiosis-specific protein required for the initiation of chromosome synapsis. Cell. 1998 May 1;93(3):349-59. doi: 10.1016/s0092-8674(00)81164-2. PMID: 9590170.

**Ciccia A, Elledge SJ.** The DNA damage response: making it safe to play with knives. Mol Cell. 2010 Oct 22;40(2):179-204. doi: 10.1016/j.molcel.2010.09.019. PMID: 20965415; PMCID: PMC2988877.

**Clerici M, Paciotti V, Baldo V, Romano M, Lucchini G, Longhese MP.** Hyperactivation of the yeast DNA damage checkpoint by TEL1 and DDC2 overexpression. EMBO J. 2001 Nov 15;20(22):6485-98. doi: 10.1093/emboj/20.22.6485. PMID: 11707419; PMCID: PMC125310.

**Clyne RK, Katis VL, Jessop L, Benjamin KR, Herskowitz I, Lichten M, Nasmyth K.** Polo-like kinase Cdc5 promotes chiasmata formation and cosegregation of sister centromeres at meiosis I. Nat Cell Biol. 2003 May;5(5):480-5. doi: 10.1038/ncb977. PMID: 12717442.

**Falck J, Coates J, Jackson SP.** Conserved modes of recruitment of ATM, ATR and DNA-PKcs to sites of DNA damage. Nature. 2005 Mar 31;434(7033):605-11. doi: 10.1038/nature03442. Epub 2005 Mar 2. PMID: 15758953.

**Gasior SL, Wong AK, Kora Y, Shinohara A, Bishop DK.** Rad52 associates with RPA and functions with rad55 and rad57 to assemble meiotic recombination complexes. Genes Dev. 1998 Jul 15;12(14):2208-21. doi: 10.1101/gad.12.14.2208. PMID: 9679065; PMCID: PMC317010.

**Gray S, Allison RM, Garcia V, Goldman AS, Neale MJ.** Positive regulation of meiotic DNA double-strand break formation by activation of the DNA damage checkpoint kinase Mec1(ATR). Open Biol. 2013 Jul 31;3(7):130019. doi: 10.1098/rsob.130019. PMID: 23902647; PMCID: PMC3728922.

**Handel MA, Schimenti JC.** Genetics of mammalian meiosis: regulation, dynamics and impact on fertility. Nat Rev Genet. 2010 Feb;11(2):124-36. doi: 10.1038/nrg2723. Epub 2010 Jan 6. PMID: 20051984.

**Hayase A, Takagi M, Miyazaki T, Oshiumi H, Shinohara M, Shinohara A.** A protein complex containing Mei5 and Sae3 promotes the assembly of the meiosis-specific RecA homolog Dmc1. Cell. 2004 Dec 29;119(7):927-40. doi: 10.1016/j.cell.2004.10.031. PMID: 15620352.

**Hochwagen A, Amon A.** Checking your breaks: surveillance mechanisms of meiotic recombination. Curr Biol. 2006 Mar 21;16(6):R217-28. doi: 10.1016/j.cub.2006.03.009. PMID: 16546077.

**Hong EJ, Roeder GS.** A role for Ddc1 in signaling meiotic double-strand breaks at the pachytene checkpoint. Genes Dev. 2002 Feb 1;16(3):363-76. doi: 10.1101/gad.938102. PMID: 11825877; PMCID: PMC155327.

**Keeney S, Giroux CN, Kleckner N.** Meiosis-specific DNA double-strand breaks are catalyzed by Spo11, a member of a widely conserved protein family. Cell. 1997 Feb 7;88(3):375-84. doi: 10.1016/s0092-8674(00)81876-0. PMID: 9039264.

**Kerr GW, Sarkar S, Arumugam P.** How to halve ploidy: lessons from budding yeast meiosis. Cell Mol Life Sci. 2012 Sep;69(18):3037-51. doi: 10.1007/s00018-012-0974-9. Epub 2012 Apr 6. PMID: 22481439.

**Klein F, Mahr P, Galova M, Buonomo SB, Michaelis C, Nairz K, Nasmyth K.** A central role for cohesins in sister chromatid cohesion, formation of axial elements, and recombination during yeast meiosis. Cell. 1999 Jul 9;98(1):91-103. doi: 10.1016/S0092-8674(00)80609-1. PMID: 10412984.

**Krogh BO, Symington LS.** Recombination proteins in yeast. Annu Rev Genet. 2004;38:233-71. doi: 10.1146/annurev.genet.38.072902.091500. PMID: 15568977.

**Leu JY, Roeder GS.** The pachytene checkpoint in S. cerevisiae depends on Swe1-mediated phosphorylation of the cyclin-dependent kinase Cdc28. Mol Cell. 1999 Nov;4(5):805-14. doi: 10.1016/s1097-2765(00)80390-1. PMID: 10619027.

**Lo HC, Kunz RC, Chen X, Marullo A, Gygi SP, Hollingsworth NM.** Cdc7-Dbf4 is a gene-specific regulator of meiotic transcription in yeast. Mol Cell Biol. 2012 Jan;32(2):541-57. doi: 10.1128/MCB.06032-11. Epub 2011 Nov 21. PMID: 22106412; PMCID: PMC3255779.

**Longhese MP, Bonetti D, Guerini I, Manfrini N, Clerici M.** DNA double-strand breaks in meiosis: checking their formation, processing and repair. DNA Repair (Amst). 2009 Sep 2;8(9):1127-38. doi: 10.1016/j.dnarep.2009.04.005. Epub 2009 May 22. PMID: 19464965.

**Lydall D, Nikolsky Y, Bishop DK, Weinert T.** A meiotic recombination checkpoint controlled by mitotic checkpoint genes. Nature. 1996 Oct 31;383(6603):840-3. doi: 10.1038/383840a0. PMID: 8893012.

**Manfrini N, Guerini I, Citterio A, Lucchini G, Longhese MP.** Processing of meiotic DNA double strand breaks requires cyclin-dependent kinase and multiple nucleases. J Biol Chem. 2010 Apr 9;285(15):11628-37. doi: 10.1074/jbc.M110.104083. Epub 2010 Feb 11. PMID: 20150422; PMCID: PMC2857040.

**Maréchal A, Zou L.** DNA damage sensing by the ATM and ATR kinases. Cold Spring Harb Perspect Biol. 2013 Sep 1;5(9):a012716. doi: 10.1101/cshperspect.a012716. PMID: 24003211; PMCID: PMC3753707.

**Marston AL, Amon A.** Meiosis: cell-cycle controls shuffle and deal. Nat Rev Mol Cell Biol. 2004 Dec;5(12):983-97. doi: 10.1038/nrm1526. Erratum in: Nat Rev Mol Cell Biol. 2005 Oct;6(10):818. PMID: 15573136.

**Matos J, Blanco MG, Maslen S, Skehel JM, West SC.** Regulatory control of the resolution of DNA recombination intermediates during meiosis and mitosis. Cell. 2011 Sep 30;147(1):158-72. doi: 10.1016/j.cell.2011.08.032. PMID: 21962513; PMCID: PMC3560330.

**Miyazaki WY, Orr-Weaver TL.** Sister-chromatid cohesion in mitosis and meiosis. Annu Rev Genet. 1994;28:167-87. doi: 10.1146/annurev.ge.28.120194.001123. PMID: 7893122.

**Nakagawa T, Ogawa H.** Involvement of the MRE2 gene of yeast in formation of meiosis-specific double-strand breaks and crossover recombination through RNA splicing. Genes Cells. 1997 Jan;2(1):65-79. doi: 10.1046/j.1365-2443.1997.d01-283.x. PMID: 9112441.

P**ablo-Hernando ME, Arnaiz-Pita Y, Tachikawa H, del Rey F, Neiman AM, Vázquez de Aldana CR.** Septins localize to microtubules during nutritional limitation in Saccharomyces cerevisiae. BMC Cell Biol. 2008 Oct 1;9:55. doi: 10.1186/1471-2121-9-55. PMID: 18826657; PMCID: PMC2584027.

**Page SL, Hawley RS.** The genetics and molecular biology of the synaptonemal complex. Annu Rev Cell Dev Biol. 2004;20:525-58. doi: 10.1146/annurev.cellbio.19.111301.155141. PMID: 15473851.

**Patricia W Greenwell, Shara L Kronmal, Stephanie E Porter, Johann Gassenhuber, Brigitte Obermaier, Thomas D Petes.** TEL1, a gene involved in controlling telomere length in S. cerevisiae, is homologous to the human ataxia telangiectasia gene, Cell, Volume 82, Issue 5, 1995, Pages 823-829, https://doi.org/10.1016/0092-8674(95)90479-4.

**Pérez-Hidalgo L, Moreno S, San-Segundo PA.** Regulation of meiotic progression by the meiosis-specific checkpoint kinase Mek1 in fission yeast. J Cell Sci. 2003 Jan 15;116(Pt 2):259-71. doi: 10.1242/jcs.00232. PMID: 12482912.

**Prieler S, Penkner A, Borde V, Klein F.** The control of Spo11's interaction with meiotic recombination hotspots. Genes Dev. 2005 Jan 15;19(2):255-69. doi: 10.1101/gad.321105. PMID: 15655113; PMCID: PMC545890.

**Primig M, Williams RM, Winzeler EA, Tevzadze GG, Conway AR, Hwang SY, Davis RW, Esposito RE.** The core meiotic transcriptome in budding yeasts. Nat Genet. 2000 Dec;26(4):415-23. doi: 10.1038/82539. PMID: 11101837.

**Rockmill B, Lefrançois P, Voelkel-Meiman K, Oke A, Roeder GS, Fung JC.** High throughput sequencing reveals alterations in the recombination signatures with diminishing Spo11 activity. PLoS Genet. 2013 Oct;9(10):e1003932. doi: 10.1371/journal.pgen.1003932. Epub 2013 Oct 31. Erratum in: PLoS Genet. 2013 Dec;9(12). doi:10.1371/annotation/b3e65d4a-f7ed-4481-9b5b-92d952d5ee02. PMID: 24204324; PMCID: PMC3814317.

**Roeder GS.** Sex and the single cell: meiosis in yeast. Proc Natl Acad Sci U S A. 1995 Nov 7;92(23):10450-6. doi: 10.1073/pnas.92.23.10450. PMID: 7479818; PMCID: PMC40629.

**Ruff P, Donnianni RA, Glancy E, Oh J, Symington LS.** RPA Stabilization of Single-Stranded DNA Is Critical for Break-Induced Replication. Cell Rep. 2016 Dec 20;17(12):3359-3368. doi: 10.1016/j.celrep.2016.12.003. PMID: 28009302; PMCID: PMC5218512.

**Schwacha A, Kleckner N.** Interhomolog bias during meiotic recombination: meiotic functions promote a highly differentiated interhomolog-only pathway. Cell. 1997 Sep 19;90(6):1123-35. doi: 10.1016/s0092-8674(00)80378-5. PMID: 9323140.

**Seeber A, Hauer M, Gasser SM.** Nucleosome remodelers in double-strand break repair. Curr Opin Genet Dev. 2013 Apr;23(2):174-84. doi: 10.1016/j.gde.2012.12.008. Epub 2013 Jan 23. PMID: 23352131.

**Shim EY, Chung WH, Nicolette ML, Zhang Y, Davis M, Zhu Z, Paull TT, Ira G, Lee SE.** Saccharomyces cerevisiae Mre11/Rad50/Xrs2 and Ku proteins regulate association of

Exo1 and Dna2 with DNA breaks. EMBO J. 2010 Oct 6;29(19):3370-80. doi: 10.1038/emboj.2010.219. Epub 2010 Sep 10. PMID: 20834227; PMCID: PMC2957216.

**Shinohara A, Ogawa H, Ogawa T.** Rad51 protein involved in repair and recombination in S. cerevisiae is a RecA-like protein. Cell. 1992 May 1;69(3):457-70. doi: 10.1016/0092-8674(92)90447-k. Erratum in: Cell 1992 Oct 2;71(1):following 180. PMID: 1581961.

**Shinohara A, Ogawa T.** Stimulation by Rad52 of yeast Rad51-mediated recombination. Nature. 1998 Jan 22;391(6665):404-7. doi: 10.1038/34943. PMID: 9450759.

**Shinohara M, Gasior SL, Bishop DK, Shinohara A.** Tid1/Rdh54 promotes colocalization of rad51 and dmc1 during meiotic recombination. Proc Natl Acad Sci U S A. 2000 Sep 26;97(20):10814-9. doi: 10.1073/pnas.97.20.10814. PMID: 11005857; PMCID: PMC27106.

**Shinohara M, Oh SD, Hunter N, Shinohara A.** Crossover assurance and crossover interference are distinctly regulated by the ZMM proteins during yeast meiosis. Nat Genet. 2008 Mar;40(3):299-309. doi: 10.1038/ng.83. Epub 2008 Feb 24. PMID: 18297071.

**Sollier J, Lin W, Soustelle C, Suhre K, Nicolas A, Géli V, de La Roche Saint-André C.** Set1 is required for meiotic S-phase onset, double-strand break formation and middle gene expression. EMBO J. 2004 May 5;23(9):1957-67. doi: 10.1038/sj.emboj.7600204. Epub 2004 Apr 8. PMID: 15071505; PMCID: PMC404324.

**Sourirajan A, Lichten M.** Polo-like kinase Cdc5 drives exit from pachytene during budding yeast meiosis. Genes Dev. 2008 Oct 1;22(19):2627-32. doi: 10.1101/gad.1711408. PMID: 18832066; PMCID: PMC2559907

**Tung KS, Hong EJ, Roeder GS.** The pachytene checkpoint prevents accumulation and phosphorylation of the meiosis-specific transcription factor Ndt80. Proc Natl Acad Sci U

S A. 2000 Oct 24;97(22):12187-92. doi: 10.1073/pnas.220464597. PMID: 11035815; PMCID: PMC17316.

**Usui T, Ogawa H, Petrini JH.** A DNA damage response pathway controlled by Tel1 and the Mre11 complex. Mol Cell. 2001 Jun;7(6):1255-66. doi: 10.1016/s1097-2765(01)00270-2. PMID: 11430828.

**Usui T, Petrini JH, Morales M.** Rad50S alleles of the Mre11 complex: questions answered and questions raised. Exp Cell Res. 2006 Aug 15;312(14):2694-9. doi: 10.1016/j.yexcr.2006.06.013. Epub 2006 Jun 20. PMID: 16857186.

**Wan L, de los Santos T, Zhang C, Shokat K, Hollingsworth NM.** Mek1 kinase activity functions downstream of RED1 in the regulation of meiotic double strand break repair in budding yeast. Mol Biol Cell. 2004 Jan;15(1):11-23. doi: 10.1091/mbc.e03-07-0499. Epub 2003 Oct 31. PMID: 14595109; PMCID: PMC307523.

**Wold MS.** Replication protein A: a heterotrimeric, single-stranded DNA-binding protein required for eukaryotic DNA metabolism. Annu Rev Biochem. 1997;66:61-92. doi: 10.1146/annurev.biochem.66.1.61. PMID: 9242902.

**Weinert TA, Kiser GL, Hartwell LH**. Mitotic checkpoint genes in budding yeast and the dependence of mitosis on DNA replication and repair. Genes Dev. 1994 Mar 15;8(6):652-65. doi: 10.1101/gad.8.6.652. PMID: 7926756.

**Xu L, Ajimura M, Padmore R, Klein C, Kleckner N.** NDT80, a meiosis-specific gene required for exit from pachytene in Saccharomyces cerevisiae. Mol Cell Biol. 1995 Dec;15(12):6572-81. doi: 10.1128/MCB.15.12.6572. PMID: 8524222; PMCID: PMC230910.

**Nishimura K, Fukagawa T, Takisawa H, Kakimoto T, Kanemaki M.** An auxin-based degron system for the rapid depletion of proteins in nonplant cells. Nat Methods. 2009 Dec;6(12):917-22. doi: 10.1038/nmeth.1401. Epub 2009 Nov 15. PMID: 19915560.

**Zou L, Elledge SJ.** Sensing DNA damage through ATRIP recognition of RPA-ssDNA complexes. Science. 2003 Jun 6;300(5625):1542-8. doi: 10.1126/science.1083430. PMID: 12791985.

# Acknowledgements

I extend my heartfelt gratitude to my parents, whose unwavering emphasis on education has been a guiding light throughout my entire life. Their steadfast belief in the transformative power of learning has shaped my academic journey and instilled in me a profound appreciation for knowledge.

I would also like to express my deepest thanks to my beloved sister for her invaluable emotional support during the challenging pursuit of my Ph.D. Her encouragement, understanding, and unwavering presence have been a source of strength, making this journey not only intellectually enriching but emotionally fulfilling.

I would like to express my sincere gratitude to Prof. Dr. Akira Shinohara for his unwavering belief in me and his invaluable guidance throughout the course of this project. Working under his mentorship has been a privilege, and I am profoundly grateful for the wealth of knowledge and experience he shared.

Special thanks to Dr. Masaru Ito for his insightful contributions and constructive feedback during the experimental phases of this research. His expertise has played a crucial role in shaping the outcome of my work.

I am immensely thankful to my fellow PhD students, Dr. Priyanka Sawant and Steve Mwaniki, for their continual support, engaging discussions, and collaborative brainstorming sessions. Their camaraderie has been a source of inspiration and encouragement.

A heartfelt appreciation goes out to all the members of the Shinohara lab whose assistance has been indispensable throughout this journey. The collective efforts of the lab community have contributed significantly to the success of this project, and I am thankful for the collaborative spirit that permeates the lab.